THE MECHANISM OF ACTION OF NOVEL GAMMA-SECRETASE MODULATORS

A Dissertation

Presented to the Faculty of the Weill Cornell Graduate School

of Medical Sciences

in Partial Fulfillment of the Requirements for the Degree of

Doctor of Philosophy

by

Chelsea Paresi

August 2016

THE MECHANISM OF ACTION OF NOVEL GAMMA-SECRETASE MODULATORS

Chelsea Paresi

Cornell University 2016

Gamma-secretase (GS) is a multi-protein, aspartyl protease complex consisting of presenilin (PS1), nicastrin (NCT), anterior pharynx-defective-1 (APH-1) and presenilin enhancer 2 (PEN-2)1,2. GS cleaves a variety of substrates, all of which are type I transmembrane proteins. The activity of GS has been most extensively studied in relation to the processing of amyloid precursor protein (APP) and Notch due to their implication in Alzheimer's disease and cancer respectively. The role of GS in these pathways makes the enzyme an attractive drug target; however, a major obstacle of using GS as a pharmacological target to treat these diseases is the development of specific inhibitors that selectively target the cleavage of only one substrate. In the case of APP processing, an ideal pharmaceutical would not only conserve cleavage of other gamma-secretase substrates, but would also maintain production of non-amyloidogenic amyloid beta (Aβ) peptides.

In an effort to discover novel GS modulators we have developed and utilized an efficient *in vitro* gamma-secretase activity assay that can be used to measure GS activity on both Notch and APP concurrently. We have shown that recombinant substrates of gamma-secretase compete for cleavage in our assay and that measured IC_{50} values are significantly different when determined in the presence of an additional

substrate. This work demonstrates the importance of using accurate biochemical assays when calculating selectivity margins.

We have utilized this assay to study novel gamma-secretase inhibitors and modulators, specifically, benzimidazoles which inhibit Notch processing while simultaneously altering APP cleavage specificity. The data presented herein suggest that similar to their mechanism of proton pump inhibition, benzimidazoles modulate gamma-secretase activity by binding to cysteine residues on Notch, PS1-NTF, PS1-CTF, and Pen-2.

A large portion of the evidence for benzimidazole binding to GS and Notch consists of protein labeling experiments performed with benzimidazole based probes. In addition to using these probes for target identification, we have also undergone a systematic comparison of available copper-free click chemistries. We have validated the use of molecular probes for target ID by showing direct labeling of the known benzimidazole target, the gastric proton pump, and have identified several novel binding partners of benzimidazole compounds.

BIOGRAPHICAL SKETCH

Chelsea Paresi was born in Salt Lake City, Utah in 1988. After graduating from Olympus High School, she remained in Utah, attending Westminster College on a Presidential Scholarship, awarded for her previous academic success. During her time at Westminster she earned the Eccles Scholarship from 2007 to 2011, the Gore Math & Science Scholarship from 2008 to 2009, and the Alumni Association Scholarship from 2009 to 2011. Chelsea was on the Dean's Honor Roll each of her four years at Westminster and was awarded the "Outstanding Student in Chemistry" award upon graduating in 2011.

Chelsea has always had a strong interest in pharmacological sciences. She received her Pharmacy Technician Certificate during high school and intended on going to Pharmacy school after college. As such, she majored in Chemistry, but quickly realized a passion for research. She completed a summer fellowship at University of California (UCSD) in 2009, where she screened a large library of compounds for inhibition or activation of PH domain and Leucine rich repeat Protein Phosphatase (PHLPP). In her junior and senior year she worked as a laboratory assistant in a small start-up called Electronic BioSciences; there she executed research aiming to develop state of the art, nanopore based systems for DNA sequencing, chemical detection and research and development applications. She performed single ion-channel studies, measuring the variance in conductance as a single strand of DNA passes through wild type and mutant forms of the biological pore, alpha-hemolysin.

Chelsea graduated *summa cud laude* from Westminster College with a B.S. in Chemistry in May 2011.

That summer Chelsea traveled with her future husband and two dogs across the country to New York City, where she entered the Pharmacology program of Weill Cornell Graduate School of Medical Sciences and was a recipient of the "Vincent du Vigneaud First-Year Poster Presentation Award." In spring 2012, she joined the lab of Dr. Yue-Ming Li at Memorial Sloan Kettering Cancer Center and began her thesis work. Chelsea was the recipient of an NIH T32 Pharmacology training grant from 2012-2014. She presented her work at annual Pharmacology retreats and student research symposiums. Her graduate career culminated in a first author paper in *Molecular BioSystems* detailing the use of copper-free click chemistry for target identification with covalent probes, in addition to two other first-author publications currently in preparation.

Chelsea was an active member in the graduate school community, serving for two years as the executive council's careers chairperson, spearheading an initiative to educate graduate students on alternative career paths, and chairing a committee to plan and execute a yearlong seminar series.

For my son, Jameson and his grandma, my mom, Shelley.

ACKNOWLEDGEMENTS

It feels very surreal to be finally writing my thesis. There were more times than I can count where I thought about giving up along the way, and I have so many people to thank for continually supporting and motivating me to keep going.

First, I'd like to thank my mentor, Dr. Yue-Ming Li. He is a brilliant scientist, an understanding boss and overall a really wonderful human being. He truly cares about the lab and his students, which has resulted in an unusually pleasant work environment. He has taught me to be a critical thinker, an expert pharmacologist and to always perform a proper triplicate. Yue-Ming was practically always available to discuss results, practice presentations, trouble-shoot protocols, or come into the lab and fix it himself when something was really broken. I'd also like to extend a huge thank you to my committee members for their time commitment and constructive criticism: Dr. Minkui Luo, Dr. Steven Gross, Dr. Lonny Levin and Dr. Xuejen Jiang. I also want to express my deepest appreciation to our secretary, Pascale Presendor, who keeps our lab running and our members happy.

I'm incredibly grateful to the entire Pharmacology Department at Weill Cornell, for an outstanding and well-rounded education and never ending support for its students. I want to thank the past and present members of the Li Lab for making lab somewhere I truly enjoyed being. I am constantly amazed at the compassionate and collaborative spirit of our lab. In particular, I want to thank Courtney Carroll, Danica Chiu, Alissa Brandes, Natalya Gertsik, Christina Crump, Deming Chau, Feng Weng, Qi Liu, Wenbo Pei. These people are extraordinarily intelligent and excellent

scientists. They have each been teachers and mentors in their own right, and I so appreciate their friendship.

Lastly, and certainly not least, I need to thank my friends and family. I have been unbelievably blessed to have an unfailing support system over the past five years. I would not be in New York, in a graduate program today without my husband, Thomas, helping me to realize my own potential, teaching me to always strive for more and constantly loving and supporting me. My friends, Courtney, Danica, Emily, Sara, Mandy, Suzanne, Jenny, Rachel, Laura and Jeff have made the past five years some of the best of my life and have continually taken such great care of me and my little family, I don't know what I would have done without them. Most importantly, I want to thank my family, my Dad, Jeff, my aunts Lulu and Becky and especially my mom, for being an unwavering source of love and support my entire life. My mom's compassion, altruistic spirit and her own battle with cancer have inspired me to spend my life striving to help others, and although she isn't here today, I would not be who I am today without her.

TABLE OF CONTENTS

LIST OF FIGURES

CHAPTER 1

CHAPTER 3

CHAPTER 4

CHAPTER 5

LIST OF TABLES

LIST OF ABBREVIATIONS

αCTF: α-Secretase cleaved C terminal fragment of APP
βCTF: β-Secretase cleaved C terminal fragment of APP
AD: Alzheimer's disease
ADAM: A disintegrin and metalloproteinase
AICD: APP intracellular domain
ANPP8: HEK293 cells overexpressing 4 components of γ-secretase (Aph1, Nct, PS, Pen2)
APH1: Anterior pharynx defective 1
APOE: Apolipoprotein E
APP: Amyloid precursor protein
ATP4A: Gene encoding gastric H+/K+-ATPase
Aβ: β-Amyloid peptide
BACE-1/β-secretase: β-Site APP Cleaving Enzyme 1
CHAPSO: 3-[(3-Cholamidopropyl)dimethylammonio]-2-hydroxy-1-propanesulfonate
COX: cyclooxygenase
CSL: CBF1/Su(H)/Lag-1, also known as RBP-Jκ family
CuAAC: Copper(I)-catalyzed Azide-Alkyne Cycloaddition, also called Azide-Alkyne Huisgen Cycloaddition
DMSO: Dimethyl sulfoxide
EM: Electron microscopy
ER: Endoplasmic reticulum
FAD: Familial Alzheimer's disease
FLIM: Fluorescence-lifetime imaging microscopy
GS: Gamma-secretase
GSAP: Gamma-Secretase activating protein
GSI: Gamma-Secretase inhibitor
GSM: Gamma-Secretase modulator
L458: L-685,458
LY450139: Also called semagacestat
MBP: Maltose binding protein
NCT: Nicastrin
NFT: Neurofibrillary tangles
NICD: Notch intracellular domain
Notch ΔE: Notch construct lacking extracellular domain
NSAIDs: Non-steroidal anti-inflammatory drugsxi
PBS: Phosphate buffered saline
PEN2: Presenilin enhancer 2
PMSF: Phenylmethanesulfonyl fluoride
PPI: proton pump inhibitor
PS: Presenilin
PS1-CTF: Presenilin1 carboxy-terminal fragment
PS1-NTF: Presenilin1 amino-terminal fragment
PS-FL: Full length presenilin

PVDF: polyvinylidene difluoride
RIP: Regulated intramembrane proteolysis
RIPA: Radioimmunoprecipitation assay buffer
sAPPα: Soluble APP, cleavage product of α-secretase
sAPPβ: Soluble APP, cleavage product of β-secretase
SAR: Structure-activity relationship
SDS: Sodium dodecyl sulfate
SDS-PAGE: SDS-polyacrylamide gel
TAMRA: 5-carboxytetramethylrhodamine
TBTA: Tris[(1-benzyl-1H-1,2,3-triazol-4-yl)methyl]amine
TCEP: Tris(2-carboxyethyl)phosphine hydrochloride
TMD: Transmembrane domain
UV: Ultra-violet

LIST OF SYMBOLS

α: Alpha
β: Beta
γ: Gamma
Δ: Delta
ε: Epsilon
κ: Kappa
μ: Mu, for micro
Å: Angstrom
˚: Degree

CHAPTER 1:

Introduction

1.1 Gamma-Secretase and Regulated Intramembrane Proteolysis

The term "Gamma-secretase" (GS) was first coined in 1993 to describe the cleavage of the Amyloid Precursor Protein (APP) within the transmembrane domain, generating the infamous beta-amyloid (Aβ) peptides that are deposited in the brains of Alzheimer disease (AD) patients[1]. While it would be at least a decade before the identity of gamma-secretase was fully elucidated, this was one of the earliest reports of regulated intramembrane proteolysis (RIP) [2]. RIP is an evolutionarily conserved mechanism that involves coordination of a water molecule within the lipid membrane to hydrolyse a peptide bond of the membrane-anchored substrate [3, 4]. In the case of aspartyl proteases such as gamma-secretase, two aspartyl residues within the active site act as an acid and a base to activate a water molecule for nucleophilic attack on the carbonyl carbon of the substrate scissile bond[5]. Cleavage of gamma-secretase substrates results in the release of both extra- and intra-cellular peptide fragments that go on to transduce cellular signals in a variety of manners[6].

1.2 The Gamma-Secretase Complex

As a result of the culmination of years of extensive research, it is now well understood that gamma-secretase is a large complex comprised of four obligatory subunits: Presenilin (PS), Nicastrin (NCT), anterior pharynx-defective-1 (Aph-1) and presenilin enhancer 2 (Pen-2)[7, 8], all of which are necessary and sufficient for catalytic activity[9] and are present in a 1:1:1:1 stoichiometry [10] (Figure 1.1). Each

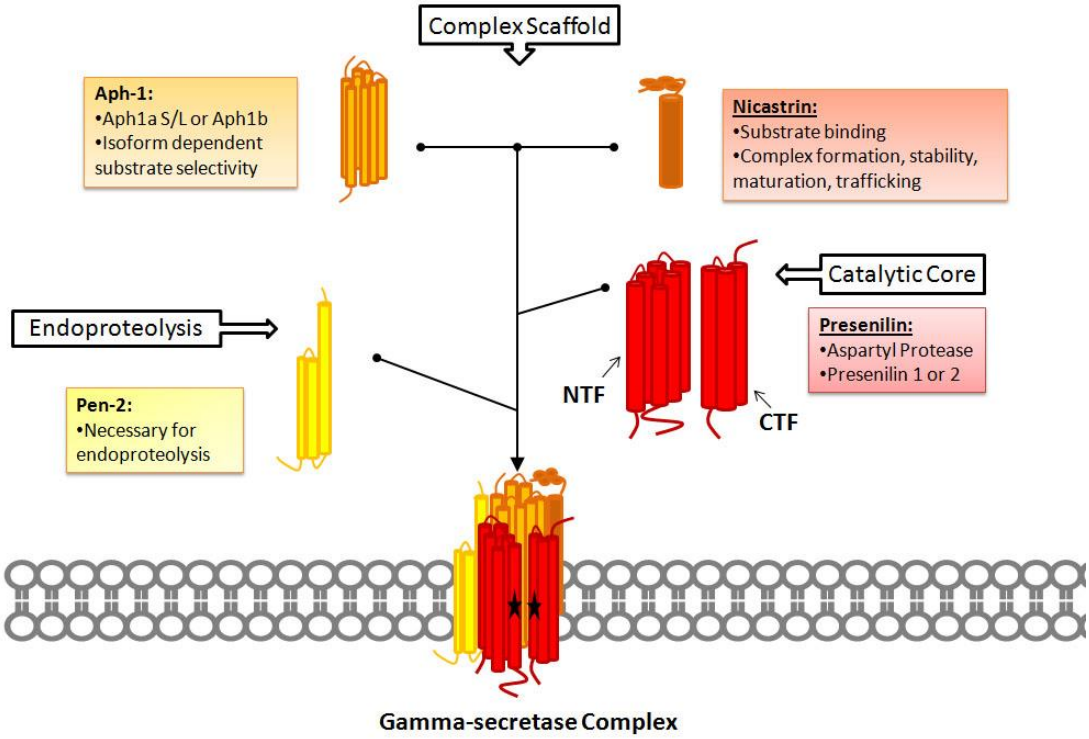

Figure 1.1: The gamma-secretase complex. The gamma-secretase complex is formed by the assembly of Aph1 and Nicastrin to create an initial sub-complex scaffold. The catalytic core, presenilin, binds next, followed by Pen-2, which results in endoproteolysis of presenilin to generate NTF and CTF, activating the complex. The black stars represent the catalytic aspartate residues of presenilin.

subunit is synthesized in the endoplasmic reticulum; NCT and APH-1 form an initial sub-complex scaffold, followed by binding of PS, then PEN-2[8]. Incorporation of PEN-2 results in rapid endoproteolysis of PS between transmembrane domains (TMD) 6 and 7 into a C-terminal fragment (CTF) and N-terminal fragment (NTF) that remain closely associated within the complex[11, 12]. Endoproteolysis generates a fully formed gamma-secretase that is trafficked through the Golgi to the plasma membrane. While the numerous mechanisms of gamma-secretase regulation will be discussed in the coming sections, it is important to note that the presence of a fully formed gamma-

secretase complex does not necessarily mean the complex is catalytically active [13-15].

Presenilin

The first identified subunit of gamma-secretase was presenilin. It was simultaneously discovered to be involved in both AD and embryonic development through two independent lines of research. Genetic analysis of Familial Alzheimer's disease (FAD) patients revealed mutations in the previously uncharacterized genes *presenilin 1* (PSEN1) [16, 17] and *presenilin 2* (PSEN2) [18]. In the same year, the PSEN gene was also identified to regulate Notch in *Caenorhabditis elegans*, which is vital for cell signaling during development [19]. It was first observed that mutations in PS result in changes in the amount of Aβ peptides generated, as well as the ratio of the longer, more aggregate prone peptide, Aβ42, to shorter peptides such as Aβ40[20-25]. Classification of PS as the catalytic core of gamma-secretase did not occur until later, when knock out of PS1 was shown to significantly reduce the production of Aβ peptides in mouse neurons[26], and deficiency of PS1 in mouse or *Drosophila* was shown to also reduce the proteolytic release of the Notch intracellular domain (NICD) [27, 28]. A gamma-secretase inhibitor was shown to block both APP and Notch processing, further confirming that PS is the protease responsible for the cleavage of both substrates[27] . Additional evidence that PS is an aspartyl protease and the catalytic subunit of GS include: the finding that mutation of two conserved aspartate residues in PS1 and PS2 result in significantly reduced Aβ production[29, 30], aspartyl protease transition state analogs directly bind PS and inhibit gamma-

secretase activity[31], and recombinant PS reconstituted into proteoliposomes is sufficient for substrate cleavage in the absence of other gamma-secretase subunits[12].

Full length PS is approximately 50kDa and has 9 TMDs [32, 33]. The protein exists as two isoforms: PS1 and PS2. PS1 is not only more abundant, but also more active and possibly more amyloidogenic [34]. The catalytic aspartate residues in both homologs are located within TMD 6 and 7, at the interface of the NTF and CTF [35]. While the identification of presenilin was a huge accomplishment in the field, it was immediately clear that it was not the only protein involved in gamma-secretase activity, as over-expression of PS is not sufficient to increase gamma-secretase activity[36].

Nicastrin (NCT)

Immunochemical purification using antibodies against PS identified Nicastrin, a 130kDa, heavily glycosylated, Type 1 integral membrane protein, as part of the gamma-secretase complex[37]. In addition to its function as a scaffold for the formation of the complete complex [38], NCT has also been found to play a role in complex stability and trafficking [8, 39, 40]. There is a large body of evidence showing that Nicastrin also plays a role in substrate docking and specificity [41-45]; however, contradictory reports have demonstrated NCT-independent gamma-secretase activity [46], suggesting it may not actually be required for substrate recognition.

Presenilin enhancer 2 (Pen-2)

Pen-2 was discovered through a genetic screen in *C. elegans* looking to identify genes that modify PS activity on the Notch homologs, *glp-1* and *lin-1 [47]*. Pen-2 is an approximately 12kDa protein that has been historically thought to be a "hairpin" like, two-transmembrane protein [47]. However, a recent report suggests the first hydrophobic domain may form a reentrant loop, while the second spans the bilayer. Knock down of Pen-2 not only drastically decreases gamma-secretase activity, but also decreases CTF and NTF levels, while increasing the stability of full length PS [48], suggesting Pen-2 plays an important role in the endoproteolysis of PS. Several groups have validated the requirement of Pen-2 for maturation of full length PS into NTF and CTF [12, 49]. Additionally, a catalytically active, endoproteolysis deficient mutant of presenilin, PS1ΔE9, was shown to have no activity when expressed in Pen-$2^{-/-}$ MEFs, suggesting that Pen-2 is still required outside of its function in endoproteolysis[50]. Interestingly, overexpression of Pen-2 shifts preference from PS1 containing complexes to PS2 containing complexes, indicating a regulatory role for the subunit as well [51].

Anterior pharynx-defective-1 (Aph-1)

Also discovered in the C. elegans screen mentioned above was Aph-1[47, 52]. Aph-1 is an approximately 29kDa protein with seven TMDs [53]. Similar to Nicastrin, Aph-1 is involved in providing the initial scaffold for complex formation [53, 54] and also in substrate selectivity. While NCT is thought to be involved in substrate selection via direct binding, Aph-1 isoform-dependent substrate processing

has been observed [55]. Humans have two Aph-1 genes, Aph-1a and Apha-1b. Aph-1a is alternatively spliced to give Aph-1aS or Aph-1aL [56]; taking the two presenilin homologs and a 1:1:1:1 stoichiometry into consideration this means there are 6 distinct gamma-secretase complexes that can be formed in the cell.

1.3 Gamma-Secretase Regulation and Substrate Specificity

In addition to processing APP and Notch, GS has been reported to process more than 90 substrates [57] (although many of these substrates have yet to be verified as physiologically relevant). Among the numerous substrates, there is no consensus sequence, and the only apparent requirement is that the substrate be a Type 1 membrane protein that has undergone ectodomain shedding [58]. To make matters more complicated, GS can cleave many of these substrates at multiple positions within the transmembrane domain. While it may appear that GS functions as a general "membrane proteasome", the regulation of its activity is actually quite complex and, the signaling pathways involved are vital to cellular function. The mechanisms that govern gamma-secretase regulation and substrate specificity are not fully understood, but clearly encompass a wide array of processes.

The requirement for each of the subunits described above provides intrinsic regulation, based on their own spatial and temporal expression patterns. Additionally, the possible heterogeneity of each complex can also dictate the activity of the complex. As briefly mentioned above, Presenilin exists in two isoforms and Aph-1 in three, which are present in a mutually exclusive manner, meaning there are 6 possible

complex compositions. It has been shown that PS1 and PS2 expression levels vary between tissues and that deficiency of either causes distinct phenotypic differences [59]. In addition to differential substrate specificity, the two isoforms also exhibit differential product preference, as PS1-containing complexes have been shown to generate more Aβ42 [60]. Aph-1 can exist in the gamma-secretase complex as three different forms. Similarly to PS, Aph-1 has tissue specific expression patterns, and the isoforms have been reported to differ in their production of longer versus shorter Aβ peptides [55].

While not absolutely required for gamma-secretase activity, additional regulatory proteins such as hypoxia inducible factor 1-α (Hif1α) [61] and gamma-secretase activating protein (GSAP) [62, 63] have been reported to directly bind to the gamma-secretase complex and regulate its activity. There have also been reports of feedback regulation by the ecto-domain shedded APP substrate itself, which can bind directly to an allosteric site on gamma-secretase to modulate Aβ production [64].

Several lines of evidence suggest that gamma-secretase contains a substrate "docking" site that is physically separate from the active site. Gamma-secretase can simultaneously bind to substrate and a transition state analogue inhibitor [65, 66], these transition state analogues show non-competitive inhibition [67, 68], and FRET analysis has shown close proximity of the APP substrate and Presenilin when PS is bound to a transition state inhibitor[69]. The exact location of the docking site and the possible existence of multiple docking sites is still unclear, but the available evidence

suggests that the large ectodomain of Nicastrin positions the substrate into a docking site located on Presenilin, approximately three amino acids from the active site[70]. The substrate then may either translocate through the membrane into the active site, or "kinks" to present the scissile bond to the catalytic aspartates.

Controlled intracellular trafficking of APP can influence the cleavage products of processing by GS, while Notch is predominantly processed at the plasma membrane [71-74]. Exciting recent studies have also shown that PS1 and PS2 are differentially trafficked within the cell, and that PS2 containing complexes localized to late endosomes/lysosomes generating a prominent pool of intracellular Aβ primarily comprised of the longer more aggregate prone species [75]. Lipid composition may also play an important role in GS regulation, as cholesterol has been repeatedly implicated in the production of Aβ and Alzheimer's disease, as it can affect trafficking of APP in lipid rafts. This is thought to sequester the necessary components for signaling into close proximity [76, 77].

1.4 Alzheimer's Disease and the Amyloid Cascade Hypothesis

Alzheimer's disease is a global health crisis characterized by diminished cognitive function, memory loss and eventual inability to perform daily tasks and execute bodily functions. Alzheimer's disease is irreversible and has no cure. More than 5 million Americans are currently living with AD. Treating dementia patients cost more than $236 billion dollars in 2015 alone, and with a large aging population, those numbers are expected to rise exponentially in the coming years (Alzheimer's Association

2015). Autosomal dominant inheritance of mutations in either PSEN or APP causes early onset and familial AD [78], and the body of evidence implicating Aβ in sporadic AD is quickly growing. Therefore, a solid understanding of gamma-secretase cleavage of APP is vital to understanding the underlying mechanisms of this debilitating disease.

While the exact pathological mechanism of AD is not fully elucidated, it is generally believed that accumulation of Aβ peptides drives a sequence of pathogenic events that ultimately lead to dementia [79]. The physiological function of APP processing is not completely understood, but is thought to play a role in neuronal and synaptic processes. On the contrary, the mechanism of processing has been generally elucidated due to its pathological consequences (Figure 2). APP is cleaved in two separate pathways involving GS and at multiple positions within its TMD. In the amyloidogenic pathway, GS cleavage of APP following ectodomain shedding by beta-secretase (BACE) leads to release of sAPPβ and ultimately to the production of amyloid beta (Aβ) peptides of various lengths and the APP intracellular domain (AICD) [80]. Recent studies suggest that APP is cleaved in a sequential manner, removing 3-4 amino acids at a time, and yielding two possible product lines depending on the initiating cleavage site [81, 82]. However, contradictory studies have been published [83-85] . In the non-amyloidogenic pathway, the ectodomain of APP is shed by α-secretase which results in the production of P3, sAPPα and AICD and precludes the formation of Aβ peptides [86, 87].

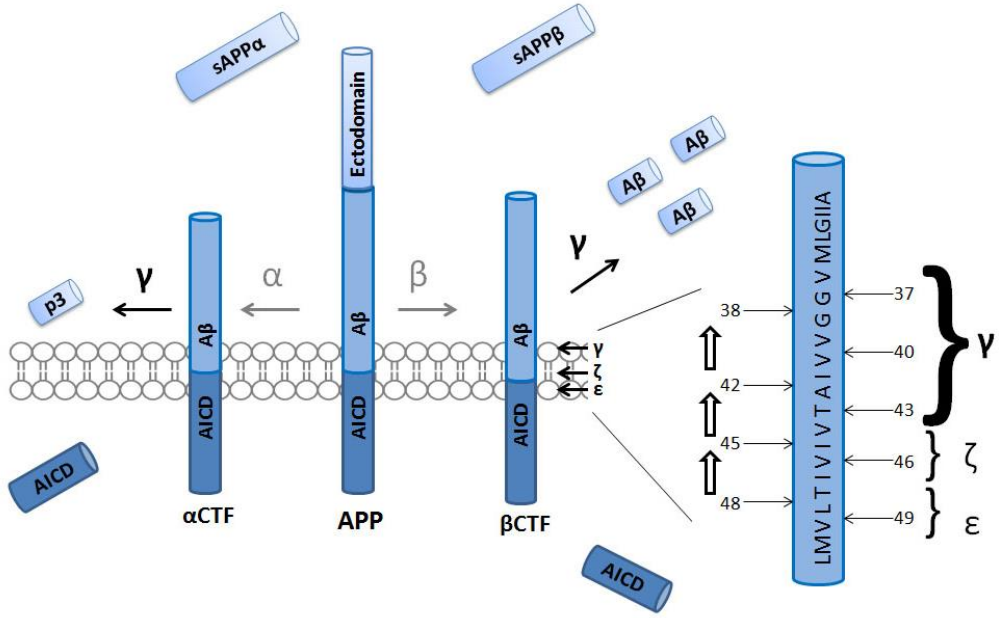

Figure 1.2: Gamma-Secretase cleavage of APP. The amyloid precursor protein (APP) can be cleaved in two separate pathways. In the non-amyloidogenic pathways (shown to the left) α-secretase cleaves APP to release sAPPα, resulting in cleavage by GS to generate p3 and AICD. In the amyloidogenic pathway (shown to the right), APP is first cleaved by β-secretase to generate βCTF, followed by sequential GS cleavage to yield AICD and Aβ peptides of various lengths. The starting cleavage site, either amino acid 48 or 49, dictates the end product, either Aβ38/42 or Aβ37/40. (*Figure adapted from Carroll et. al. Brain. Res. Bull. 2016)*

It is the longer, more hydrophobic and aggregate prone peptides, such as Aβ42, that are thought to be the more "toxic" species of the Aβ peptides. Aβ42 is the more abundant species found in brain plaques [88] and a higher ratio of Aβ42:Aβ40 has been found to increase the toxicity and aggregation potential for total Aβ [89].Not surprisingly, many of the reported FAD mutations result in an increase in Aβ42, and all presenilin FAD mutations result in an increase in the ratio of Aβ42: Aβ40 [78], which correlates more closely to the age of onset of FAD than total Aβ [90]. In addition to the direct genetic link between gamma-secretase processing of APP and FAD, extensive research suggests that this mechanism is involved in early onset and sporadic AD as well. All AD patients exhibit Aβ deposition in brain regions serving

memory and cognition, and Aβ42 oligomers isolated from late-onset AD brains decrease synapse density, inhibit long-term potentiation, and enhance long-term synaptic depression in the rodent hippocampus [79]. A protective mutation in APP has been identified and shown to decrease the production and aggregation of Aβ peptides [91]. Additionally, the only identified major risk factor for AD, APOE4, has been shown to contribute to excess Aβ aggregation by decreasing its clearance from the brain [92-94].

1.5 The Notch Signaling Pathway

The *Notch* gene was discovered 97 years ago, with the observation that haploinsufficiency results in notches at the wing margin of *Drosophila melanogaster [95]*. Nearly a century later, it is now recognized that Notch plays a fundamental role in cell-fate determination. Notch dictates vital cell processes such as differentiation, proliferation and apoptosis in developing and adult tissues in organisms from sea urchin to humans [96] [97].

The Notch family of receptors includes four paralogues (Notch 1-4) [98] that are all type 1 transmembrane proteins of approximately 300kDa [96]. Notch proteins are synthesized as a precursor that is cleaved by a furin-like convertase (S1 cleavage) to generate a mature, calcium dependent, non-covalent heterodimer [99]. Although the Notch signaling pathway is recognized to be extraordinarily complex and not completely understood, a general mechanism for canonical Notch signaling is widely accepted (Figure 1.3) [97]. Ligands of the Delta-Serrate-Lag2 (DSL) family (in

mammals these include Jagged (JAG) 1,2 and Delta-Ligand Like (DLL) 1,3 and 4) expressed on an adjacent cell can bind to the Notch receptor, resulting in a conformational change that exposes the S2 cleavage site to the metalloproteinase tumor necrosis factor-α-converting enzyme (TACE; also known as ADAM17). S2 cleavage allows for further processing by gamma-secretase at the S3 site and subsequent release of the Notch intracellular domain (NICD). NICD travels to the nucleus, converting CBF1-Su(H)-lag1 (CSL) from a repressor complex to an activating complex, which recruits other co-activating proteins, such as mastermind-like 1(MAML1), to regulate the transcription of target genes [100]. The accessory transcription factors present in each cellular context dictate the outcome of signaling in different cell types. Some of the most well characterized Notch target genes include the basic-helix-loop-helix (bHLH) transcriptional repressors hairy enhancer of split (HES) and the hairy-related transcription factor (HRT or HEY), cyclin D1 and MYC [100, 101]. Notch target genes subsequently regulate the expression of genes involved in cell-fate determination such as differentiation, proliferation, stem-cell maintenance and self-renewal and apoptosis (Figure 1.3).

Although the core components of Notch signaling are ubiquitous, the environmental context of Notch signaling dictates the outcome, such that the cell exerts multiple levels of regulation. Spatial and temporal expression of ligand and receptor is vital, as Notch signaling is extremely sensitive to gene dosage. Additionally, biosynthesis, post-translation modifications, trafficking and degradation

of core components or accessory modifiers can also influence the role Notch signaling plays in a cell [100].

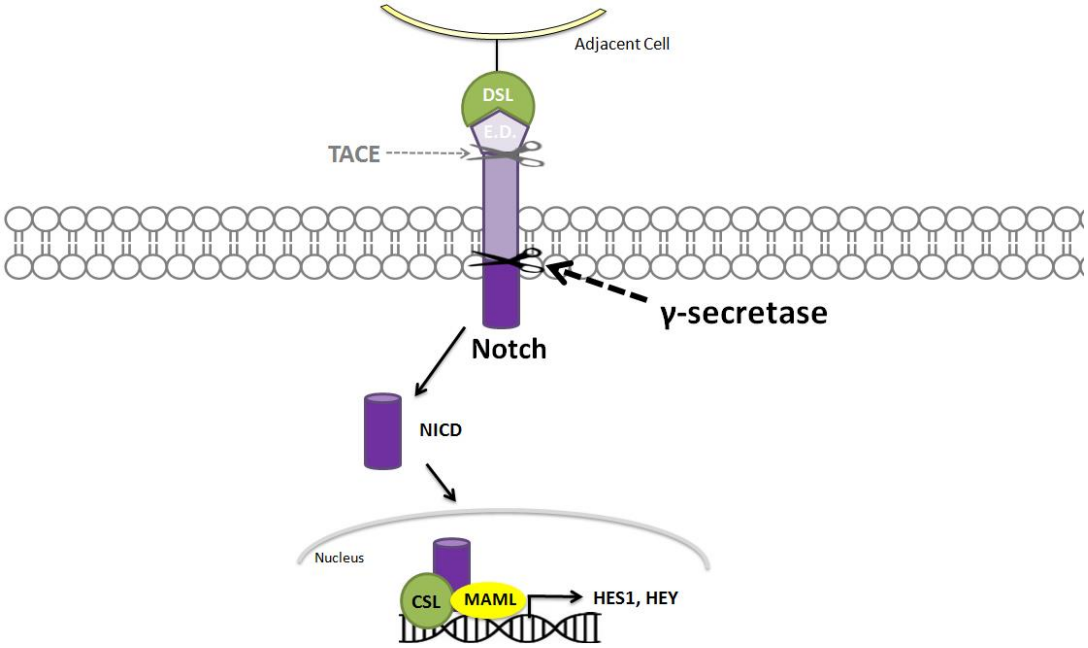

Figure 1.3: The Notch signaling pathway. Ligands of the DSL family expressed on adjacent cells bind the extracellular domain (E.D.) of the Notch receptor resulting in sequential cleavage by TACE and GS to release the Notch Intracellular domain (NICD), which travels to the nucleus to cooperate with other transcription factors and regulates expression of target genes.

Consistent with its pivotal role in determining cell-fate, Notch pathway perturbations are implicated in numerous disease states, including genetic disorders and cancer. The first reports of oncogenic Notch were identified in T-cell acute lymphoblastic leukemia (T-ALL), where chromosomal translocation involving Notch results in constitutively active NICD signaling [102]. It was later discovered that more than 50% of human T-ALL's have activating mutations in the Notch locus. These mutations also cause constitutive activation of NICD involving ligand independent

signaling and/or impaired proteasome degradation of NICD [103]. To date, oncogenic Notch has been reported in numerous lymphoid neoplasms such as Human multiple myeloma [104], acute myelogenous leukemia (AML) [105], and chronic lymphocytic leukemia (CLL) [106].

While the role of Notch signaling in hematopoietic cancers is well established, the role of Notch in solid tumors is highly context dependent (Table 1). Notch has been implicated in breast, colon, pancreas, prostate, central nervous system and skin cancers; acting as an oncogene in most, but as a tumor suppressor in others (Table 1). Unlike leukemias, deregulation of Notch signaling in solid tumors is rarely due to genetic alterations, but rather inappropriate activation through the loss of a negative regulator or deregulated expression of signaling components[107]. Not only is Notch oncogenicity tissue specific, it's also been shown that Notch signaling during the early stages of tumorigenesis can prevent tumor growth, while Notch activation is required in later stages for tumor progression [108, 109].

Whether aberrant signaling is caused by genetic or molecular alterations, they often lead to cancer by resulting in increased self-renewal and inhibition of cell differentiation [110]. Notch signaling has also been reported to play a role in the epithelial to mesenchymal transition (EMT), which results in decreased expression of adhesion molecules, allowing cells to transverse the extracellular matrix and migrate through the vasculature [111]. It may also contribute to cancer progression via cross-talk with other important signaling pathways such as EGFR, RAS, and MYC [107].

Table 1.1: Multiple roles of Notch signaling in solid tumors. *Adapted from Ranganathan, P. et. al., Nature Review Cancer 11, 3380351 (May 2011).*

Tumour type	Oncogenic	Tumour suppressor	Tumour progression	Tumour maintenance	Drug resistance
Breast	✓	✓	✓	✓	✓
Colorectal	✓		✓		✓
Prostate		✓	✓		
Liver		✓	✓		✓
Pancreatic	✓		✓		✓
Glioblastoma		✓	✓	✓	✓
Cervical	✓		✓		✓
Oral SCC	✓	✓			
Skin		✓			
Head and neck					✓
Medulloblastoma			✓	✓	
Melanoma			✓	✓	
Lung	✓	✓	✓		

1.6 Gamma-Secretase as a Therapeutic Target

Targeting Gamma-Secretase for Treatment of Alzheimer's disease

Based on the pivotal role gamma-secretase plays in prime signaling pathways of both Alzheimer's disease and cancer, small molecule inhibition of the protease has been extensively explored. Multiple gamma-secretase inhibitors (GSI's) have been reported, used to investigate gamma-secretase function and several even entered the clinic. Active site directed GSI's, such as the hydroxyethylene dipeptide isostere, L-685,458, have been extensively utilized in research laboratories and further developed into activity-based molecular probes for identification, localization and isolation of gamma-secretase components[31, 51, 64, 66, 112-118].

While incredibly useful in the research laboratory, complete inhibition of gamma-secretase abolishes cleavage of all substrates, resulting in an array of

unwanted side effects when used in humans. These include increased risk of skin cancer due to inhibition of Notch signaling and worsening memory, as evident by the failed clinical trial for LY450139 (Semagacestat, Eli Lily) [119]). In efforts to overcome these toxicities, the use of "Notch-sparing" compounds such as GSI-953 (Begacestat, Wyeth [now Pfizer]) and BMS-708,163 (Avagacestat, Bristol-Myer Squibb) was proposed [120, 121]. However, Avagacestat has been shown in follow-up studies to have very little selectivity for Aβ42 over Notch [122, 123], and showed major adverse side effects, including but not limited to gastrointestinal disruption, dermatologic complications and cognitive worsening [124]. A phase 1 clinical trial testing Begacestat was discontinued in 2010 for unknown reasons.

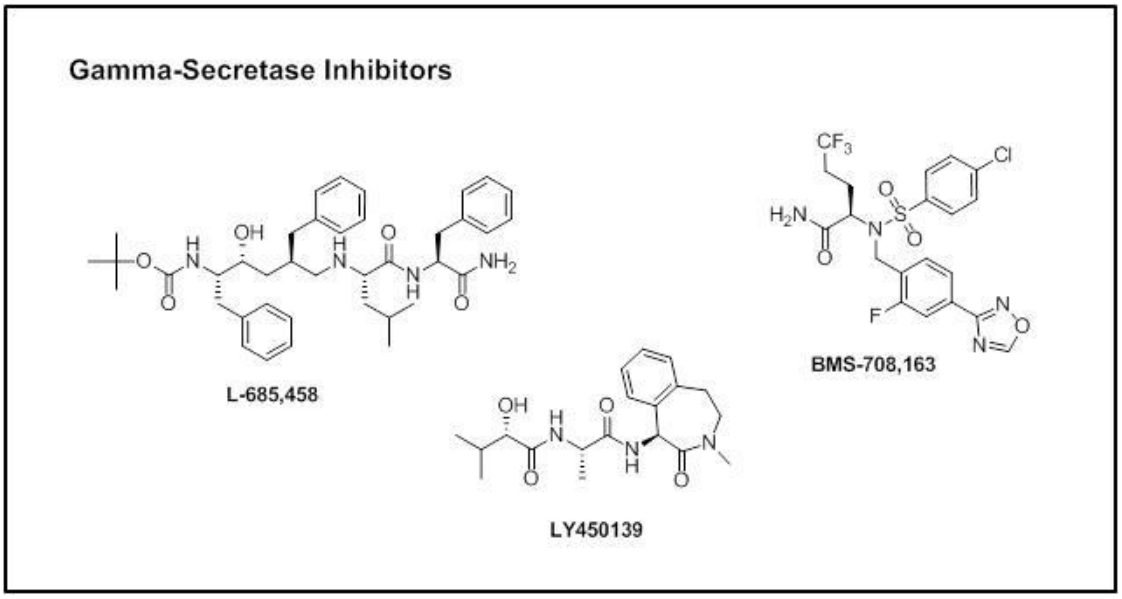

Figure 1.4: Chemical structures of select gamma-secretase inhibitors.

Not only does complete inhibition of gamma-secretase have unwanted effects due to nondiscriminatory inhibition of Notch processing, but it appears that non-

selective inhibition of APP processing can be damaging in its own right. In a physiological setting, APP processing has been shown to be important for various neuronal and synaptic functions [125]. Complete GS inhibition results in an accumulation of the direct substrate, APP βCTF, which appears to be neurotoxic at high concentrations [126], and it has also been found to impact total Aβ42:Aβ40 ratio [127].

Reports of the subsequent cognitive worsening with GSI treatment in clinical trials have made it very clear that the ideal therapeutic candidate must not only protect Notch signaling function, but also conserve total Aβ production. Such gamma-secretase modulators (GSMs) were discovered when certain non-steroidal anti-inflammatory drugs (NSAIDs) such as ibuprofen, indomethacin and sulindac sulfide were found to selectivity inhibit Aβ42 production while increasing Aβ38 production, thus maintaining total Aβ levels. Furthermore, these compounds do not inhibit Notch cleavage and function outside of their activity on cyclooxygenase (COX) [128]. Unfortunately, due to poor brain penetration and low *in vitro* potency (Aβ42 IC_{50}>10μm), these compounds did not proceed into clinical trials (with the exception of R-flurbiprofen which did not achieve statistically significant outcomes in a Phase III clinical trial [129]). However, they demonstrate the promise of selective gamma-secretase modulation and paved the way for the development of second generation GSM's with more favorable profiles.

In an effort to increase potency and permeability of the blood brain barrier (BBB), second generation GSM's were developed. These include compounds which can be classified into three categories: NSAID-derived carboxylic acid molecules, non-NSAID-derived heterocyclic chemotypes, and natural product-derived compounds [130].

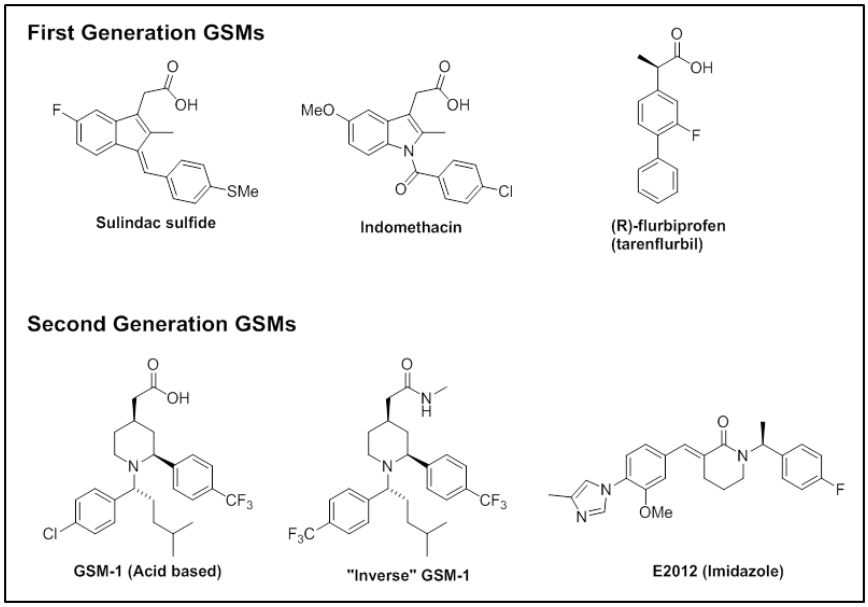

Figure 1.5: Chemical structures of "typical" gamma-secretase modulators.

GSM-1 exemplifies a typical 2nd generation, acid GSM, as it reduces Aβ42 production, promotes the generation of Aβ38 and has negligible effects on Aβ40, total Aβ, NICD or AICD [84]. Structure activity relationship studies have shown the carboxylic acid moiety is not only critical for modulatory activity, but the corresponding ester or amide compounds acts as an "inverse" GSM, increasing the level of Aβ42 production [131, 132].

The imidazole compound, E2012, exemplifies the non-NSAID-derived, 2nd generation GSMs, shifting cleavage site preference to decrease the production of both Aβ40 and Aβ42, and simultaneously increasing Aβ37 and Aβ38 [133, 134]. E2012 entered clinical trials in 2006, but was halted in favor of the development of an improved compound, E2212, that is reported to be more potent and also has a wider safety margin, however no updates have been reported thus far (ClinicalTrials.gov identifier NCT01221259.)

The binding site of 1st generation GSMs remains elusive as contradictory models have been reported; these fall into three possibilities: GSM's bind gamma-secretase [13, 135, 136], GSM's bind the APP substrate [137-139], or GSMs bind both gamma-secretase and APP [140, 141]. The relatively low potency of these compounds required high concentrations for many of these studies, likely resulting in the detection of unspecific interactions being mistaken for the true drug target. However, 2nd generation GSM's of all chemotypes have been shown by various groups to bind presenilin [142-147] and induce conformational changes in gamma-secretase ([117, 118, 141, 145]. Furthermore, a series of elegant photolabeling experiments have also demonstrated that each class of 2nd generation GSM occupies a distinct binding site on presenilin [117, 147].

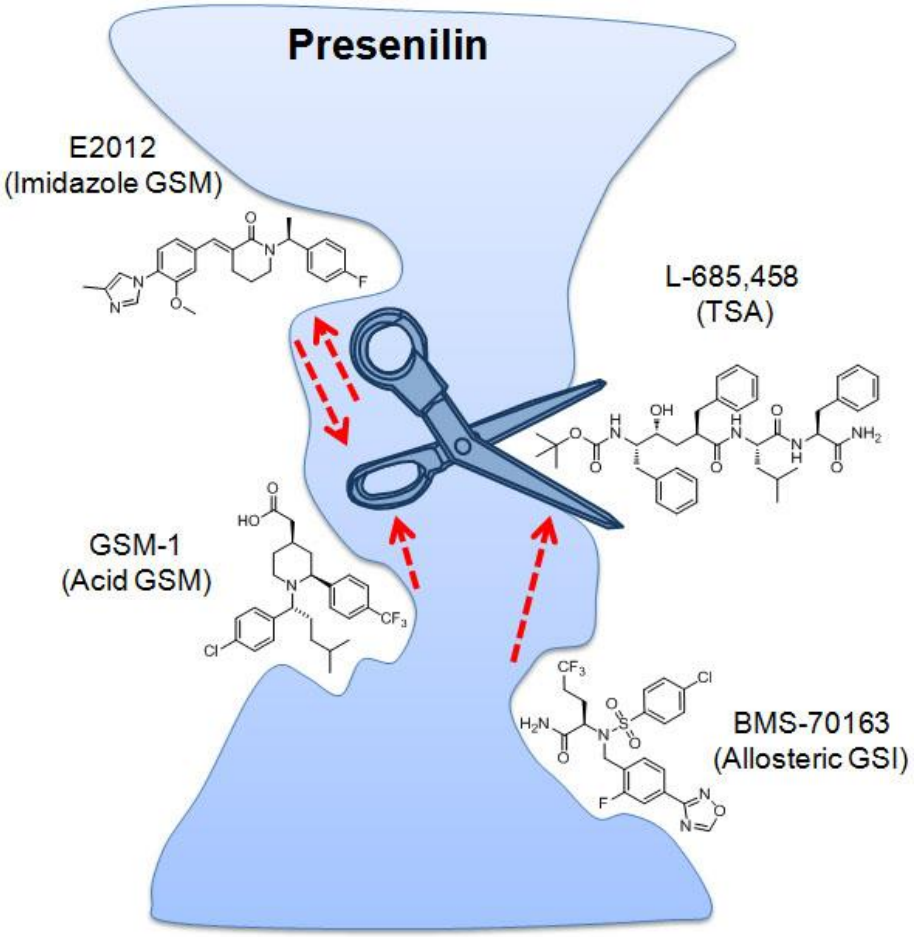

Figure 1.6: Structurally diverse GSIs and GSMs bind to presenilin on distinct allosteric sites (*Adapted from Crump et al. 2013).*

While critics of the amyloid cascade hypothesis often cite failure of GSI's and GSM's to treat AD in the clinic as evidence against the prevailing model, it is more likely that failure has been due not only to unwanted side effects on other gamma-secretase targets, but also to sub-optimal dosing regiments[148]. Furthermore, the continued success of active and passive immunotherapy for lowering amyloid in the clinic support the amyloid cascade hypothesis and validate the importance of targeting this pathway to treat AD[79].

Gamma-Secretase Inhibitors for Cancer Treatment

The extreme toxicity observed with GSI's in the clinic may not be acceptable for treatment of AD, where patients are likely to require extended dosing regiments, but the threshold of acceptable toxicity for cancer treatment is much higher. The use of GSIs to repress cancer stem cell growth has been successful in an *in vitro* experimental setting [149], providing evidence that GSIs may represent a viable therapeutic strategy. As such, several compounds have entered the clinic and are at various stages in the drug development pipeline for cancer therapy.

RO4929097 has been shown to decrease proliferation and impair the ability to form colonies in human primary melanoma cell lines and effect tumor formation and growth in human primary melanoma xenografts [150]. It demonstrates minimal single agent efficacy [151-153], but was found to be safely tolerated and achieve clinical benefit when used in combination with standard chemotherapies in several clinical trials [154-156]. Furthermore, RO4929097 significantly sensitized breast cancer stem cells to ionizing radiation in a pre-clinical model [157].

MRK-0752 is an oral GSI that was reported to reduce stem cell sub populations *in vitro* and in human tissues from clinical trials [158]. The compound was shown to effectively modulate Notch signaling and exert anti-tumor activity in a Phase I study of patients with advance solid tumors [159]. It was also shown to be well-tolerated and effective in treating children with refractory or recurrent CNS malignancies; however, extreme gastrointestinal side effects were reported [160]. It is

currently being tested in several Phase I trials for breast cancer in combination with standard chemotherapies [161].

Among other promising pre-clinical results [162], PF-03084014 was reported to selectively induce apoptosis in chronic lymphocytic leukemia cells bearing Notch mutations, while having relatively little effect on normal T cells or T cells from patients that do not carry Notch mutations [163], mimicking "selective" Notch-target therapy. Interestingly, the toxicity of PF-03084014 has been found to be somewhat mild when compared to other agents in the same class [164]. PF-03084014 is currently in multiple ongoing Phase I and II trials alone and in combination with other therapies [161].

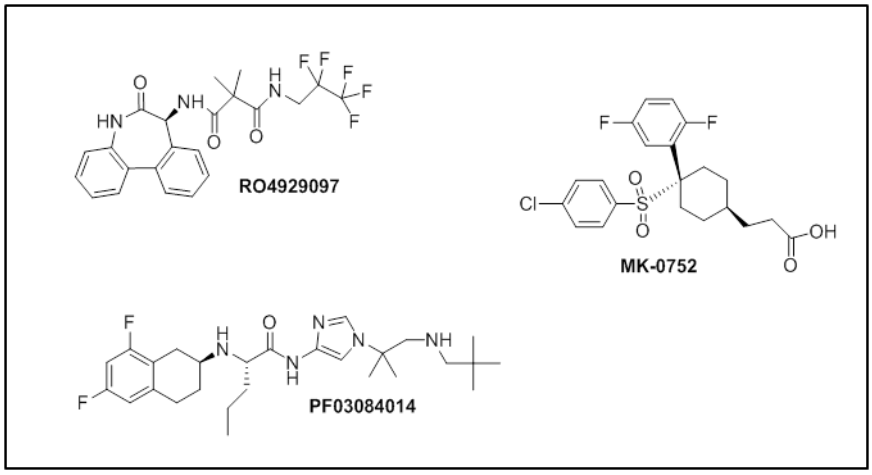

Figure 1.7: Chemical structures of gamma-secretase inhibitors in clinical trials for cancer treatment

While relative success has been achieved in the clinic thus far, there is still much work to be done. In order to maximize therapeutic effects and minimize toxicity, it will be beneficial to show tumor dependency on Notch activation and treat those cancers accordingly. Moreover, based on the data thus far, the use of GSI's in

combination with other therapies such as traditional chemotherapy or ionizing radiation will yield the most curative effect [162].

1.7 Hypothesis and Thesis Overview

It seems to be fully accepted in the Alzheimer's disease field that therapeutically targeting gamma-secretase will ideally be achieved through the use of gamma-secretase modulators. In the cancer field, however, treatment with pan GSI's has prevailed. While the threshold of acceptable toxicity is much higher for cancer treatment, the development of GSMs demonstrates that this may not necessary. Notch-selective compounds have been reported in the literature, but there has been little intentional research for such compounds. We believe that the discovery and development of such compounds would provide an excellent therapeutic option for Notch dependent cancers.

In an effort to discover Notch-specific inhibitors of gamma-secretase we have developed and optimized a "one-pot", *in vitro*, gamma-secretase activity assay that can be used to measure gamma-secretase cleavage of Notch and APP simultaneously. This assay allows for screening of large compound sets with more accurate selectivity calculations.

Using our *in vitro* assay, we have discovered that substituted benzimidazole compounds, which are known proton pump inhibitors widely used for gastrointestinal issues, are also modulators of gamma-secretase activity. Benzimidazoles potently

inhibit NICD production and increase Aβ peptides. We hypothesize that benzimidazole compounds share a similar mechanism of action with proton pump inhibition, meaning that they form a disulfide bond with their molecular target.

Because there is no crystal structure of γ-secretase, we have a limited understanding of where previously reported GSIs/GSMs bind and how the location of binding impacts the modulation profile. Additionally, whether the recent high resolution electron microscopy (EM) structure of γ-secretase [165] illustrates an active enzyme complex is questionable. Due to this, alternative methods must be utilized in order to elucidate the targets of GSIs and GSMs. Labeling using photoaffinity probes has been extremely successful in the past, and we have applied these techniques to our studies. Additionally, because we are working with a covalent inhibitor, we can utilize various copper-free click chemistry techniques in conjunction with covalent probes.

This work presents a novel assay for screening potential GSIs and GSMs, demonstrates a novel mechanism of action for Notch-specific inhibition and gamma-secretase modulation and provides insight into the optimal conditions for labeling with covalent probes for target identification.

CHAPTER 2:

Materials and Overview of General Methodologies

2.1 Materials

HeLa (S3) cell pellet (mid-log) for membrane preparation was purchased from Biovest. ANPP8 (HEK293 cells that overexpress PS1, Aph1, NCT, and Pen2) were a gift from Dr. Sangram Sisodia and were grown in-house for membrane preparation and use in labeling experiments. Fresh porcine stomachs were ordered from Innovative Research Inc. and used for collection of the gastric mucosa and subsequent membrane preparation and vesicle isolation. Biotin-PEG2-azide for azide-alkyne cycloaddition was purchased from ChemPep. Streptavidin Plus UltraLink Resin was purchased from Pierce. Trans-cyclooctene biotin and trans-cyclooctene-TAMRA were synthesized in house by Dr. Qi Liu. Protease Inhibitor cocktail was made in house from powders purchased from Sigma Aldrich and used at final concentrations as follows: 1 mM benzamidine, 2.9 μM leupeptin, 5 μM antipain, 100 μM EDTA, and 100 μM phenylmethanesulfonyl fluoride (PMSF). The PiColorLock Gold Phosphate detection system was purchased from Innova Biosciences and used for ATPase activity assays. Typhoon Trio Variable Mode Imager (GE Healthcare) was used for in-gel fluorescence scans. Western blots were developed either with film or scanned with Odyssey CLx from LI-COR.

Primary antibodies for Western blot: anti-Aph1a 28-3600 was purchased from Invitrogen. Anti-PS1-CTF loop MAB 5232 was purchased from Millipore. Anti-Pen2 18189 rabbit polyclonal was purchased from Abcam. Anti-PS1-NTF was provided by

Dr. Min-Tain Lai (Merck Research Laboratories). The antibody against Nicastrin was generated by immunizing rabbits with a peptide epitope. Anti-ATP4A (ab174293) was purchased from AbCam. Secondary antibodies for Western blots scanned on Odyssey were purchased from LI-COR: IRDye 800 CW goat anti-rabbit and IRDye 680 RD goat anti-mouse.

AlphaLISA detection reagents for γ-secretase activity assays including Streptavidin coated donor beads, anti-mouse acceptor beads, protein-A coated acceptor beads were purchased from Perkin Elmer. G2-10 conjugated acceptor beads were made in-house according to the protocol provided by Perkin Elmer. The Aβ42 cleavage specific antibody 10-G3 was kindly provided as a gift from Douglas Johnson (Pfizer); the Aβ40 cleavage specific antibody G2-10 was a gift from Merck Research Labs; and the Notch1 intracellular domain cleavage specific antibody SM320 was generated by Deming Chau. AlphaLISA signal was detected with an EnVision multilabel plate reader (PerkinElmer).

2.2 Expression and Purification of Recombinant Substrates

Recombinant substrates were expressed and purified as previously reported [64, 166]. Briefly, plasmids encoding for recombinant Notch (rNotch) and APP (rAPP) substrates, PIad16-rNotch-Avi or PIad16-rAPP-Avi, were separately co-transformed into BL21 (DE3) *E.Coli* with pACYC184, which encodes for biotin ligase (*BirA).* Bacteria were incubated at 37°C until growth reached 0.4-0.8 at A600, then recombinant substrate expression was induced by the addition of isopropyl 1-thio-β-D-galactopyransoide

(100μM) in the presence of 50μM biotin for 5 hrs at 20°C. To generate non-biotinylated substrates, the same protocol was followed in the absence of biotin during induction. Cells were pelleted and lysed by French press (Spectronic Instruments). The soluble fraction was isolated by centrifugation at 17,000g for 30min then subjected to amylose affinity chromatography, purifying target proteins via a maltose binding protein (MBP) tag present on both substrates. The MBP tag was removed by overnight thrombin treatment at 16°C to generate biotinylated, recombinant proteins. Mutant substrates were generated using Agilent QuickChange Lightening mutagenesis kit, expressed and purified as described above.

2.3 Membrane Preparation

Gamma-secretase containing HeLa or ANPP membranes were prepared as previously reported [31, 112]. Frozen cells were resuspended in 1X MES buffer (50mM MES, pH 6.0, 5 mM $MgCl_2$, 5 mM $CaCl_2$, 150 mM KCl) containing "complete" protease inhibitors, PI and PMSF, (Boehringer Mannheim, Gaithersburg, MA) and lysed by French Press (Spectronic Instruments). Cell debris and nuclei were removed by centrifugation at 800g for 10min. Supernatants were collected and centrifuged at 100,000g for 60min. Pellets were resuspended in a minimal amount of 1X MES buffer and re-centrifuged at 100,000g for 60min. The final pellet was suspended in MES buffer and stored at -80°C.

2.4 *In Vitro* Gamma-Secretase Activity Assay

Gamma-secretase present in HeLa membrane is incubated with recombinant, biotinylated substrate (0.4μM rNotch, 1μM rAPP) in the presence of 0.25% CHAPSO and PIPES buffer (50mM PIPES, 150mM KCl, 5mM $CaCl_2$, 5mM $MgCl_2$, pH=7.0) for 3 hours at 37C. In a "two-pot" assay, substrates are separately incubated with HeLa

membrane. In the "one-pot" assay format, both substrates are incubated with HeLa in the same reaction. Afterwards, an antibody specific to the cleavage site is added in the presence of streptavidin-conjugated donor beads (40ug/mL in APP assays and 20ug/mL in Notch assays) and Protein A-conjugated acceptor beads (5ug/mL) and incubated at room temperature overnight. The AlphaLISA signal is measured the next day using an Envision plate reader (Perkin Elmer, Waltham MA). A pan GS inhibitor is used to determine background and vehicle (DMSO) is used as a positive control. For IC_{50} assays, normalized AlphaLISA signals were converted to percent vehicle values and used to create dose-response curves which were fitted to 3 parameter curves using GraphPad Prism version 6 (GraphPad Software, San Diego, CA).

2.5 Cell-Based Gamma-Secretase Activity Assay

For the Aβ cell-based γ-secretase activity assays, 35,000 HEK-APP cells were seeded in DMEM-HG media in a 96 well plate in order to achieve a confluency of 50% in 24 hrs, at which point cells were treated with desired compounds or vehicle (0.1% DMSO). Background signal is determined from a negative control sample with 1 μM JC2 (Compound E racemate). After 24 hours of treatment, cells are approximately 80% confluent and 25 μL of media is removed for testing using the suggested protocol for the Aβ three-plex (4G8) Meso Scale Discovery kit.

For the NICD cell-based γ-secretase activity assays, 35,000 HEK293-NΔE cells were seeded in DMEM-HG media in a 96 well plate in order to achieve a confluency of 50% in 24 hrs, at which point cells were treated with desired

compounds or vehicle (0.1% DMSO). Background signal is determined from a negative control sample with 1 μM JC2 (Compound E racemate). After 24 hours of treatment cells should be ~80% confluent, then aspirate media from cells and replace with 25μL ice cold lysis buffer (0.25 % CHAPSO in PBS with PI cocktail) and shake for 45min at 4C. Once cells are completely lysed, remove 5 μL lysate and add to 20 μL of detection mix (0.6 μg/mL biotin-anti-Myc antibody, 0.2 μg/mL SM320 antibody, 5 μg/mL protein A acceptor beads, 10 μg/mL streptavidin coated donor beads in assay buffer containing 50mM HEPEs pH 7.5, 150 mM NaCl, 0.1% BSA, 0.1% (Tween-20) in a 384 well plate. Read plate on Envision the next day.

2.4 Photoaffinity labeling (PAL) with PPI-BP probes in HeLa membrane followed by western blot analysis

Clickable PPI based probes were incubated with 600-800 μg of HeLa cell membranes at 37 °C for 1 hr in the presence or absence of parent compound in 1 mL of PBS, and then UV irradiated at 350 nm for 45 min to crosslink the benzophenone probe to nearby proteins. The samples were then ultracentrifuged at 90,000 ×*g* and the pellets were resuspended with 200 μL PBS buffer by homogenization with the TissueLyser at 25 rps for 2 min (Qiagen). Proteins were labeled with biotin by using Cu2+ catalyzed azide alkyne cycloaddition (CuAAC) click chemistry with 1 mM CuSO4, 1 mM TCEP, 0.1 mM TBTA, 100 μM biotin-azide, in PBS with 5% t-butanol, 2% DMSO, and shaking for 1 hr at 25 °C. The samples were then ultracentrifuged at 90,000 ×*g* to remove click chemistry reagents and the pellets were

again resuspended by homogenization and solubilized in 500 μL of RIPA buffer (50 mM Tris pH 8, 150 mM NaCl, 0.1% SDS, 1% NP40, 0.5% deoxycholate), followed by centrifugation at 12,000 rpm to remove particulate matter. The supernatant was added to 20 μL of streptavidin ultralink resin slurry, and incubated overnight at 4 °C. The streptavidin resin was washed 3 times by centrifugation at 0.5 ×*g* with 500 μL of RIPA buffer and then washed an additional time with Tris-Buffered Saline with 0.1% Tween-20. Biotinylated proteins were eluted by heating with 30 μL of 2X SDS sample buffer for 10 min at 70 °C. Then 25 μL of the eluent was loaded on to an SDS- PAGE gel for protein band separation and then transferred to PVDF membrane and blotted for target proteins with indicated primary antibodies.

2.4 Direct labeling with tetrazine probes followed by western blot analysis

HeLa membrane (800ug) or ANPP membrane (100 to 300ug) was incubated with Rabe-Tz in PBS for 1 hour at 37°C while shaking. After incubation, copper free click reactions were initiated by adding trans-cyclooctene-biotin (16μM) to conjugate a biotin to labeled proteins for pull down. Click reactions were allowed to proceed for 1 hour at room temperature. Reactions were centrifuged at 90,000 x *g* for 40 min at 4°C. Supernatants were aspirated, thus removing excess click reagents. The pellets were resuspended by homogenization with a TissueLyser (Qiagen) at 25 rps for 2 min and solubilized in RIPA buffer (50 mM Tris (pH= 8), 150 mM NaCl, 0.1% SDS, 1% NP40, 0.5% deoxycholate) then centrifuged at 12,000 rpm to remove particulate matter. To show specificity, 50mM DTT was added to select samples and incubated for 5 minutes at RT. Streptavidin ultralink resin slurry (Pierce) was added to all

supernatants and incubated overnight at 4C. Streptavidin resins were washed 4 times by centrifugation at 0.5 x *g* followed by aspiration of supernatant and addition of 500µL RIPA buffer. Labeled proteins were eluted by incubation with excess biotin (2mM) in 2X Laemmli sample buffer (BioRad) at 70°C for 10min. Eluates were loaded onto a precast 4–20% Criterion™ Tris-HCl gel (BioRad) for protein separation, transferred to a PVDF membrane and blotted for target proteins with indicated primary antibodies.

2.5 Direct labeling with tetrazine probes followed by fluorescence gel-scanning

For labeling of gamma-secretase components benzimidazole probe, Rabe-Tz (1µM), was incubated with ANPP membrane (50ug) in PBS for 1h at 37°C in the presence or absence of 50mM DTT. Targeted proteins were labeled with tetramethyl rhodamine via spontaneous reaction of trans-cyclooctene-TAMRA (16uM) and the tetrazine present on Rabe-Tz for 1 hr at room temperature in the dark. Labeled proteins were centrifuged at 9,000 x *g* for 40 min at 4°C and the supernatant removed. Protein pellets were resuspended in 45µL PBS using the TissueLyser for 2min at 25rps, followed by the addition of 15µL 4x Laemmli Sample buffer (BioRad) which was solubilized for 5min at 15prs, then centrifuged at 13,000 rpm to remove particulate matter. Samples were heated for 10min at 70°C and then loaded onto an SDS-PAGE gel for band separation and scanned for fluorescent bands. The same gel was then immediately stained with Coomassie blue (BioRad) to compare the total amount of protein in each sample.

For labeling of recombinant substrates, Rabe-Tz (1μM) was incubated with either wild type or mutant substrate (1-5μM) in the presence and absence of 50mM DTT and brought to a total reaction volume of 20μL with buffer either PBS or glycine buffer. Targeted proteins were labeled with tetramethyl rhodamine via spontaneous reaction of trans-cyclooctene-TAMRA (16uM) and the tetrazine present on Rabe-Tz for 1 hr at room temperature in the dark. Dye-free Laemmli SDS sample buffer (6μL) was added to samples, mixed well, and heated for 10min at 70°C. Samples were loaded onto a 16% pre-cast Tricine gel for band separation and scanned for fluorescent bands. The same gel was later analyzed for total protein by using the Thermo SilverQuest silver staining kit.

CHAPTER 3:

Discovering Novel Gamma-Secretase Modulators- Development of One-Pot In Vitro *Gamma-Secretase Activity Assay*

3.1 Background

The pivotal role of gamma-secretase in both Alzheimer's Disease and cancer makes the enzyme an attractive drug target; however, a major obstacle of targeting GS to treat these diseases is the need for specific inhibitors that selectively target the cleavage of only one substrate[130, 167]. This is evident based on the failure of several GSIs in clinical trials for AD, which failed primarily due to cytotoxicity in the gastrointestinal tract and severe immunosuppression as a result of unwanted suppression of Notch signaling[168, 169], and possibly unknown side-effects on other gamma-secretase substrates. As such, there is a need to develop substrate specific inhibitors and modulators. To do so efficiently requires superior *in vitro* assays that can accurately detect the production of specific gamma-secretase cleavage products; for example, assays that can distinguish Aβ peptides of various lengths.

Production of Aβ peptides is commonly measured using enzyme-linked immunosorbent assays (ELISA)[170-172], western blot with cleavage site specific antibodies[173, 174], or mass-spectrometry[13, 82] while NICD production is most often studied using western blot[173, 175], RT-PCR of target genes[176] or reporter systems[177-180]. In addition to being indirect measures of gamma-secretase enzyme activity, these methods are often multi-step, labor intensive processes which are relatively low through-put. Other reported methodologies include

electrochemiluminescence based detection [64, 112, 127, 181] , homogeneous time-resolved fluorescence (HTFR)[182] and flow cytometry using xMAP [183], but these are much less common.

Our lab has developed a superior *in vitro* gamma-secretase assay utilizing AlphaLISA technology to detect the generation of specific gamma-secretase products [142, 166, 184]. This assay uses cleavage site specific antibodies in conjunction with FRET based donor and acceptor beads. When the beads are brought into close proximity to one another, via interaction with either the cleavage site antibody or a recombinant biotin tag, excitation at 680nm can be used to transfer a singlet oxygen from donor to acceptor bead generating a luminescent signal (615nm) which can be measured and quantified (Figure 3.1A). This assay system is less time consuming than other available methods, easy to automate [185], and relatively inexpensive.

However, in its current state, cleavage of each substrate is assayed individually using a "two-pot" format (Figure 3.1B). This requires additional time and reagents than if production of each species is assayed simultaneously. Using the two-pot assay as a platform, we have developed a "one-pot" assay that can be used to detect the products of both APP and Notch cleavage simultaneously (Figure 3.2B). Rather than separately incubating substrates with gamma-secretase containing membranes, recombinant Notch (rNotch) and recombinant APP (rAPP) are incubated in the same reaction vessel, followed by sample separation for product detection. Not only does this assay save time and reagents, but it also allows for evaluation of therapeutic

candidates in an environment more similar to *in vivo*, where multiple substrates are present, allowing for more accurate calculation of selectivity margins.

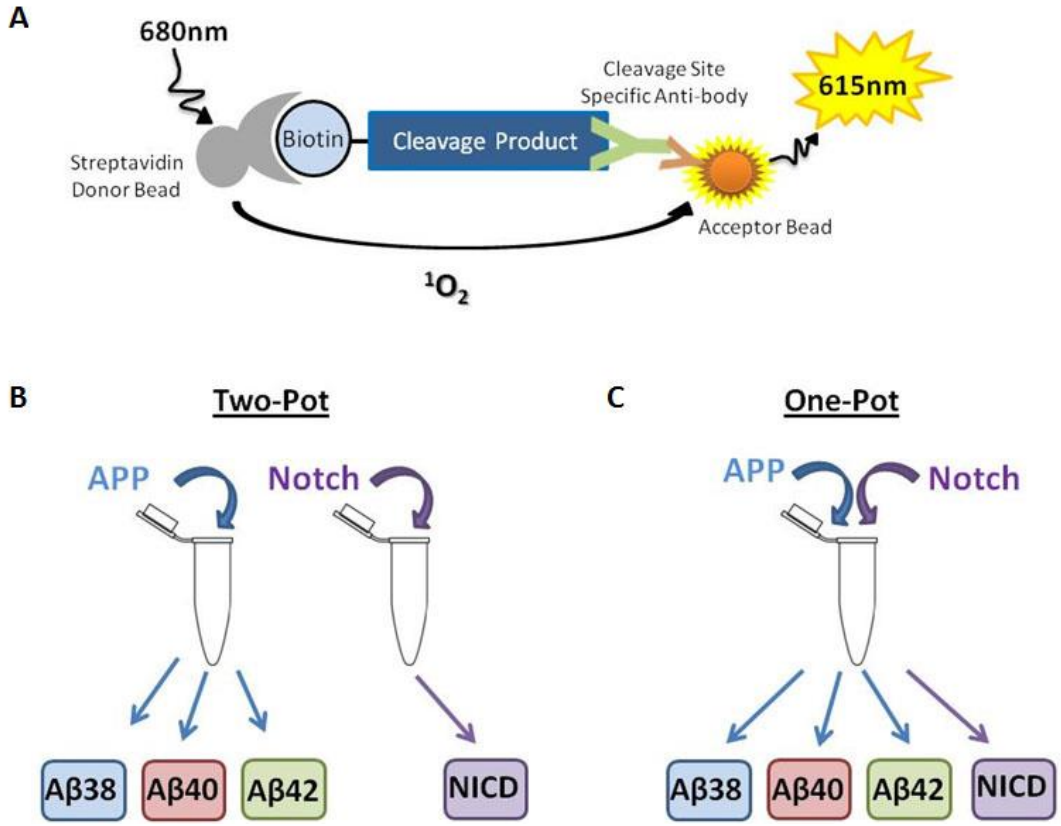

Figure 3.1: Schematic of *In Vitro* Gamma-secretase activity assay. A) Schematic representation of AlphaLISA detection technology. Protein-A acceptor beads bind to cleavage site specific anti-bodies while streptavidin donor beads bind biotin at the opposite terminus of the protein. When the two beads are in close proximity, AlphaLISA signal is generated by excitation of the donor beads at 680nm, transfer of singlet oxygen to the acceptor bead and subsequent emission at 615nm. **B)**. In the traditional "two-pot" AlphaLISA assay, each substrate is incubated with gamma-secretase individually, then reactions are split for detection of individual products. **C)** In the "one-pot" AlphaLISA assay both APP and Notch are incubated with gamma-secretase in the same reaction vessel.

A cell-based method for detecting APP and Notch cleavage simultaneously has recently been reported, termed the "dual substrate assay", and has already

illustrated an over-estimation of selectivity margins as a result of testing compounds for activity against APP and Notch processing separately[186]. They have demonstrated in several instances that selectivity was drastically reduced or completely eliminated when both substrates are present, providing a plausible explanation for why GSI's and GSM's have not been successful in the clinic to date. While cell-based assays are invaluable for testing if compounds have physiological activity, *in vitro* assays provide a faster means to screen a large number of compounds. Here, we have developed and implemented a one-pot *in vitro* assay for measuring gamma-secretase cleavage of Notch and APP simultaneously.

3.2 Results

One-Pot Assay Optimization

We first wanted to optimize the conditions for our one-pot assay to maximize signal and reduce background. To determine the optimal amount of CHAPSO-solubilized GS to be added to the *in vitro* reaction, the amount of GS containing HeLa membrane was titrated and enzyme activity was assayed using the one-pot activity assay format. Figure 3.2A shows a concentration dependent increase in the generation of each product up to 120μg/mL. Next, we varied the length of time the enzyme is incubated with recombinant substrates between 2 and 4 hours. At the end of each time point an aliquot of the reaction volume was removed and stored at 4C. After the last time point, detection reagents were added to all samples and product generation was quantified the next day and plotted as seen in Figure 3.2B. Gamma-secretase cleavage of both substrates and at each position in rAPP increased over time up to 4 hours.

Lastly, the amount of streptavidin donor beads (SAD) added to the detection mix was varied between 10 and 40µg/mL (Figure 3.2C). In order to remain in the dynamic, linear range of detection, 80µg HeLa membrane was incubated with recombinant substrates for 3 hours for all subsequent experiments. For the detection of Aβ products, 20µg/mL SAD was used and for the detection of NICD 10µg/mL SAD was used.

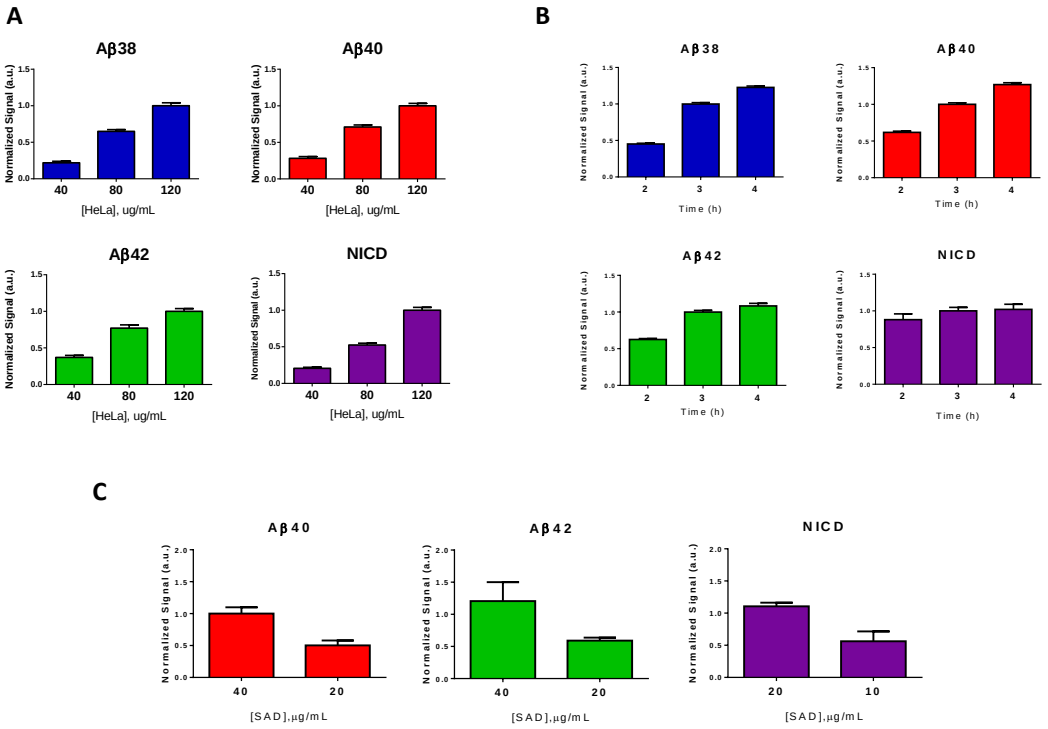

Figure 3.2: One-pot assay optimization. A) The amount of solubilized gamma-secretase added to the assay was titrated by adding various concentrations of HeLa membrane to each reaction. **B)** The time of the reaction was varied from 2 to 4 hours. **C)** The concentration of streptavidin donor beads (SAD) was titrated in the detection reaction. The final parameters for subsequent experiments were chosen to be 80ug/mL HeLa for each reaction, incubated for 3 hours using 40ug/mL streptavidin donor beads for detection of Aβ products and 20ug/mL for detection of NICD. Data shown are means +/- SEM (n=3).

Substrate Characterization

While the topic of competition between endogenous APP and Notch for cleavage by gamma-secretase has been explored previously, results have been controversial [41, 187]. It was important for us to determine if our recombinant substrates compete for cleavage by gamma-secretase in our assay. To explore this issue, we titrated the amount of one recombinant substrate, while keeping the concentration of the other constant. Both substrates were expressed without the addition of biotin and the non-biotinylated proteins were used as the variable substrate, so as to isolate the effects of enzyme competition without any interference based on competition for donor beads. Previous work by Svedruzic et al. using a similar in vitro system has shown that the presence of a recombinant Notch construct, NotchΔE, can have either activating or inhibitory effects on AICD production depending on the concentration used[188]. Reminiscent of that, we observe a slight initial increase in gamma-secretase activity for all products other than Aβ42 at the lowest concentrations of alternate substrate, followed by a dose dependent decrease in activity at higher concentrations (Figure 3.3A).

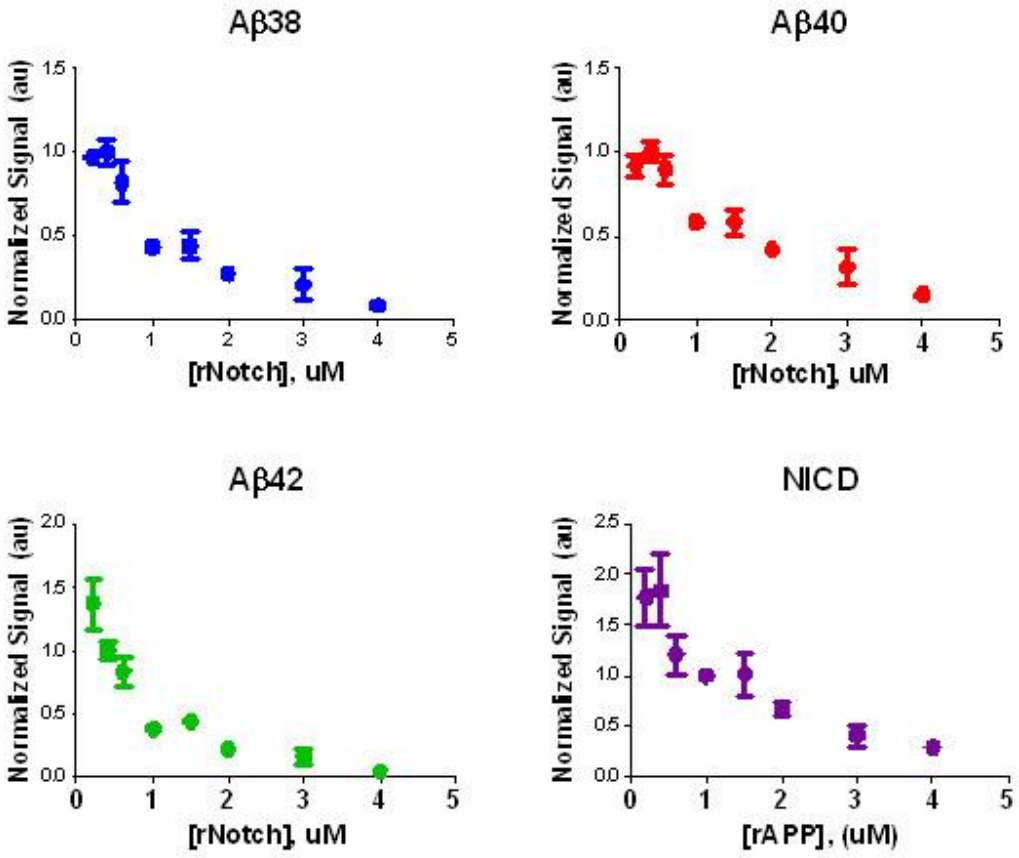

Figure 3.3: rNotch and rAPP compete for cleavage by gamma-secretase. Competition was assayed by titrating the concentration of one non-biotinylated substrate while keeping the concentration of the other biotinylated substrate constant and assaying for the cleavage of that substrate. For NICD detection the concentration of rAPP was kept at 1μM. For Aβ detection the concentration of rNotch was 0.4μM

Several lines of evidence suggest the existence of a substrate docking site that is physically distinct from the active site and that gamma-secretase can bind and cleave multiple substrates per one catalytic turn over[67, 68, 189]. According to this model, the two substrates compete for cleavage only at sufficiently high concentrations (Figure 3.4).

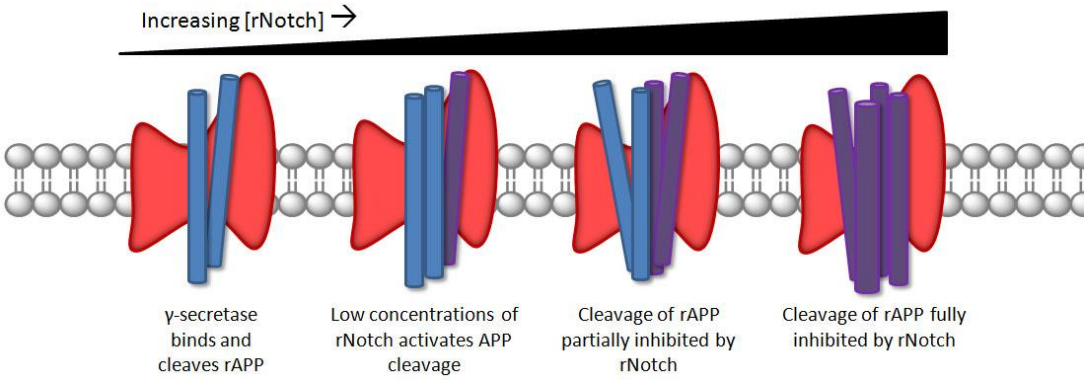

Figure 3.4: Model of substrate competition for cleavage by gamma-secretase. (*Adapted from Svedruzic et. al. PLoS One. 2012.*

In support of this model, kinetic analysis showed an approximate two-fold increase in K_m for the one-pot assay compared to individual assays, but little to no change in V_{max} or K_{cat} for all products, indicating that the addition of the alternate substrate affects binding, but does not affect catalytic efficiency.

Table 3.1: Summary of calculated kinetic parameters of one-pot assay.

	Aβ38			Aβ40			Aβ42			NICD		
	V_{max} (nM min^{-1})	K_m (μM)	K_{cat}	V_{max} (nM min^{-1})	K_m (μM)	K_{cat}	V_{max} (nM min^{-1})	K_m (μM)	K_{cat}	V_{max} (nM min^{-1})	K_m (μM)	K_{cat}
One-Pot	2.45 ± 0.16	1.64 ± 0.22	0.03 ± 0.002	1.48 ± 0.12	0.59 ± 0.13	0.02 ± 0.002	1.40± 0.12	0.78± 0.16	0.02 ± 0.001	1.36 ± 0.08	0.17 ± 0.03	0.02± 0.001
Control	2.72 ± 0.20	2.18 ± 0.29	0.03 ± 0.003	1.50 ± 0.14	1.10 ± 0.22	0.02 ± 0.002	1.32± 0.21	1.84± 0.55	0.02 ± 0.002	1.37 ± 0.17	0.45 ± 0.13	0.02± 0.002

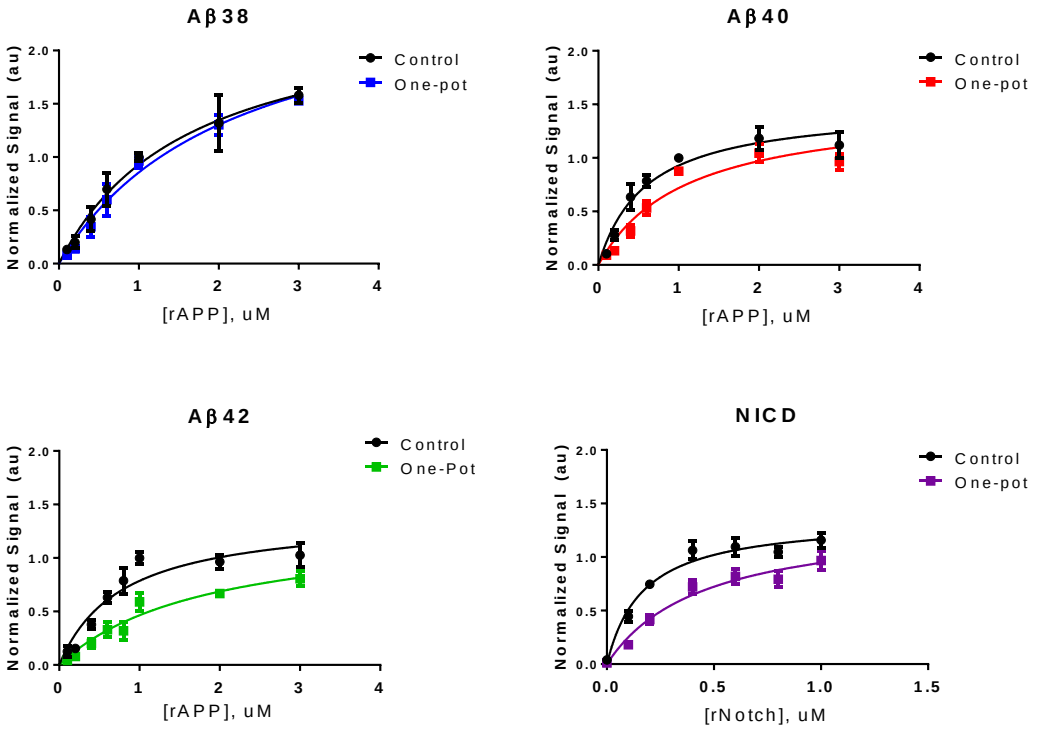

Figure 3.5: Kinetic analysis of substrate cleavage in the one-pot assay was performed by titrating the concentration of one substrate while keeping the concentration of the other constant and assaying for the cleavage of the substrate being titrated. The kinetic parameters K_m and V_{max} were calculated using a non-linear curve fit with the Michaelis-Menten equation and compared between the one-pot assay with both substrates present and a control assay with only the substrate being assayed for cleavage present. ($N \geq 8$).

One-Pot AlphaLISA Assay Can Be Used to Screen GSMs and GSIs

One of the most useful applications of our one-pot assay is in screening for novel gamma-secretase modulators and/or Notch-selective inhibitors. For "proof-of-concept" we aimed to show that our assay could be used to screen the activity of numerous compounds against each gamma-secretase product simultaneously in a quick and efficient manner. Using one 384-well opti-plate our one-pot assay was

prepared with 11 test compounds, plus vehicle for a positive control, and we assayed for the modulation of Aβ38, Aβ40, Aβ42 and NICD production simultaneously. As seen in Figure 3.6, one can generate a heat map of one-pot assay results to quickly screen for compounds with unique modulatory activity. At 1μM compound, the four GSI's tested (JC2, L458, JC34 and GSI-139) were all shown to have equal potency for inhibition of all products, while gamma-secretase modulators from various classes such as NGP-555, E2012, GSM-067, GSM-1, and GSM 616 selectively inhibit Aβ42 production while increasing Aβ38 and having little effect on NICD, and the inverse GSM, iGSM-893, has the opposite effect, drastically increasing Aβ42 production. Not surprisingly, the reported "Notch-sparing" inhibitor BMS708-163, was found to have no selectivity towards any of the gamma-secretase products supporting previously reported data from our lab [123].

Figure 3.6: Using the one-pot AlphaLISA assay to screen numerous compounds simultaneously. Each compound was tested at 1μM for gamma-secretase modulating activity and the results were graphed as a heat map based on percent activity remaining as compared to vehicle (DMSO).

Testing GSI and GSM IC_{50} in the One-Pot Assay

Previous work has shown that the concentration of the APP substrate, as well as the presence of the Notch substrate in a cellular assay are sufficient to shift IC_{50} values for several GSM's[186, 190]. We directly compared IC_{50} calculations between the one-pot assay and a two-pot assay control for compounds representative of several chemotypes.

L-685,458 (L458) is a peptide based, transition-state mimic, which directly targets the active site to halt cleavage of all substrates with equal potency[191]. No significant difference was observed in the IC_{50} between the one-pot and two-pot assay (Figure 3.7), consistent with findings in the equivalent cellular dual substrate assay [186].

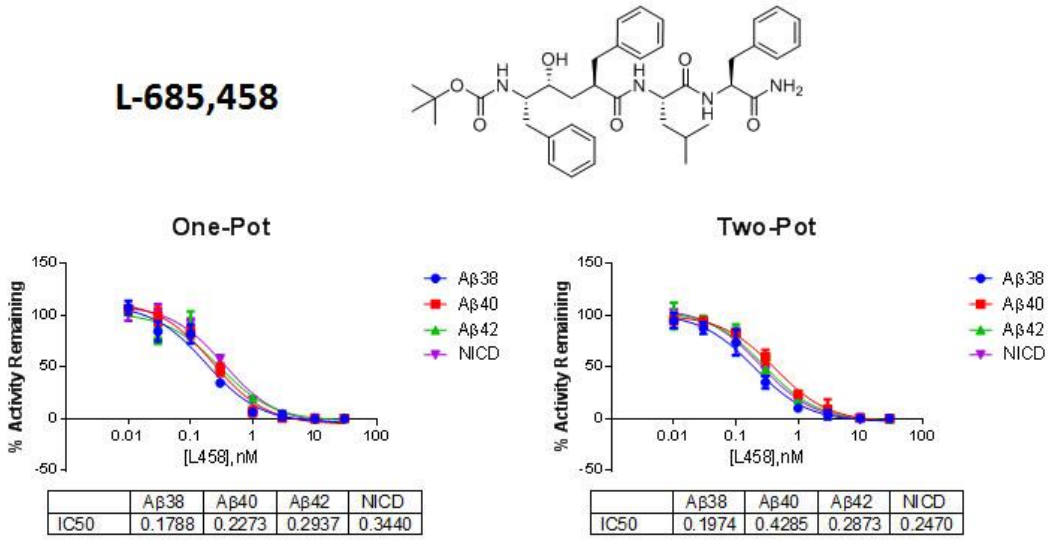

	Aβ38	Aβ40	Aβ42	NICD
IC50	0.1788	0.2273	0.2937	0.3440

	Aβ38	Aβ40	Aβ42	NICD
IC50	0.1974	0.4285	0.2873	0.2470

Figure 3.7: Chemical structure of L-685,458 and one-pot vs. two-pot IC_{50} curves. IC_{50} values are reported in nM.

Semagacestat (LY-450139) has been studied in numerous clinical trials testing multiple dosing regiments with little success due to unwanted toxicity [148, 192]. This is not surprising as Chavez et al. reported the compound to preferentially inhibit cleavage of Notch to produce NICD over the cleavage of APP to generate AICD, however, reported selectivity margins for this compound vary widely[122, 186, 192]. Similarly, we observe selectivity for NICD inhibition over Aβ peptides in our two-pot AlphaLISA assay (Figure 3.8). However, when we test this compound in our one-pot assay, we see a drop in selectivity from 0.16 fold to 1.3 fold, consistent with results reported by McKee et al. where they report 0.6 selectivity in their cellular, dual substrate system[186]. It appears that the inconsistency in selectivity margins reported for this compound could be due not only to differences in assay systems, but also to the presence and local concentration of additional substrates.

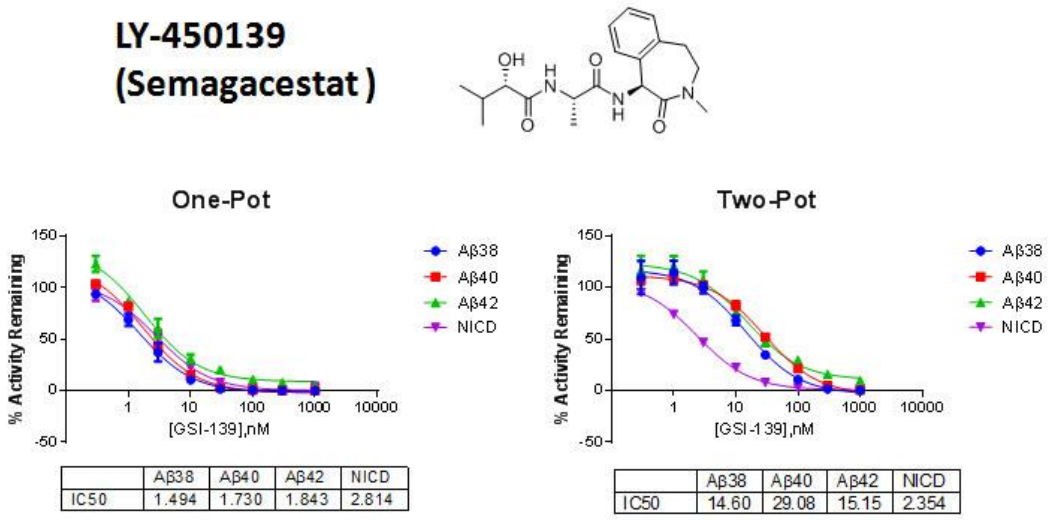

Figure 3.8: Chemical structure of LY-450139 and one-pot vs. two-pot IC_{50} curves. IC_{50} values are reported in nM.

In an effort to overcome the challenges faced with using traditional GSI's in the clinic, two classes of gamma-secretase modulators (GSMs) have evolved. The first are NSAID derived, acid GSMs, typified by GSM-1 which has been reported to be more than 30 times selective for inhibiting Aβ42 production over Notch cleavage[145]. In our two-pot assay we observe 210 fold selectivity, however in the one-pot assay, we see a drastic drop in selectivity to only 54-fold, as well as a drop in selectivity for Aβ42 over Aβ40 (from ≈8x to ≈4x) and Aβ42 over Notch (from ≈400x to ≈40x), verifying previously reported shifts in IC_{50} values at higher concentration of substrate. The loss in selectivity is not due to a decrease in potency for Aβ42 inhibition, but rather a result of increased potency in inhibiting the other production of the other species (Figure 3.9). Interestingly, this trend was not observed with the structurally distinct imidazole compound, GSM-25, where we saw little difference between the one-pot and two-pot assay (Figure 3.10), but was repeatable when tested with un-biotinylated substrates (data not shown). It has been previously shown that GSM-1 has a binding site that is distinct from the binding site for imidazole GSMs [117, 147], which could explain why we do not see this phenomenon with GSM-25.

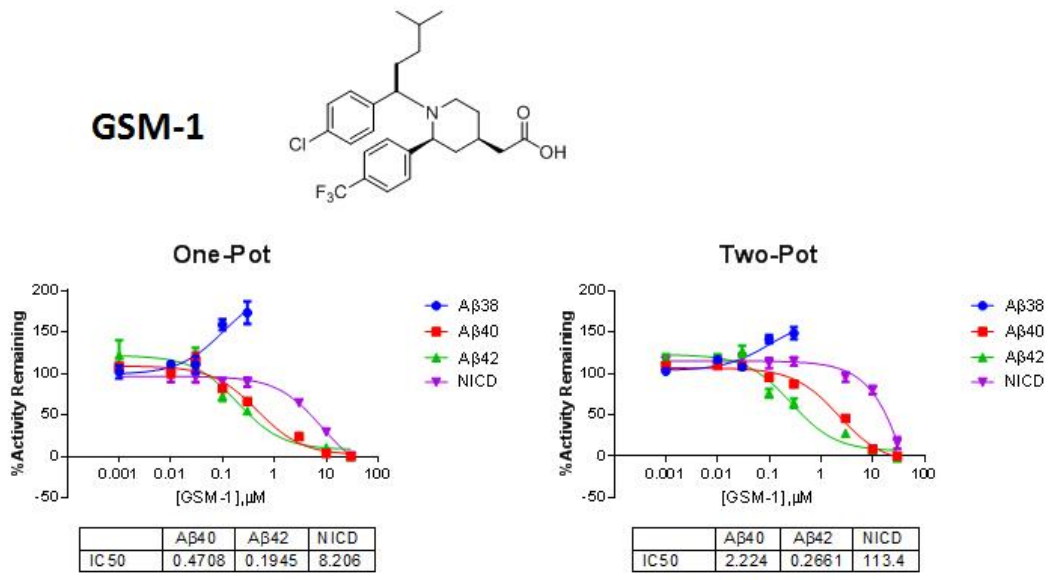

Figure 3.9: Chemical structure of GSM-1 and one-pot vs. two-pot IC_{50} curves. IC_{50} values are reported in µM.

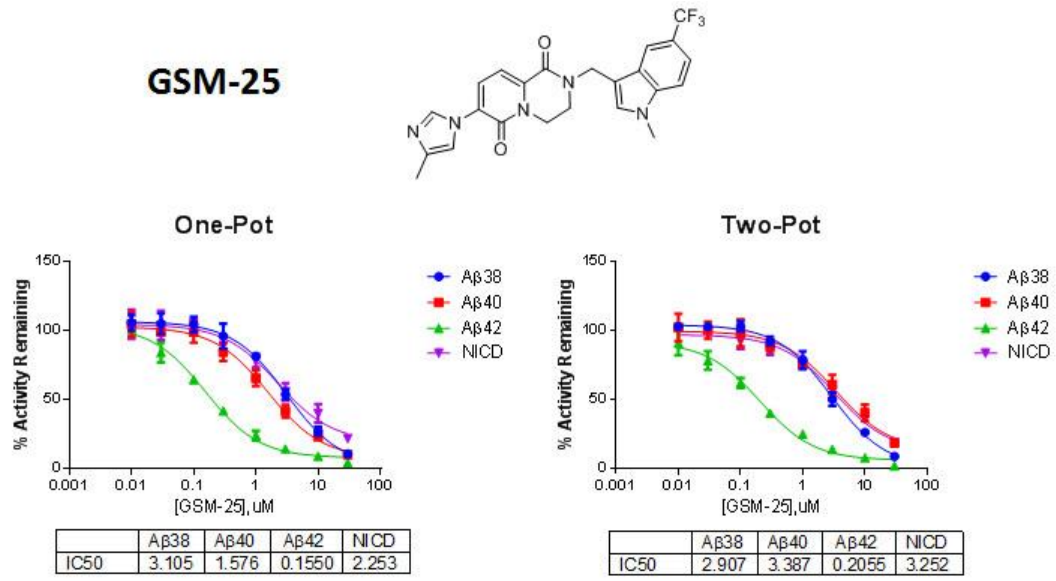

Figure 3.10: Chemical structure of GSM-25 and one-pot vs. two-pot IC_{50} curves. IC_{50} values are reported in µM.

Consistent with previous reports from our lab and others, we found that the supposed "Notch-Sparing" compound**,** BMS-708,163, has a mere two-fold selectivity for Aβ42 over Aβ40 or Notch when tested in our traditional assay [123], and the small window of selectivity is completely abolished when tested in our one-pot assay (Figure 3.11).

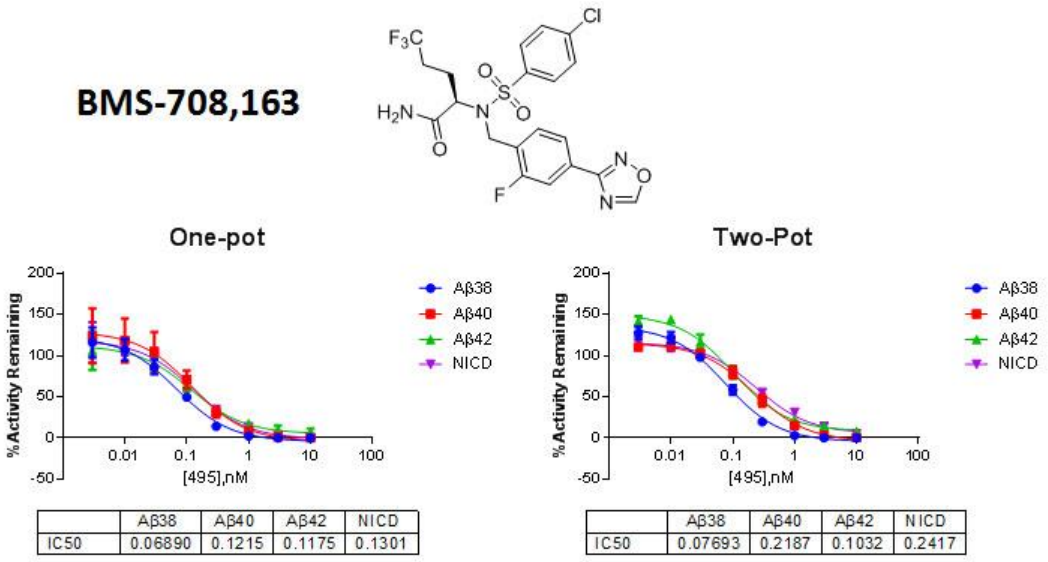

	Aβ38	Aβ40	Aβ42	NICD
IC50	0.06890	0.1215	0.1175	0.1301

	Aβ38	Aβ40	Aβ42	NICD
IC50	0.07693	0.2187	0.1032	0.2417

Figure 3.11: Chemical structure of BMS-708,163 and one-pot vs. two-pot IC_{50} curves. IC_{50} values are reported in nM.

3.3 Discussion and Conclusions

Gamma-secretase is a prime target for therapeutic intervention in both Alzheimer's disease and cancer. However, because gamma-secretase has numerous substrates, there is a need for compounds that selectively inhibit the cleavage of one substrate over the other in order to minimize unwanted side-effects. We have developed an *in vitro* "one-pot" gamma-secretase activity assay that can be used to

measure the production of several Aβ species and NICD simultaneously, and provides an ideal platform for drug discovery. We have optimized the concentrations of each component in the reaction in order to maximize signal strength and reduce background noise. We have evidence for direct competition between the rNotch and rAPP substrates for cleavage by GS in our assay, but have used analysis of enzyme kinetics to demonstrate that while the additional substrate may affect binding or docking, it does not affect catalytic turnover.

As evident by the discrepancies we've observed in IC_{50} values between the one-pot and two-pot assays and with the failure of Semagacestat in clinical trials, it is clear that having accurate and efficient assays to determine potency and selectivity margins between APP and Notch is vital to the success of using GSIs or GSMs to treat patients in the clinic. Furthermore, maintaining the production of Aβ40 may be equally as important as maintaining Notch signaling [126], so the ability to simultaneously detect multiple Aβ species is also imperative. Use of the one-pot *in vitro* assay has the potential to save not only time and money, but could also prevent patients in clinical trials from experiencing unnecessary harm.

On a small scale, we have shown the utility of the one-pot assay to screen for drug candidates with ideal modulatory profiles. We are particularly interested in further developing the assay to be used in high-throughput screens, similar to our recent report on a Notch HTS assay [185], but believe that the one-pot assay has countless applications for investigation of gamma-secretase.

CHAPTER 4:

Benzimidazoles are Novel Gamma-Secretase Modulators

4.1 Background

Gamma-secretase is a prime therapeutic target for both AD and cancer, but it is clear that using gamma-secretase modulators will be necessary to overcome unwanted side effects that are a result of the wide array of gamma-secretase substrates present in each cell. While extensive research has been done to develop gamma-secretase modulators for treatment of Alzheimer's disease, the pursuit of Notch-specific gamma-secretase inhibitors has been lacking. The compound LY-450,139, originally intended to be used for AD treatment but found to be Notch-selective [122], demonstrates the existence of such compounds but has not been used for this purpose. There are currently no other Notch-selective compounds reported. Although the threshold of toxicity may be higher for potential cancer therapeutics, this may not be necessary if Notch-selective inhibitors can be discovered, optimized and utilized on Notch addicted cancers.

The traditional *in vitro* gamma-secretase activity assay commonly utilized in our lab [166] has been developed into a 384-well and 1536-well microtiter plate format that can be used as a high-throughput screen for novel gamma-secretase inhibitors and modulators [185]. During validation of this assay, several proton-pump inhibitors such as Lansoprazole, Omeprazole and Rabeprazole (Figure 4.1) were identified to specifically inhibit NICD over Aβ40 production and found to have IC_{50}

values for Notch inhibition of 3μM, 2.5μM, and 1μM respectively. Additionally, they cause a modest increase in Aβ production, most potently Aβ42.

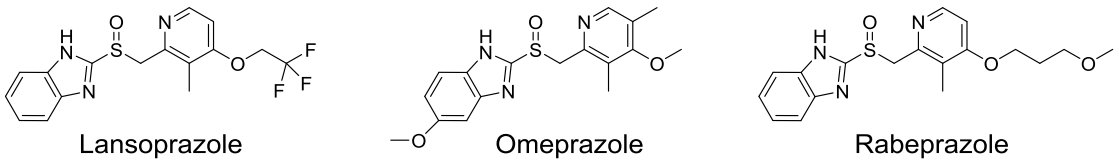

Figure 4.1: Chemical structures of proton pump inhibitors identified in HTS for Notch-selective inhibitors of gamma-secretase

Proton pump inhibitors (PPIs) are substituted 2-pyridylmethylsulfinyl benzimidazole compounds that require acid activation before binding to their intended molecular target, the proton pump, or gastric H+/K+-ATPase. PPIs are administered orally, and remain relatively inert until they reach the acidic environment of the parietal cell where they are protonated, undergo spontaneous rearrangement to active sulfenamide and sulfenic acid derivatives, and react with accessible cysteine residues in the proton pump to form a disulfide bond, irreversibly inactivating the enzyme[193, 194] (Figure 4.2). Extensive research has verified this mechanism and shown that PPIs can react with several cysteine residues in the proton pump, but binding of any benzimidazole to Cys- 813 is sufficient to inhibit ATPase activity [195]. Benzimidazoles with high reactivity and activation rates, such as lansoprazole and omeprazole, generally bind Cys-813 exclusively, while slowly activated benzimidazoles such as pantoprazole are able to reach and inactivate less accessible cysteines as well [196].

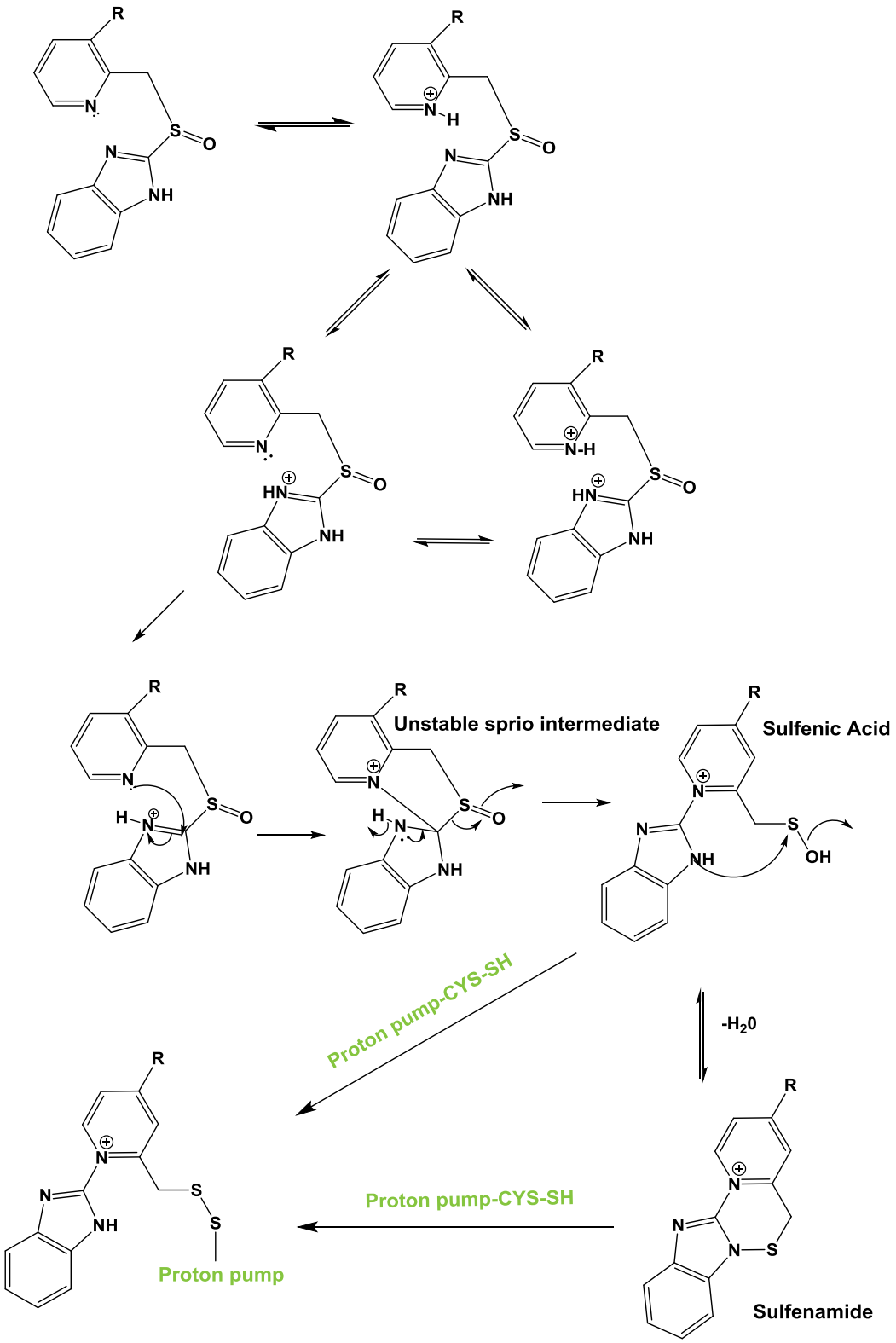

Figure 4.2: Activation of substituted benzimidazoles under acidic conditions to react with cysteine residues in the gastric proton pump.

Based on the known mechanism of action of PPIs and the proton pump, we hypothesized that benzimidazole compounds share a similar mechanism of action in inhibiting gamma-secretase cleavage of Notch. In this study, we show several lines of evidence suggesting that benzimidazoles do in fact undergo a similar activation reaction and form a disulfide bond with a cysteine residue near the scissile bond of the Notch substrate, as well as bind to cysteines in NTF, CTF, and PEN-2. These results represent a novel mechanism of action for gamma-secretase modulation and while selective inhibition of NICD is promising as a cancer treatment strategy, the potential for benzimidazoles is dampened by the observed increase in Aβ peptides. This data may shed light on recent findings that PPIs may not be as safe as originally assumed and should be taken into consideration before administering PPIs to patients.

4.2 Results

The Effect of Benzimidazole Treatment on Gamma-Secretase Activity in Biochemical and Cell-Based Assays

Figure 4.3A shows a prototypical benzimidazole compounds and the effect on *in vitro* gamma-secretase activity in our one-pot assay (Figure 4.3B). The IC_{50} for Notch cleavage is just under 1μM and we observe a slight increase in the production of Aβ peptides, most pronounced for Aβ42. HEK293 cells stably expressing the NΔE Notch construct (which lacks the extra-cellular domain and does not require ligand binding for signaling) were treated with vehicle, GSI, or benzimidazole compound for 24 hours, lysed and NICD levels were assayed using our AlphaLISA activity assay.

HEK293 cells stably overexpressing APP were treated similarly and Meso Scale Discovery (MSD) Aβ peptide kit was used to measure Aβ production in the media. Similar to our *in vitro* data, we observe a dose-dependent increase in Aβ peptides and a dose-dependent decrease in NICD (Figure 4.3D). Interestingly, Lansoprazole and Omeprazole have been previously reported to enhance amyloid beta production in cell models and transgenic mice [197], but researchers did not postulate on the mechanism of action.

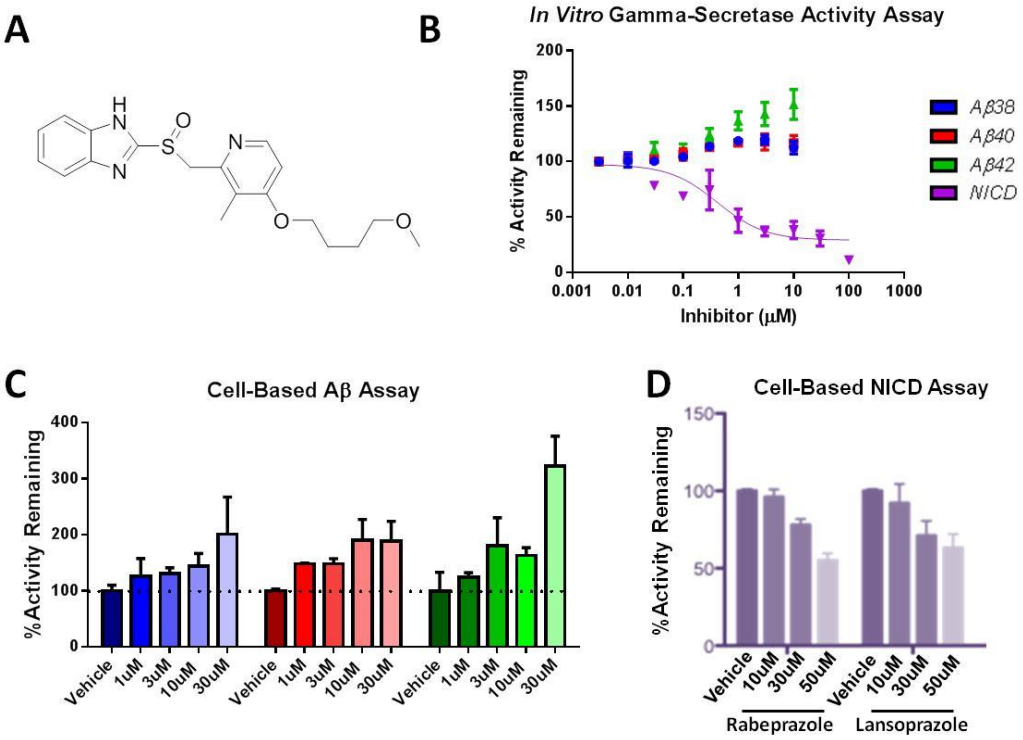

Figure 4.3: Benzimidazole compounds inhibit NICD production and increase Aβ peptides. A) Chemical structure of prototypical benzimidazole compound used in our studies**. B)** *In Vitro* , one-pot gamma-secretase activity assay shows IC50 for NICD production of less than 1uM and modest increase in Aβ production. **C)** Cell-based assay for Aβ detection demonstrates dose-dependent increases in each peptide with increasing concentrations of benzimidazole compound. **D)** Cell-based assay for NICD production shows dose-dependent decrease in NICD production with Rabeprazole and Lansoprazole treatment. *Cell-based NICD assay was performed by Dr. Deming Chau

Structure-Activity Relationship Analysis

Our working hypothesis is that benzimidazoles are modulating gamma-secretase through a mechanism similar to inhibition of the proton pump. The first step in benzimidazole activation is protonation of the nitrogen on the pyridine ring (Figure 4.2). Therefore, if these compounds are modulating gamma-secretase via a similar mechanism, removal of this nitrogen should impede inhibition of Notch cleavage. We have synthesized an analogue, PPI-benzene, and shown that it does not inhibit Notch cleavage (Figure 4.4B). Furthermore, the sulfoxide of PPIs rearranges to a sulfonamide during acid activation and analogues in which the sulfoxide moiety has been removed and replaced with either a sulfone or sulfoxide, also lose the ability to inhibit Notch cleavage (Figures 4.4C,D).

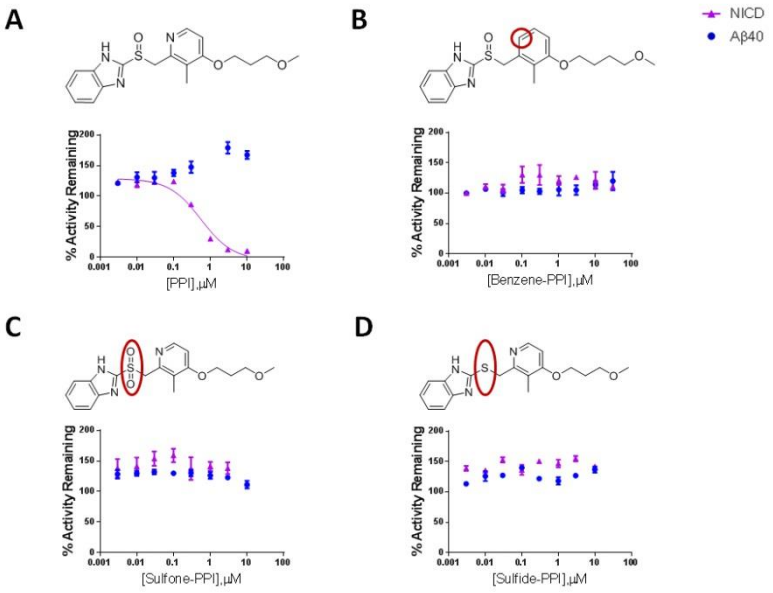

Figure 4.4: Structure activity relationship analysis A) The standard benzimidazole compound is a potent inhibitor of NICD production. **B)** Removal of the pyridine nitrogen abolishes inhibitory activity. Changing the sulfoxide moiety to a sulfone **C)** or sulfide **D)** also results in loss of NICD inhibition.

Reducing Agents Prevent Benzimidazole Inhibition of Notch Cleavage

Based on the above structure-activity relationship data, which suggests a similar mechanism of activation may be required for benzimidazole modulation of Gamma-Secretase activity, we next asked if disulfide bond formation was also involved. In order to test this, we added the reducing agent DTT to our Notch IC_{50} assay and found that this resulted in loss of Notch inhibition (Figure 4.5A). Conversely, addition of DTT to an IC_{50} assay for the transition state mimic, L458, does not have any effect on inhibition. The same results were observed with other reducing agents such as TCEP (data not shown).

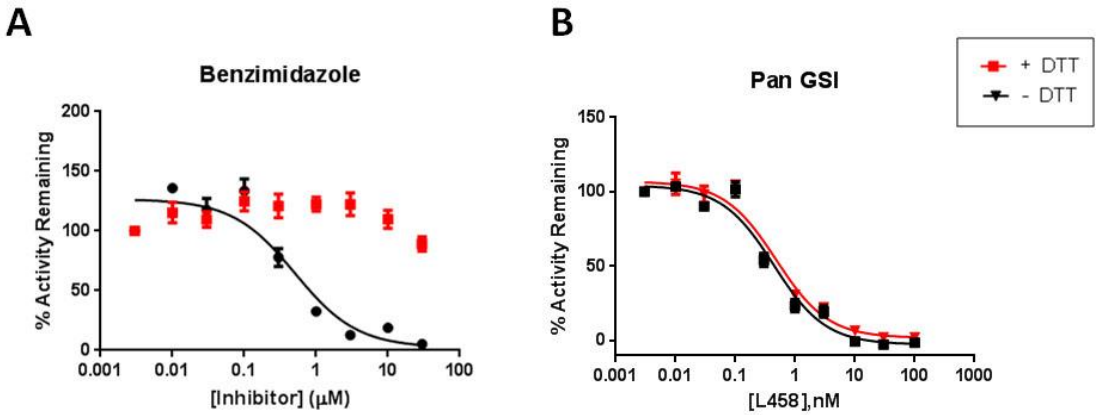

Figure 4.5: Reducing agents abolish benzimidazole inhibition of Notch cleavage. **A)** The effect of 50Mm DTT on NICD IC_{50} **B)** 50mM DTT has no effect on inhibition of gamma-secretase by a pan GSI, such as the transition state mimic, L458.

Enzyme Kinetics Demonstrate a Non-Competitive Mechanism of Action

To investigate where benzimidazoles are binding to modulate gamma-secretase, we first analyzed enzyme kinetics and found that Rabeprazole does not affect K_m for Notch cleavage, but lowers V_{max} (Figure 4.6A). Further double-

reciprocal plot shows intersection at the x-intercept, suggesting non-competitive inhibition through allosteric binding (Figure 4.6B). This means that substrate binding to enzyme and inhibitor binding to enzyme is not mutually exclusive, and it is the formation of the enzyme-substrate-inhibitor complex that is catalytically inactive.

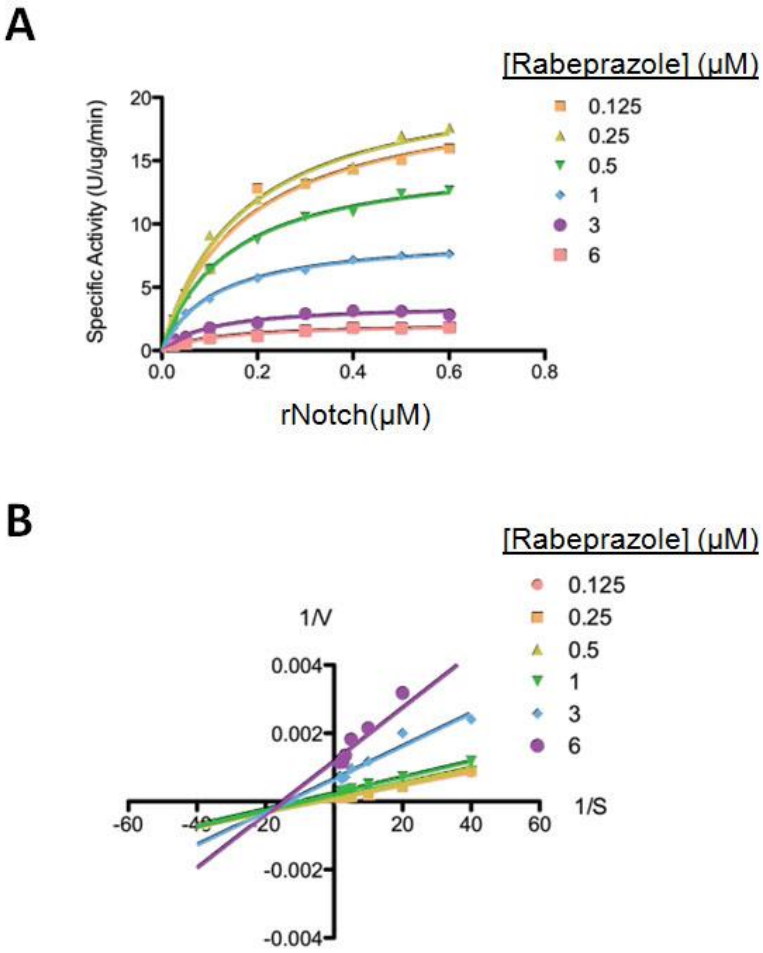

Figure 4.6: Rabeprazole is a non-competitive gamma-secretase inhibitor. A) Increasing concentrations of Rabeprazole results in decreased Vmax, but has no effect on Km. **B)** Double-reciprocal plot shows lines share the same x-intercept, suggesting Rabeprazole binds allosterically as a non-competitive inhibitor. *These experiments were performed by Dr. Deming Chau.

Mutation of Recombinant Substrates Suggests P2 Cysteine of Notch is Binding Site for Benzimidazole Compounds

There are five cysteines in presenilin, three in nicastrin, three in Aph-1, one in Pen-2, and seven in the recombinant Notch (rNotch) substrate used in our assays. There are no cysteine residues in the recombinant APP used. Therefore, benzimidazoles could be binding to gamma-secretase, or the Notch substrate, or both. Interestingly, one of the cysteine residues, Cys-1752 in Notch, is located just two residues away from the scissile bond, at the P2 position according to common protease nomenclature [198] (Figure 4.7). Furthermore, past studies in our lab have shown that substitution of this cysteine to other amino acids can result in changes to gamma-secretase processing and specificity [166]. Therefore, we hypothesized that benzimidazoles could be binding to the P2 cysteine of Notch resulting in inhibited cleavage by gamma-secretase.

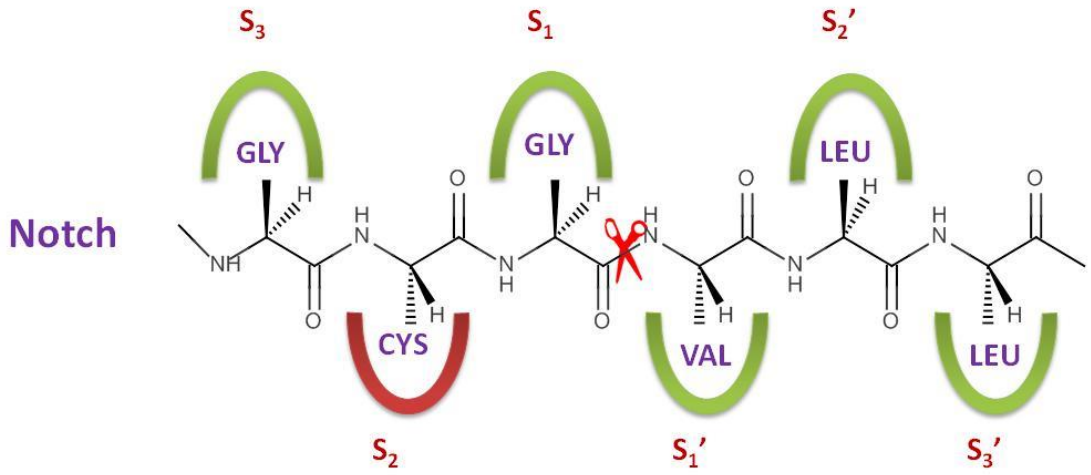

Figure 4.7: Schematic of the Notch substrate within the active site of gamma-secretase. According to Schechter and Berger nomenclature, residues to the right of the scissile bond are referred to as P1', P2', etc. and the corresponding enzyme subpockets S1', S2', etc. To the left of the cleavage site residues are designated P1, P2, etc. and enzyme subpockets S1, S2, etc.

In order to test our hypothesis, we generated a series of P2 rNotch mutants and tested them in an IC_{50} assay with a benzimidazole compound. Mutation of the P2 cysteine residue to any amino acid tested resulted in complete loss of gamma-secretase inhibition. Furthermore, if we re-introduce a cysteine at the P1 or P3 position on the P2 methionine rNotch mutant, we see nearly complete rescue of inhibition by benzimidazole. This data supports our hypothesis that benzimidazoles bind to the P2 cysteine of rNotch to inhibit gamma-secretase cleavage.

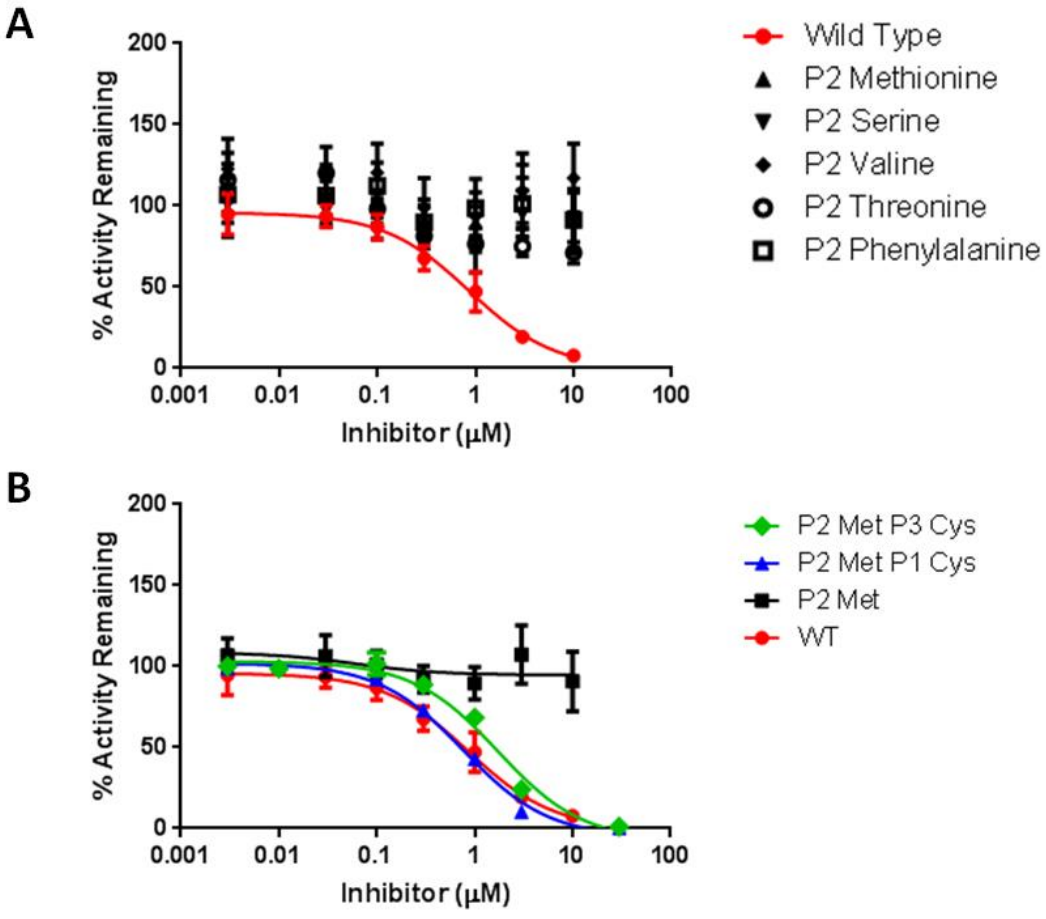

Figure 4.8: P2 cysteine of rNotch is vital for inhibition by benzimidazoles. **A)** Mutation of rNotch P2 cysteine to various amino acids results in loss of inhibition. **B)** Re-introduction of cysteine at P1 or P3 in P2 methionine mutant rescues inhibition by benzimidazoles.

Gamma-secretase cleaves APP at multiple positions within the transmembrane domain to release Aβ peptides of various lengths as well as the APP intracellular domain (AICD), which is synonymous to gamma-secretase cleavage of Notch to release NICD. APP contains a threonine residue at the P2 position, relative to AICD cleavage. Benzimidazole compounds do not inhibit the production of wild type AICD, however, mutation of P2 threonine to cysteine, results in benzimidazole inhibition of AICD production (Figure 4.9), further supporting our hypothesis that benzimidazole binding to the P2 position of the substrate is sufficient to inhibit cleavage.

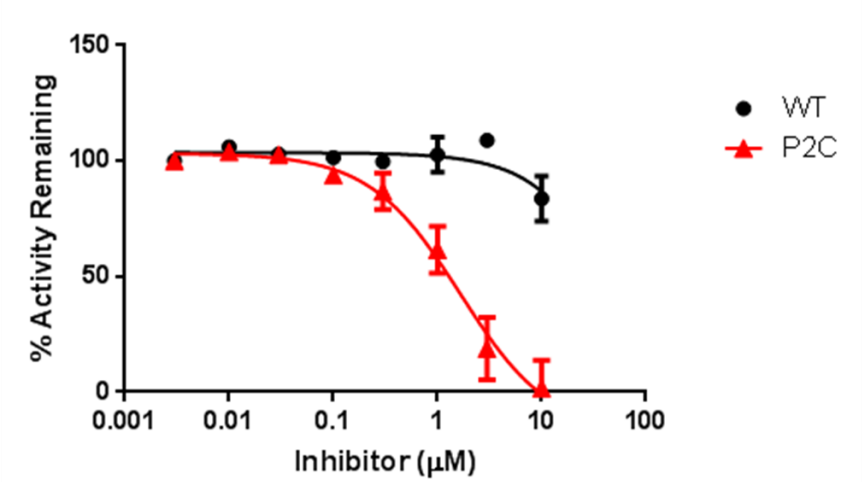

Figure 4.9: Production of AICD from mutant P2C APP is inhibited by benzimidazoles, while there is no effect on cleavage of WT APP.

Labeling with Benzimidazole Based Probes Demonstrates Binding to Gamma-Secretase on PS1-NTF, PSI-CTF and Pen-2

Evidence of benzimidazoles binding to the Notch substrate does not eliminate the possibility that these compounds are also binding to gamma-secretase. In order to explore this possibility, we first utilized photoaffinity labeling (PAL) with benzimidazole based benzophenone probes. PAL has previously been shown to be a useful method for target identification [199], and has proven to be a valuable tool for the study of GSIs and GSMs in the past [31, 116, 117, 200, 201]. PAL utilizes the addition of a photoreactive group, such as a benzophenone, into the compound of interest to covalently capture the targets of small molecules. Biotin is often incorporated into the photoreactive probe as a means to isolate the labeled target; however, use of such a large group can often impair the inhibitory activity of a compound by reducing potency or limiting access to the site of action. Clickable photoaffinity probes have the advantage of using a much smaller chemical group, such as a terminal alkyne, that can be "clicked" to another reactive group, such as biotin-azide, which facilitates enrichment with streptavidin (SAD) beads. A clickable, photoaffinity probe, PPI-BP, was designed based on the structure of Rabeprazole, has been synthesized and was shown to have similar activity and potency to that of the parent compound against NICD, Aβ40, and Aβ42 generation (Figure 4.10A,B). PPI-BP was incubated with gamma-secretase containing HeLa membranes in the presence and absence of the parent compound, then UV irradiated to cross-link to nearby proteins. Copper(I)-catalyzed Azide-Alkyne Cycloaddition (CuAAC), also called Azide-Alkyne Huisgen Cycloaddition, was utilized to click a biotin-azide group to the

probe, followed by capture with streptavidin beads and analysis by western blot using anti-bodies for each component of gamma-secretase. PS1-NTF was found to be robustly and specifically labeled by PPI-BP (Figure 4.10C). The other gamma-secretase components tested were not labeled, but this does not necessarily rule out the possibility that PPIs interact with these components, as PAL is highly dependent on the proper orientation of probe in relation to nearby residues.

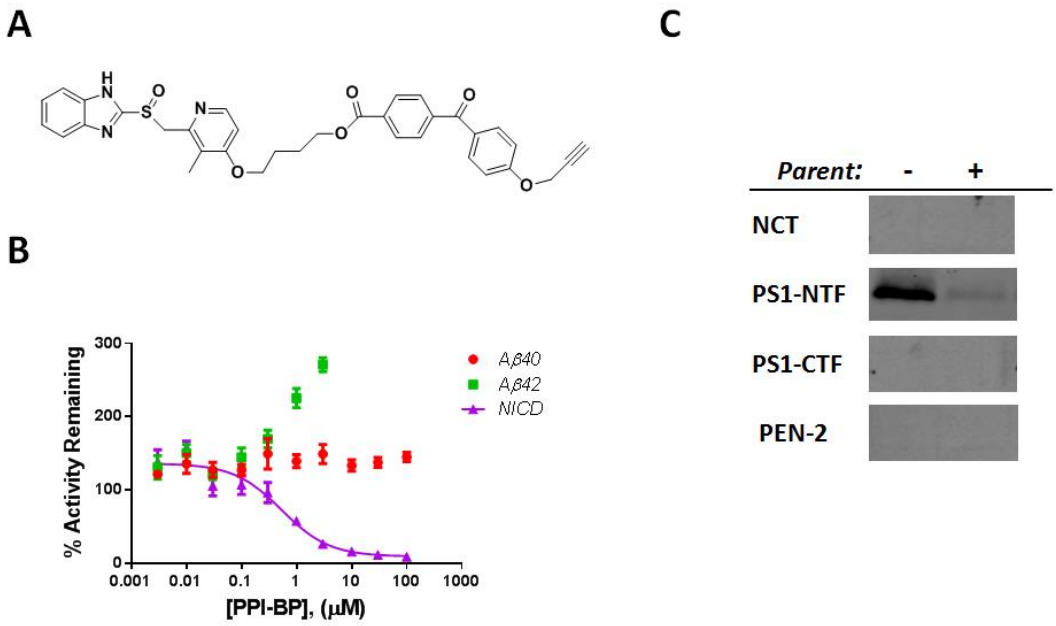

Figure 4.10: Photoaffinity labeling with PPI-BP shows specific labeling of PS1-NTF in HeLa membranes. A) Chemical structure of PPI-BP **B)** One-pot IC_{50} assay shows that PPI-BP potently inhibits NICD and increases production of Aβ42 **C)** Photoaffinity labeling with PPI-BP (1μM) shows specific labeling of PS1-NTF that is blockable with 25μM parent compound. Note: Levels of Aph-1 in HeLa membranes are not sufficient for detection by western blot

Because we believe that PPIs are binding their target via a disulfide bond, this represents a unique opportunity to use labeling techniques not available to compounds that non-covalently bind their target. It does, however, require the use of copper-free

click chemistry in order to maintain the bond between probe and target. We have synthesized a tetrazine probe, PPI-Tz, that is a potent gamma-secretase modulator and can be reacted with trans-cyclooctene conjugated to biotin or a reporter dye for target identification (Figure 4.11A,B). Additionally, rather than using HeLa membranes, we have utilized a HEK293 cell line that overexpresses each component of Gamma-Secretase, to ensure that insufficient protein levels are not an issue. ANPP membranes were incubated with PPI-Tz, and copper-free click chemistry was utilized to attach a biotin tag. A streptavidin resin was then used to enrich for labeled proteins, followed by western blot analysis using primary antibodies for each gamma-secretase component. Again, we observe specific labeling of PS1-NTF, in addition to labeling of PS1-CTF and Pen-2. Because DTT is used in this experiment for blocking, this also indicates that benzimidazoles are covalently binding gamma-secretase sub-units by disulfide linkage.

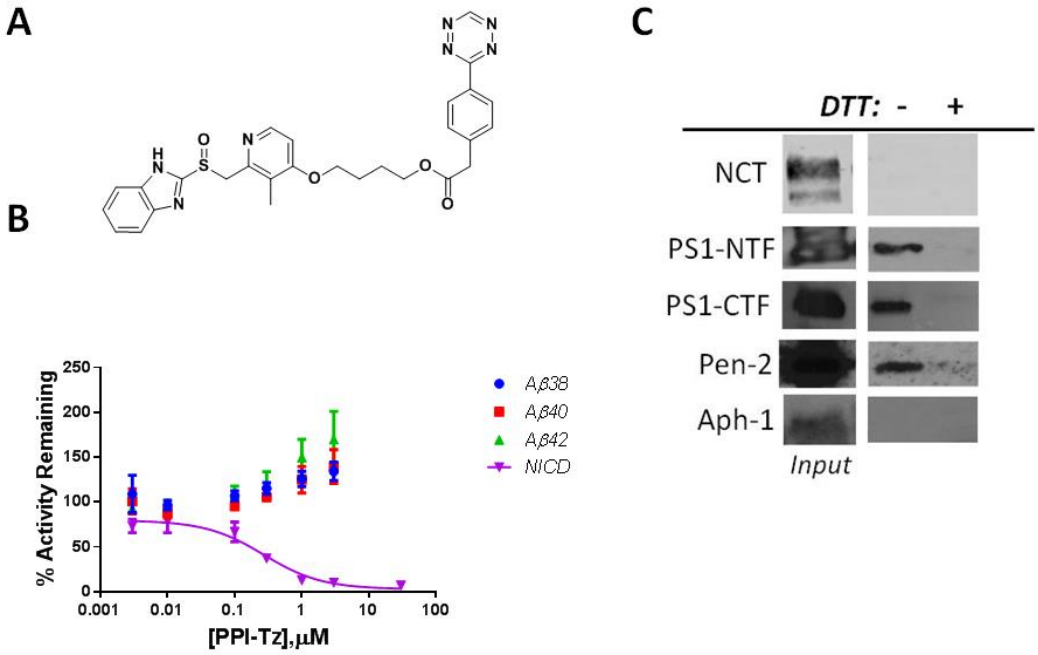

Figure 4.11: Benzimidazole based tetrazine probe specifically labels PS1-NTF, PS1-CTF and Pen-2. A) Chemical structure of PPI-Tz **B)** One-pot IC_{50} assay shows that PPI-Tz potently inhibits NICD and increases production of Aβ42 **C)** Direct labeling with PPI-Tz (1μM) demonstrates disulfide bond formation between benzimidazole probe and PS1-NTF, PS1-CTF and Pen-2, that is blockable with 50mM DTT. Input in the first lane is 5μg ANPP membrane.

Fluorescent Labeling Shows Benzimidazoles Bind to PS1-NTF, PS1-CTF, Pen-2, and rNotch substrate

To confirm these findings, we aimed to show specific labeling of gamma-secretase through an additional method, as well as show specific labeling of the recombinant Notch substrate. Copper free click chemistry between PPI-Tz and trans-cyclooctene-TAMRA was used to conjugate a fluorescent dye to benzimidazole targets in ANPP membranes. Consistent with the results of western blot analysis we see labeling of three proteins at approximately 30, 20, and 12 kDa, corresponding to PS1-NTF, PS1-CTF and Pen-2 respectively (Figure 4.12). Interestingly, the intensity

of fluorescent bands is increased with the addition of rNotch substrate, suggesting the formation of a stable enzyme-inhibitor-substrate triplex.

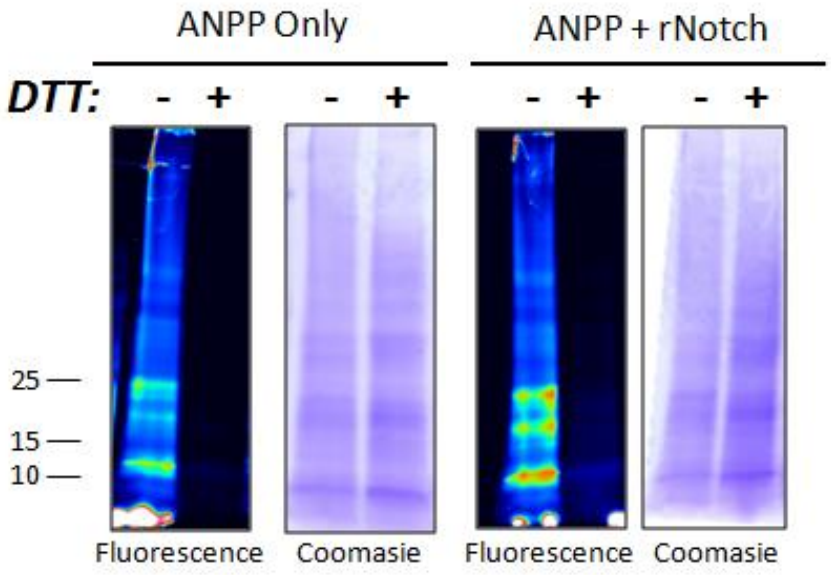

Figure 4.12: TAMRA labeling with PPI-Tz (1μM) probe shows molecular targets of approximately 25kDa, 20kDa, and 12kDa in ANPP membrane. The addition of 50mM DTT demonstrates specificity and Coomassie staining confirms equivalent amounts of protein loaded in each lane.

Furthermore, the rNotch substrate was robustly and specifically labeled, while the P2 methionine mutant was not (Figure 4.13). Additionally, no labeling was seen with the wild-type rAPP substrate, but was seen in the P2 cysteine rAPP mutant (Figure 4.13). This data coincides with our IC_{50} studies and further supports our hypothesis that the P2 cysteine of the Notch substrate is a binding site for benzimidazoles.

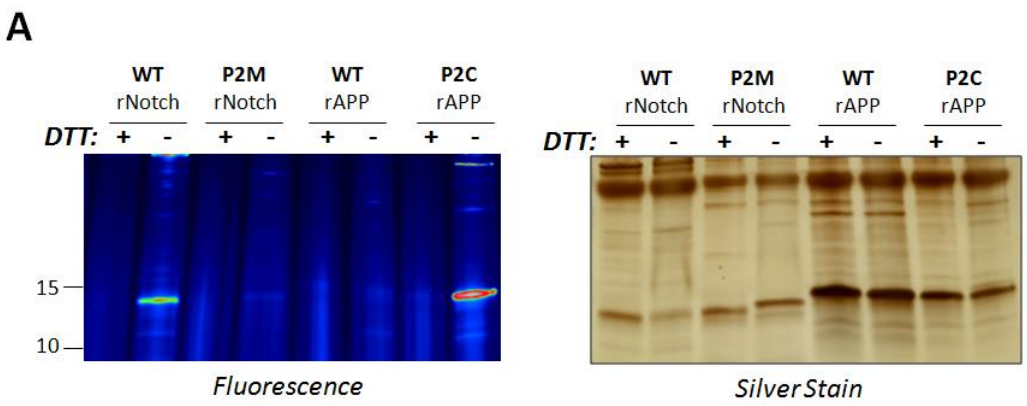

Figure 4.13: P2C in recombinant substrates is specifically labeled by PPI-Tz and TAMRA. A) Wild type rNotch is specifically labeled by PPI-Tz, while the P2 methionine mutant is not. Additionally, the mutant P2 cysteine rAPP is also specifically labeled. The addition of 50mM DTT shows specificity of labeling while silver stain for total protein confirms equivalent amounts of protein were added to each lane

4.3 Discussion and Conclusions

While all the data presented thus far provides strong evidence that benzimidazoles act through a similar mechanism to modulate gamma-secretase as they do inhibiting the proton pump, there is one important detail that must not be overlooked: all of our IC_{50} assays and labeling experiments are performed at an essentially neutral pH, so how are these compounds being activated to form disulfide bonds with gamma-secretase and rNotch? The pKa of the pyridine nitrogen is 4.53, and according to the Henderson-Hasslebach equation, at a pH near seven, less than 0.1% of benzimidazole molecules will be protonated. Additionally, the pKa of the second nitrogen to be protonated in the activation cascade is 0.63, indicating that an even lower percentage of molecules will be protonated at this nitrogen under assay conditions.

We originally hypothesized the existence of an acidic microenvironment within the gamma-secretase complex where benzimidazoles could be activated before binding the rNotch P2 cysteine. The existence of an acidic pocket is not without precedent, as many aspartyl proteases such as pepsin, chymosin, cathepsin D, and nepenthesin have been reported to have highest enzymatic activity at pH's ranging from 2.5 to 3.8[202-204]; although, a large body of current research suggests that the gamma-secretase active site is water accessible and that the optimal pH for cleavage is 7 [112, 205, 206]. Furthermore, the TAMRA labeling experiments using recombinant substrates were performed in the absence of the gamma-secretase complex and we still observe labeling. We think perhaps the local concentration of substrate and/or are high enough to react with the small fraction of activated benzimidazole molecules. In order to test this, we wanted to see if we see increased labeling in buffers with lower pH, where there should be a higher fraction of benzimidazole molecules activated. Indeed, if we perform the same labeling experiment using PPI-Tz and TAMRA with wild-type rNotch, we see an increase in labeling intensity with decrease in the pH of the buffer (Figure 4.14).

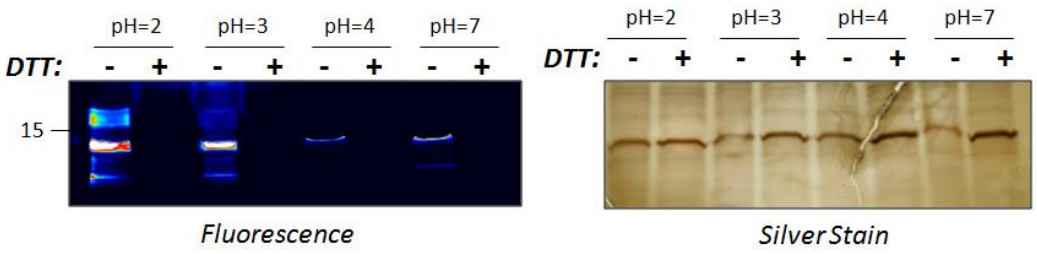

Figure 4.14: TAMRA labeling of WT rNotch is increased with decreasing pH.

Another important caveat we must consider is the fact that we observe direct binding to rNotch, *and* modulation of APP processing. While we do have evidence that benzimidazoles are also directly binding to gamma-secretase, based on the location of the target Notch cysteine, so close to the scissile bond, it seems likely that Notch cleavage is being inhibited based solely on steric hinderance from the active site when bound to benzimidazole. Competition studies performed using our one-pot activity assay suggest that the two substrates compete for cleavage (Figure 4.15), so we hypothesized that the increase in Aβ production is due to increased availability of gamma-secretase active sites when Notch is blocked from binding. In support of this hypothesis, we've found that the increase in Aβ42 is eliminated when we assay benzimidazole IC_{50} with the P2 methionine rNotch mutant.

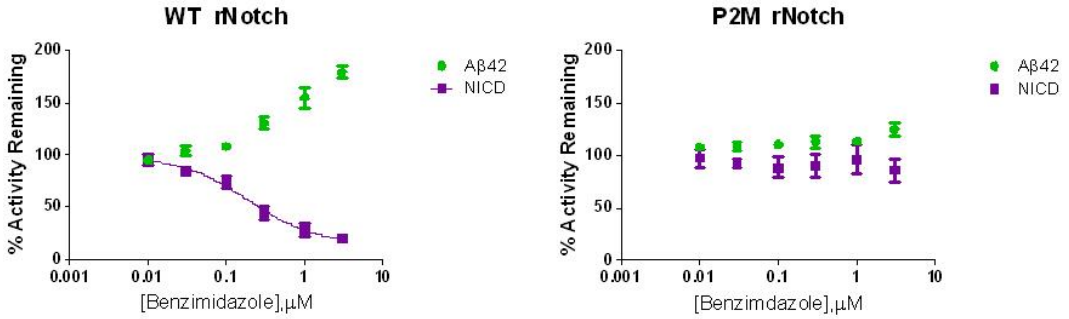

Figure 4.15: Benzimidazole compounds do not increase Aβ42 when assayed with mutant P2 methionine rNotch in the one-pot gamma-secretase activity assay.

In summary, we have discovered that benzimidazoles are novel modulators of gamma-secretase activity. They inhibit the production of NICD, while increasing production of Aβ peptides. Our studies strongly suggest that benzimidazoles bind to the P2 cysteine of the Notch substrate, as well as to cysteine residues in PS1-NTF,

PS1-CTF, and Pen-2. Further analysis using mass-spectrometry will confirm our findings (See Appendix A). How these compounds are being activated at a neutral pH remains to be elucidated, but we plan to utilize NMR analysis to determine exactly which species are present under our assay conditions. The increase in Aβ peptides observed with benzimidazole treatment may preclude these molecules from being used in the clinic, but this work demonstrates the possibility of a Notch specific inhibitor and provides important rationale for clinicians to use caution before indiscriminately prescribing proton pump inhibitors to patients.

CHAPTER 5:

Benzimidazole Covalent Probes and the Gastric H+/K+-ATPase as a Model System for Protein Labeling in a Copper-free Setting[1]

5.1 Background

The discovery of benzimidazoles as novel gamma-secretase modulator presented an opportunity to utilize methods exclusive to working with covalent probes. The development of covalent enzyme inhibitors is often avoided due to concerns of selectivity and possible immunogenicity of enzyme-inhibitors adducts. This is unfortunate, as covalent inhibitors often have increased efficiency and duration of action and also unnecessary as the development of clickable covalent probes can allow researchers to determine possible off-target effects[207-209]. Some of the most successful therapeutics in history are covalent inhibitors. For example, aspirin works as an NSAID by irreversibly acetylating a serine residue in the active site of cyclooxygenase COX-1 and COX-2[210, 211].

As detailed in Chapter 3, substituted benzimidazole compounds are covalent inhibitors widely used for the treatment of acid-related gastric diseases such as peptic ulcers and gastroesophageal reflux disease[212, 213]. Benzimidazole compounds are pro-drugs that must first undergo two protonations and a subsequent spontaneous rearrangement to become sufficiently reactive[194, 214]. Once activated, they form a disulfide bond with cysteine residues within the proton pump, the gastric H^+/K^+-ATPase, resulting in irreversible inhibition of enzymatic activity[193, 215-218]. Because this reaction has been extensively studied and the target irrefutably identified

as the catalytic subunit of the H^+/K^+-ATPase [195, 218], ATP4A, covalent probes derived from these compounds can serve as a useful model system for testing the efficiency of different bioorthogonal reactions in protein labeling.

The copper(I)-catalyzed azide-alkyne cycloaddition (CuAAC) reaction has widespread use in bioorthogonal labeling; however, this type of reaction is not always ideal because it requires a copper catalyst. In the case of benzimidazoles, reducing agents disrupt the disulfide bond between inhibitor and enzyme making CuAAC unsuitable for protein labeling with these compounds. By incorporating clickable moieties compatible with copper-free click chemistries, one can utilize covalent probes without being limited by toxicity or solubility issues[219-221]. Subsequently, the strain-promoted azide-alkyne cycloaddition (SPAAC)[222, 223] and inverse electron demand diels-Alder (iEDDA)[224-226] reaction for tetrazine ligation have become increasingly popular for protein labeling applications.

We have synthesized a series of benzimidazole analogues containing different "clickable" moieties that can be used in a copper free setting to directly label the molecular target of these compounds: the H+/K+ exchanging ATPase or the gastric proton pump. We have directly compared tetrazine ligation and SPAAC and found that tetrazine ligation is far superior; not only in regard to reaction rate, but efficiency as well. Our results validate the development of chemical probes for discovery of unknown targets and also emphasize the ease of implementation when using copper-

free clickable systems. In particular, this study highlights the utility and efficiency of tetrazine covalent probes.

5.2 Results

Benzimidazole Probes are Potent Proton-Pump Inhibitors

We synthesized two benzimidazole probes, Rabe-Tz and Rabe-N_3 (Figure 5.1A). Tetrazines and trans-cyclooctenes undergo a rapid inverse-demand Diels Alder reaction followed by a retro-Diels Alder reaction to eliminate nitrogen gas and can be used for bioconjugation at extremely low concentrations [227]. Conjugated dibenzocyclooctene reacts with terminal azide via strain promoted azide-alkyne cycloaddition in an alternate copper-free click reaction(Figure 5.1B) [222].

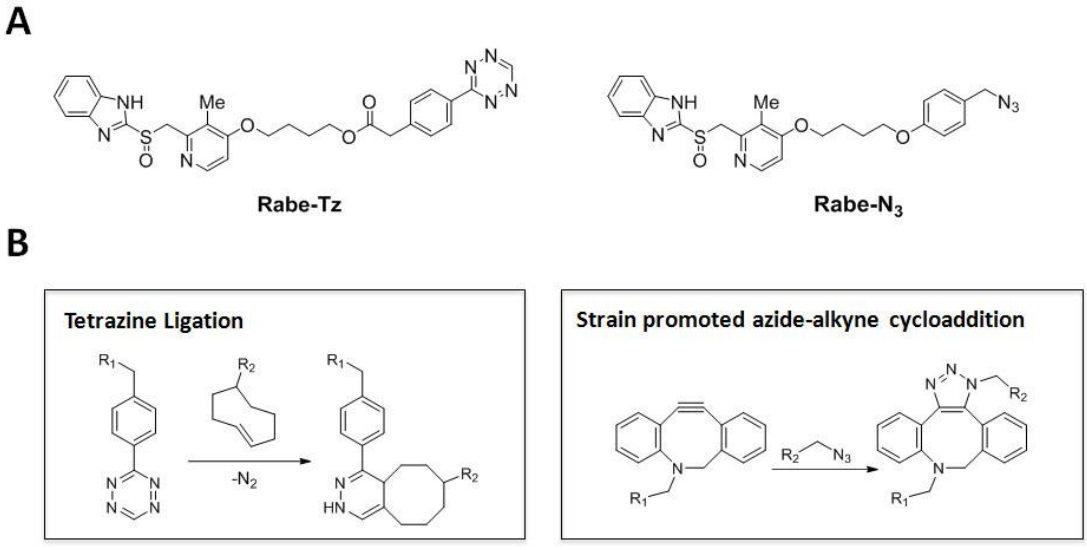

Figure 5.1: Structures of synthesized benzimidazole probes and the corresponding copper-free click chemistries available to each.

In order to determine if the synthesized analogues retain inhibitory activity against the proton pump, we prepared gastric H^+/K^+-ATPase containing vesicles for use in a colorimetric activity assay. Differential centrifugation of gastric mucosa from pig stomachs, with slight modifications from procedures previously reported [228-230], was used for vesicle isolation (Figure 5.2A). To characterize the gastric H^+/K^+-ATPase in our sample, enzyme activity was detected by measuring the amount of inorganic phosphate released using the PiColorLock Gold Phosphate Detection System. Background phosphate release was measured using reactions carried out in the absence of $MgCl_2$, in which gastric H^+/K^+-ATPase is inactive, as described previously by Shin et al[231]. Gastric H^+/K^+-ATPase activity was defined by the difference in signal in the absence and the presence of 100 μM Rabeprazole, a known proton-pump inhibitor (Figure 5.2B,C).

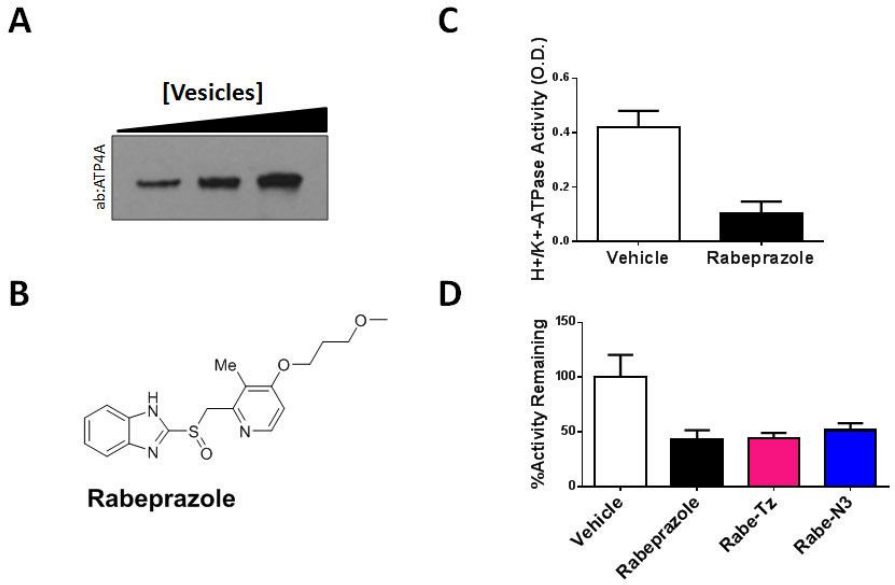

Figure 5.2: **Benzimidazole probes inhibit gastric H+/K+-ATPase activity. A)** Western blot analysis confirming the presence of the gastric H+/K+-ATPase, ATP4A, in isolated vesicles. **B)** Structure of known proton-pump inhibitor, Rabeprazole **C)** Gastric H+/K+-ATPase activity is inhibited by 100μM Rabeprazole and **D)** benzimidazole probes inhibit ATPase activity by approximately 50% at 10μM compound.

Each benzimidazole probe (10μM) was incubated with H^+,K^+-ATPase containing vesicles to determine their potency. Figure 5.2D shows the inhibitory activity of synthesized compounds in our assay. We tested both analogues in comparison to the known inhibitor, Rabeprazole, and found that all compounds tested inhibit the enzyme at similar levels. This suggests that the modifications to the core benzimidazole structure did not change potency of either compound.

Direct Labeling of Gastric H^+/K^+-ATPase, ATP4A, with Benzimidazole Analogues

Since the analogues completely retained inhibitory activity, we tested if they still directly bind and label their target. Gastric H^+/K^+-ATPase containing membranes were prepared using differential centrifugation, incubated with each probe, and copper-free click chemistry (Figure 5.1B) was utilized to attach a biotin tag. A streptavidin resin is then used to enrich for labeled proteins, which can be analyzed using western blot (Figure 5.3A). Because these compounds require low pH for activation, labeling should only occur under sufficiently acidic conditions. We performed the labeling experiment using Rabe-Tz at a pH of 2, 3, 4 and 7 and observed labeling of a protein with apparent molecular weight of 270kDa at pH=3 (Figure 5.3B). While a recent study proposes that the active form of the ATPase is the monomeric form (≈114kDa)[230], extensive early research suggest the enzyme functions as a dimer or higher oligomer in conjunction with the β subunit[232-237]. Our finding suggests that active ATP4A is a dimer. Surprisingly, no labeled ATP4A was detected at pH 2, in which Rabe-Tz should be activated for covalently binding to the target. We reasoned that ATP4A is less soluble when it was treated at pH 2 and extracted from the membrane environment. For this reason, all subsequent experiments were run at pH=3. Specificity of labeling was shown by addition of a reducing agent, used to break the disulfide bond between the probe and its target. For both compounds, labeling is completely abolished by the addition of 50mM DTT (Figure 5.3C). Next, we directly compared the labeling efficiency of the

two analogues by titrating the dose of probe used for labeling between 0.3 and 3.0 μM. As shown in Figure 5.3D, each compound labels ATP4A in a dose dependent manner, but Rabe-Tz is clearly more efficient, labeling with much stronger intensity at similar concentrations.

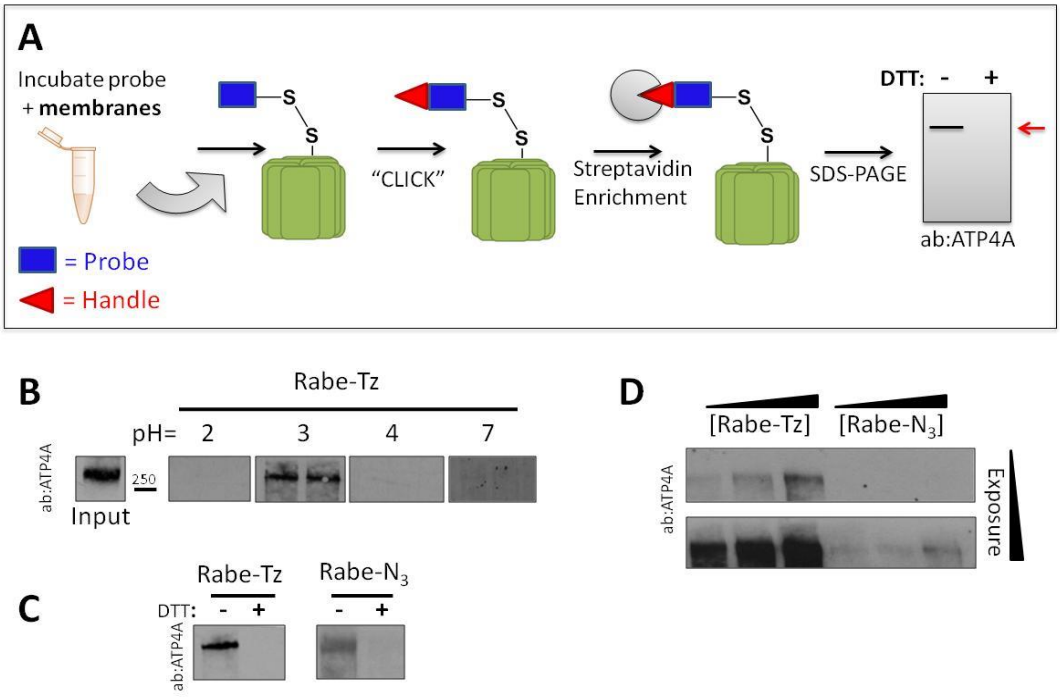

Figure 5.3: **Benzimidazole probes label the gastric H+/K+-ATPase, ATP4A**. **A)** Schematic drawing of labeling protocol. After incubation of probe and gastric membranes biotin is "clicked" onto the probe, the target enriched using streptavidin beads, separated using SDS-PAGE and analyzed by western blot. **B)** Labeling is pH dependent, requiring a pH of 3.0 for acid activation of benzimidazole compounds. **C)** Direct comparison of labeling efficiency between probes at 1μM shows that labeling is blockable with DTT (50mM). **D)** Labeling with 0.3, 1, and 3μM probe shows that labeling is dose dependent and Rabe-Tz labels more efficiently than Rabe-N_3 at equivalent concentrations.

There are two possibilities that explain the differences in labeling efficiency between Rabe-Tz and Rabe-N_3. The first possibility is that Rabe-Tz binds to the proton pump with a higher affinity. The second option is that tetrazine ligation is more efficient than SPAAC, resulting in superior labeling. Based on the activity data showing that each analogue inhibits the proton pump with similar potency, it is plausible to assume that Rabe-Tz labels more strongly due to a more efficient click reaction[238].

Fluorescent Imaging of Labeled Proteins

To take advantage of the efficient labeling of ATP4A with Rabe-Tz, we sought to identify Rabe-Tz labeled proteins using an unbiased approach: direct labeling with tetramethyl rhodamine (TAMRA) dye (Figure 5.4A). Following incubation of gastric vesicles with the tetrazine probe, we clicked a trans-cyclooctene-TAMRA dye to labeled proteins for visualization on SDS-PAGE gel. Figure 4B shows that Rabe-Tz directly labels two protein bands with apparent molecular weight of approximately 270 kDa and approximately 70kDa. Moreover, both bands are eliminated with the addition of DTT, and Coomassie blue staining confirms that equal amounts of protein were loaded to each lane (Figure 5.4B).

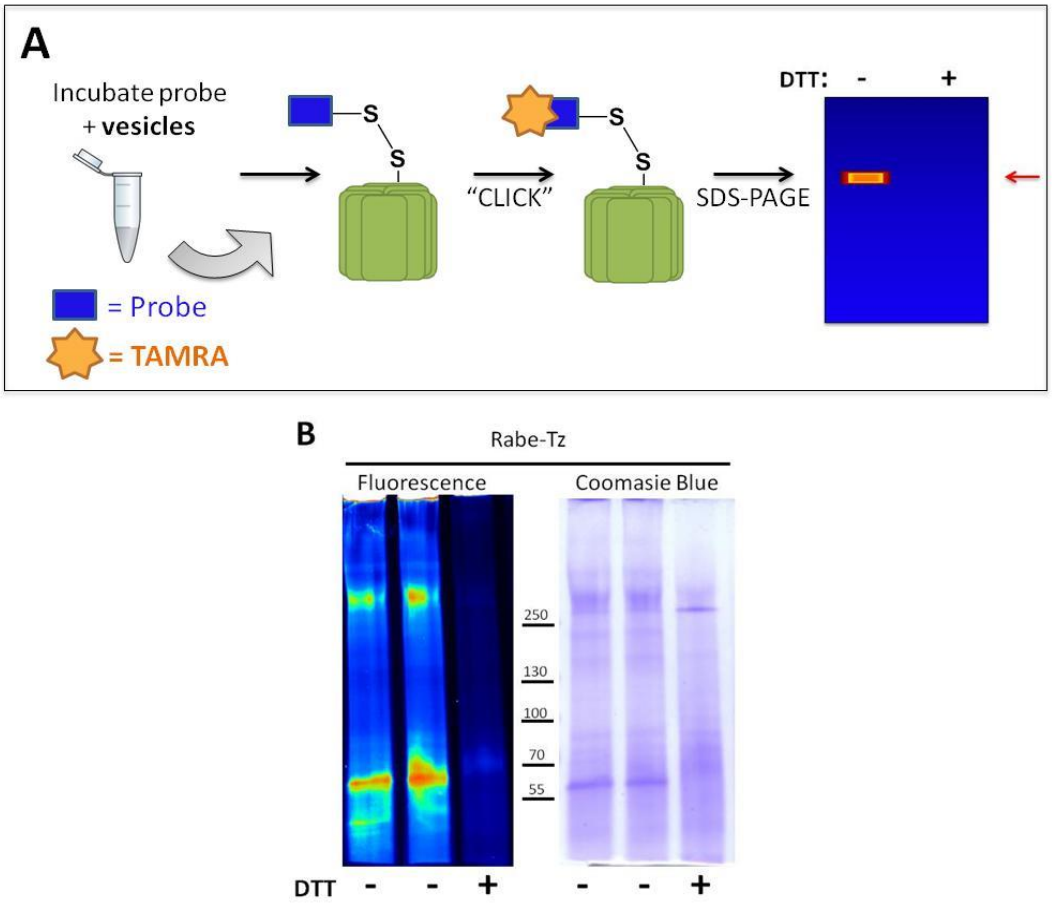

Figure 5.4: TAMRA labeling with Rabe-Tz. A) Schematic representation of protocol used for unbiased protein labeling with TAMRA dye. **B)** Rabe-Tz probe specifically labels protein at >250kDa and approximately 70kDa. . Lane 1 and 2 are duplicate samples while Lane 3 demonstrates that labeling is blocked by 50mM DTT.

In order to identify these TAMRA labeled proteins, we performed a pull down experiment based on the protocol shown in Figure 3A, however, following SDS-PAGE, we stained the gel with Coomassie blue. No clear bands were visible, so gel slices at approximately 250kDa and ~70 kDa, where TAMRA labeling was observed, were excised and digested for liquid chromatography-tandem mass spectrometry (LC-MS/MS) analysis. Peptide identifications were accepted if they could be established at greater than 95% probability to achieve an FDR less than 1.0% by the Scaffold Local FDR

algorithm. Protein identifications were accepted if they contained at least 4 identified peptides.

Table 5.1. Proteins identified by MS analysis of Rabe-Tz pull down

Protein	Accession number	Molecular weight (kDa)
Gastric H^+/K^+ ATPase	ATP4A_PIG	114
Isoform 2 of deleted in malignant brain tumors 1 protein	Q4A3R3-2	148
Uncharacterized protein	F1SKJ1	225
Uncharacterized protein	F1SHC1	50
Uncharacterized protein	I3LT38	202

The band at 70kDa was found to correspond to serum albumin and is likely pulled down as a result of its extremely high abundance. For the higher molecular weight band, five proteins were identified exclusively in the sample not treated with DTT and can be seen in Table 5.1. As expected, the catalytic subunit of the gastric H^+/K^+-ATPase was a top hit, further confirming ATP4A as the target of Rabe-Tz. In addition, Isoform 2 of deleted in malignant brain tumors 1 protein (DMBT1) was also identified. This protein is a secreted scavenger receptor cysteine-rich protein that has been reported to be deleted in numerous human cancers including: brain[239], lung[240], and gastrointestinal cancers[241]. It is thought to play a role in both immune defense and epithelial differentiation[242] and has also been reported to bind Helicobacter pylori[243]. Interestingly, Benzimidazole compounds are commonly used to treat *H.pylori* infection[244] with an unknown cellular target and both DMBT1 and benzimidazole compounds have been reported to play a protective role for

gastrointestinal mucosa[245, 246]. It would be interesting to carry out more studies to examine the physiological interaction between DMBT1 and benzimidazole compounds.

Alternatively, the abundance of cysteine residues in this protein could account for benzimidazole binding under low pH. The remaining three proteins are currently uncharacterized in the literature, although, according to www.uniport.org, F1SKJ1 is inferred to have actin-dependent ATPase activity based on electronic annotation through Ensembl. Whether our probes bind to these proteins due to unrecognized ATPase activity or whether they only bind benzimidazoles under artificially low pH remains to be investigated.

5.3 Discussion and Conclusions

We have synthesized two benzimidazole based probes and shown that both specifically label the catalytic component of the gastric H^+/K^+-ATPase, ATP4A. By directly comparing protein labeling using tetrazine ligation and SPAAC, we have demonstrated that tetrazine ligation is more useful; not only is tetrazine ligation faster, it is also more efficient. If tetrazine modification is tolerated on compounds of interest, we recommend this as the preferred approach for copper-free bio-orthogonal reactions.

Moreover, MS analysis of proteins targeted by benzimidazole probes confirm the use of covalent probes for target identification, as well as revealed

a potential link between benzimidazole compounds and DMBT1 for H. pylori eradication and mucosal protection.

5.4 Detailed methods

Compound Synthesis

Benzimidazole probes were synthesized by Dr. Qi Liu as previously reported[247].

Preparation of Porcine Gastric H+/K+-ATPase Enzyme

Gastric H+/K+-ATPase was isolated using a protocol adapted from Dach et al. 2012[230] and Skrabanka et al 1984[229]. Fresh porcine stomachs were obtained from Innovative Research Inc (Novi, MI) and kept on ice during each step. Gastric mucosa was scraped from the stomachs with a cell scraper and homogenized 1:1 v/v in homogenization buffer (0.25M Sucrose, 20mM TRIS-HCl, pH=7.4) using an immersion blender. The mucosa was further homogenized with 8 passes of piston-based motorized homogenizer. The sample was centrifuged at 27,000g (17,235rpm) for 20 minutes in a Sorval T-1250 rotor. The supernatant was transferred to a clean tube and re-centrifuged at 100,000g (33,000rpm in Sorval T-1250) for 1 hour. The pellet was re-suspended in homogenization buffer, homogenized with 5 passes of the motorized homogenizer and layered on a two-step gradient consisting of 37% sucrose (w/v) and 20 mM Tris-HCl (pH 7.4) at the bottom with 7% Ficoll at the top (GE Healthcare), 0.25 M sucrose, and 20 mM Tris-HCl (pH 7.4). The sample was

centrifuged at 217,000g (35,000rpm in Thermo Scientific TH-641 rotor) for 1 hour H^+/K^+-ATPase containing vesicles were collected from the top of the ficoll layer and diluted with 20mM Tris buffer (pH=7.4) and centrifuged at 217,000g (49,000rpm in Sorval T-1250) for 30minutes. The pellet containing the vesicles was re-suspended in 20mM Tris (pH=7.4) and kept frozen in small aliquots at -20°C for short term and -80°C for long term storage.

Gastric H^+/K^+-ATPase Activity Assay

Isolated vesicles (15ug/mL) were pre-incubated for 15 minutes at 37°C with compound or vehicle in assay buffer (20mM TRIS-HCl, (pH=7), 10mM KCl, 2mM $MgCl_2$) in the presence of 1ug/mL nigericin. The gastric H+/K+-ATPase was activated by the addition of 2mM NaATP (Sigma) and incubated at 37°C for 45 minutes. Activity was determined by measuring inorganic phosphate release using the PiColorLock Gold Phosphate Detection System (Innova Biosciences, Cambridge, UK). Assay background was measured by carrying out reactions in the absence of vesicles; while background phosphate release was measured using reactions carried out in the absence of $MgCl_2$ Reactions without compounds were run with vehicle, DMSO, as a positive control. The following equations were used to calculate potency of inhibition:

$$\boldsymbol{Background} = Signal\ at\ 100uM\ Rabeprazole$$

$$\boldsymbol{\delta} = Signal - Background$$

$$\%\boldsymbol{Acitivity\ Remaining} = \frac{\delta_{treatment}}{\delta_{DMSO}}\ X\ 100$$

Preparation of Gastric Mucosa Membranes

Fresh porcine stomachs were obtained from Innovative Research Inc (Novi, MI) and kept on ice during each step. Gastric mucosa was scraped from the stomachs with a cell scraper and homogenized 1:1 v/v in buffer A (50 mM MES, pH 6.0, 5 mM $MgCl_2$, 5 mM $CaCl_2$, 150 mM KCl) using an immersion blender. The mucosa was further homogenized with 10 passes of a piston-based motorized homogenizer. The homogenate was centrifuged at 800g for 10 minutes to remove cell debris and nuclei. The supernatant was centrifuged at 100,000g for 1 hour at 4°C. The pellet was resuspended in buffer A and the centrifugation at 100,000g repeated. The final membrane pellet was resuspended and homogenized in buffer A to a final concentration of approximately 18mg/mL and stored at -80°C.

Labeling of Mucosa Membrane with Benzimidazole Probes and Western Blot Analysis

Membrane fractions containing endogenous H^+/K^+-ATPase were isolated from porcine gastric mucosa using ultracentrifugation methods described above. Isolated membrane (800ug) was incubated with each benzimidazole analogue (1uM) in a glycine buffer at pH=3 for 1 hour at 37°C while shaking. After incubation, copper free click reactions were initiated by adding Dibenzocyclooctene-PEG4-biotin (Sigma) (100uM) to reactions with Rabe-N3 and trans-cyclooctene-biotin, (16uM) to reactions with Rabe-Tz. Reaction with either handle allows for conjugation of biotin to labeled proteins for pull down. Click reactions were allowed to proceed for three hours at room temperature. Reactions were centrifuged at 90,000g for 40 min at 4°C.

Supernatants were aspirated, thus removing excess click reagents. The pellets were resuspended by homogenization with a TissueLyser (Qiagen) at 25 rps for 2 min and solubilized in RIPA buffer (50 mM Tris (pH= 8), 150 mM NaCl, 0.1% SDS, 1% NP40, 0.5% deoxycholate) then centrifuged at 12,000 rpm to remove particulate matter. To show blocking of labeling, 50mM DTT was added to select samples and incubated for 5 minutes at RT. Streptavidin ultralink resin slurry (Pierce) was added to all supernatants and incubated overnight at 4C. Streptavidin resins were washed 4 times by centrifugation at 0.5g followed by aspiration of supernatant and addition of 500µL RIPA buffer. Labeled proteins were eluted by incubation with excess biotin (2mM) in 2X Laemmli sample buffer (Biorad) at 70°C for 10min. Eluates were loaded onto a precast 4–15% Criterion™ Tris-HCl gel (BioRad) for protein separation, transferred to a PVDF membrane and blotted for the H,K-ATPase with Anti-ATP4A antibody (ab174293) (AbCam).

Fluorescent Labeling

Benzimidazole probe, Rabe-Tz (2uM), was incubated with 150ug of gastric vesicles (preparation described above) in Glycine buffer (pH=3) for 1h at 37°C in the presence or absence of 50mM DTT or TCEP. Targeted proteins were labeled with tetramethyl rhodamine via spontaneous reaction of trans-cyclooctene-TAMRA (16uM) and the tetrazine present on Rabe-Tz for 1 hr at room temperature in the dark. Labeled proteins were then precipitated with 1mL of cold acetone at -20°C for 2 hours, washed once with 500µL ammonium bicarbonate (100mM), then again with 500µL cold acetone. Precipitated proteins were centrifuged at 15,000g for 10 min, the

acetone was removed, and the protein pellet was air-dried for 10 min. Protein pellets were resolubilized in 45µL PBS + 15µL 4x Laemmli Sample buffer (BioRad) while rotating at RT for 2 h. Lowry assay was used for total protein quantification and 25ug of each sample was loaded onto an SDS-PAGE gel for band separation and then scanned for fluorescent bands. The same gel was then immediately stained with Coomassie blue (BioRad) to compare the total amount of protein in each sample.

Pull down with Rabe-Tz for LC- MS/MS Analysis

The protocol described for "Labeling of Mucosa Membrane with Benzimidazole Probes" was followed using Rabe-Tz (1uM) and trans-cyclooctene-biotin (16uM) with the exception that the click reaction was only allowed to proceed for 1 hour. Following protein separation by SDS-PAGE protein bands of interest were excised, destained and SDS removed by washes with 50% methanol (v/v). These gel pieces were then dried using a speed-vac. To reduce the disulfide bonds, 10 mM DTT in 25 mM ammonium bicarbonate was added until the pieces were covered with 10 mM DTT in 25 mM ammonium bicarbonate for 1 hour at 56°C. For alkylation, the reducing agent was removed and the gel pieces were covered with freshly made 55 mM iodoacetamide in 25 mM ammonium bicarbonate at room temperature in the dark. After 45 minutes, the supernatant was removed and gel pieces were rinsed with 100 mM ammonium bicarbonate three times. Gel pieces were again dried using a speed-vac. To dried, gel-bound protein, 200 ng of trypsin (modified, sequencing grade, Promega) in 10 µl of 100 mM ammonium bicarbonate was added to swell the gel piece. Then an additional 90 µl of 100 mM ammonium bicarbonate was added or

until the gel piece was covered with the digestion solution. Tryptic digestion was allowed to proceed at 37°C overnight. The supernatant containing the generated peptides was removed and desalted using Poros R2 beads as described in Erdjument-Bromage et al (1998). Peptides were eluted with 3 μl of 40% (v/v) acetonitrile containing 0.1% (v/v) formic acid and stored at -20°C if not analyzed immediately.

The purified peptides were diluted to 0.1% formic acid and each gel section was analyzed separately by microcapillary liquid chromatography with tandem mass spectrometry using the NanoAcquity (Waters) with a 100-μm-inner-diameter × 10-cm-length C18 column (1.7 um BEH130, Waters) configured with a 180-um x 2-cm trap column coupled to an OrbiElite mass spectrometer(Thermo Fisher Scientific) scanning 300-1650 m/z at 120000 resolution with AGC set at 1 x 10(6). Peptides were eluted with a linear gradient of 0-50% acetonitrile (0.1% formic acid) in water (0.1% formic acid) over 90 mins with a flow rate of 300nL/min. Key parameters for the data dependent MS were top 10 DDA, AGC 1e4, and CID ms/ms collected in the linear ion trap.

Database searching

Tandem mass spectra were extracted by ProteoWizard version 3.0.7529 from the raw files. Charge state deconvolution and deisotoping were not performed. All MS/MS samples were analyzed using Mascot (Matrix Science, London, UK; version 2.3.02) and X! Tandem (The GPM, thegpm.org; version CYCLONE (2010.12.01.1)). Mascot was set up to search the uniprot_pig_20150721 database (selected for Mammalia, unknown version, 26153 entries) assuming the digestion enzyme trypsin.

X! Tandem was set up to search a subset of the uniprot_sprot_20150223 database also assuming trypsin. Mascot and X! Tandem were searched with a fragment ion mass tolerance of 0.80 Da and a parent ion tolerance of 10.0 PPM. Carbamidomethyl of cysteine was specified in Mascot and X! Tandem as a fixed modification. Deamidation of asparagine and glutamine, oxidation of methionine, acetyl of the n-terminus and phospho of serine, threonine and tyrosine were specified in Mascot as variable modifications. Glu->pyro-Glu of the n-terminus, ammonia-loss of the n-terminus, gln->pyro-Glu of the n-terminus, deamidated of asparagine and glutamine, oxidation of methionine, acetyl of the n-terminus, carbamidomethyl of cysteine and phospho of serine, threonine and tyrosine were specified in X! Tandem as variable modifications.

Criteria for Protein Identification

Scaffold (version Scaffold_4.4.3, Proteome Software Inc., Portland, OR) was used to validate MS/MS based peptide and protein identifications. Peptide identifications were accepted if they could be established at greater than 95% probability to achieve an FDR less than 1.0% by the Scaffold Local FDR algorithm. Protein identifications were accepted if they could be established at greater than 99.9% probability to achieve an FDR less than 1.0% and contained at least 4 identified peptides. Protein probabilities were assigned by the Protein Prophet algorithm (Nesvizhskii, Al et al Anal. Chem. 2003;75(17):4646-58). Proteins that contained similar peptides and could not be differentiated based on MS/MS analysis alone were grouped to satisfy the principles of parsimony. Proteins sharing significant peptide

evidence were grouped into clusters. Proteins were annotated with GO terms from NCBI (downloaded Jul 22, 2015). (Ashburner, M et al Nat. Genet. 2000;25(1):25-9).

CHAPTER 6

Thesis Summary and Major Implications

We have successfully developed and utilized an efficient and applicable *in vitro* one-pot assay for measurement of gamma-secretase activity against APP and Notch simultaneously. This assay has provided important insight into the enzyme kinetics of *in vitro* gamma-secretase activity and provides evidence for direct competition between Notch and APP for gamma-secretase cleavage at sufficiently high concentrations. Not only have we have shown that this assay can be used to screen for novel gamma-secretase modulators, but it also demonstrates the importance of using assays with both substrates present in order to accurately calculate selectivity margins. The widespread failure of gamma-secretase inhibitors in the clinic thus far, makes it clear that more stringent testing is necessary before compounds advance past pre-clinical trials. Use of our assay has the potential to save researchers valuable time and money by accurately determining selectivity for APP or Notch from the early stages of drug development.

The fact that we observe a shift in selectivity for only certain compounds when compared between our one-pot and two-pot assay is intriguing and we are eager to determine the mechanism. Furthermore, it's interesting that we observe this phenomenon with both a Notch targeted compound, LY-450,139, and an Aβ42 targeted compound, GSM-1. The binding sight of GSM-1 has been shown to be PS-NTF, but the binding site of LY-450,139 remains to be elucidated. It would be interesting to see if the two compounds have overlapping binding sites. We could

perform photoaffinity labeling with GSM-1 based probes and see if LY-450,139 is able to block labeling in order to determine if a similar binding site is the reason for similar behavior in our one-pot versus two-pot assay.

While similar binding sites could explain why we see the same phenomenon with two distinct chemotypes, it still does not explain the mechanism for a shift in selectivity in the one-pot assay. Our prevailing hypothesis is that different GSIs and GSMs are actually targeting different gamma-secretase enzymes. As mentioned previously in the introduction, both Aph-1 and PS exist as multiple isoforms, allowing for the formation of six distinct complexes. Furthermore, an increase in PS2 containing complexes has been shown to be positively correlated with increased Aβ42:Aβ40 ratios [51], demonstrating differential processing of APP by distinct gamma-secretase complexes. Perhaps the compounds that experience a selectivity shift are actually binding to Aph-1a containing compounds, while compounds that do not experience a shift bind to Aph-1b containing compounds, or vice versa. Isoform dependent substrate selectivity has been observed, suggesting that each isoform of Aph-1 may contain unique substrate docking sites. Perhaps the addition of the alternate substrate only effects compounds that target Aph-1a because the substrate binds to a docking site resulting in a conformational change that alters active site structure or binding site structure and changes the potency for the other gamma-secretase products. In order to test this, one could overexpress different complexes in separate cell lines, isolate gamma-secretase containing membranes and compare compound IC_{50} in the one-pot and two-pot assays. Alternatively, you could use

CRISPR to selectively knock out a certain isoform and test the effect of compound IC_{50} in this model.

It's important to note that the loss in selectivity is not due to a loss in potency for inhibiting the production of the targeted species, but rather is due to an increase in potency for inhibiting the production of the off-target species. Another possible, but unlikely explanation is that the increase in potency for the off-target species is due to a decrease in available enzyme as a result of the inhibitor "locking" the enzyme in place the alternate substrate. This is not probable, as the IC_{50} of our compounds should not vary this drastically with subtle changes in enzyme concentration, but may be worth looking into. We could begin by testing the effect of lower enzyme concentration on the IC_{50} of these compounds. If we see a change similar to the magnitude that we see when comparing our one-pot to two-pot assay, we could continue on to pull-down experiments to further study enzyme-inhibitor-substrate interactions.

It would also be interesting to see if the IC_{50} of GSIs and GSMs differ for gamma-secretase complexes isolated from different regions of the brain, specifically disease relevant tissues such as the hippocampus or tissues where Notch plays a tumor suppressor role such as the skin. PS1 and PS2 have both been shown to be expressed in neurons, glial cells and astrocytes, but are enriched in neurons of the hippocampal formation and entorhinal cortex [257]. Differential expression of accessory proteins in different tissues could also play a role in gamma-secretase activity and susceptibility to modulation by various compounds.

Our one-pot assay was used extensively in determining the mechanism of action of benzimidazole modulation of gamma-secretase activity. All of our data thus far suggests that these compounds are binding to an acidic pocket within gamma-secretase, and being activated to form disulfide bonds with nearby cysteine residues within the Notch substrate as well as several components of gamma-secretase, similar to their activity on the gastric proton-pump.

In the future, we plan to confirm our findings from labeling experiments by using LC-MS to show direct binding of benzimidazoles to a synthetic Notch peptide as well as the identified components of gamma-secretase: PS-NTF, PS-CTF, and PEN-2. Additionally, we are able to circumvent the inherent difficulty of crystallizing complex membrane proteins by using a combination of photoaffinity labeling and proteomics to determine the exact binding site of these compounds. We will use a benzophenone containing probe to covalently modify benzimidazole targets through UV cross-linking and then identify the exact targeted cysteine residues using LC-MS. Use of the benzophenone allows us to overcome any limitations due to the reducibility of a disulfide bond. The most recent atomic structure of gamma-secretase, published in Nature by Bai et. al., will provide valuable insight into the positioning of these cysteine residues at the interface of presenilin and pen-2.

Although our current model is plausible, as it's been shown in several instances in the past that the local chemical environment of an enzyme active site is sufficient to drastically change pKa, it would also be interesting to test if the lipid composition of our sample is sufficient to affect the pKa as well. We could test this by

determining the pKa's of relevant nitrogen's in the presence of various lipids using UV spectroscopy or NMR.

The fact that we observe a selective increase in the production of Aβ, most dramatically the production of Aβ42, suggests that direct binding to the P2 cysteine of Notch is not the only mechanism of action, and supports our hypothesis stated above. Moving forward, it will be important to ensure that the observed increase in Aβ is not due to any artifact of our assay conditions (ie. an increase in available acceptor or donor beads concurrent with a decrease in detectable NICD). In order to test this, we will need to assay the effect of benzimidazoles on gamma-secretase activity using another method. For example, detecting gamma-secretase products using mass-spectrometry could provide an alternative method and could also be used to test the effect of benzimidazoles on the production of other Aβ peptides such as Aβ37, 43, 46 etc.

The implications of our findings merit immediate consideration granted the fact that Americans filled more than 170 million prescriptions for acid blockers last year, falling only behind statins in total cost expenditure worldwide (IMS Health, U.S. Pharmaceutical Market Performance Review™ 2015) and PPIs constitute the majority of this class. Recent epidemiological studies have reported an increased risk of dementia in elderly patients using proton-pump inhibitors [248, 249], which can be explained by the findings in our lab and others [197] that benzimidazoles increase Aβ peptide production. Even more concerning is the fact that the aggregate prone Aβ42 is the most strongly effected species. Considering the fact that these compounds have

been shown to pass the blood brain barrier and exert effects on brain tissue [250], these findings are extremely concerning. Additional studies have reported a significantly higher risk of heart attack in PPI users compared to those on other antacid medication [251, 252], which could also be potentially explained by PPI inhibition of Notch cleavage by gamma-secretase. Not only is Notch signaling vital for proper heart development, but it has also been shown to play a role in adult cardiac repair [253] and long-term inhibition of Notch signaling in cardiac tissues has been postulated to cause cardiomyocyte and endothelial dysfunction [254].

Our work using benzimidazole based covalent probes, has also brought forth several important findings. First, this study validates the use of chemical probes for target identification, as our tetrazine probe successfully pulled down the known target of PPIs, the gastric proton pump. Second, we have demonstrated the superior efficiency of working with tetrazine probes when copper-free click chemistry is required and suggest their use whenever tolerated on compounds of interest. Lastly, we have identified several novel binding partners of benzimidazole probes, including Isoform 2 of deleted in malignant brain tumors 1 protein (DMBT1), which has been reported to bind *H. pylori* and could potentially provide a link between benzimidazole use and the eradication of *H. pylori* infection.

The one-pot assay has also been utilized in two additional studies of GSIs and GSMs that are presented in Appendices B and C. Further discovery and development of Notch-specific gamma-secretase inhibitors is a key step in using gamma-secretase as a drug target to successfully treat Notch addicted cancers.

APPENDIX A: *Preliminary LC-MS Analysis of Benzimidazole-Notch Adduct Formation*

The most straightforward, and arguably the most convincing, evidence for target identification is the detection of a drug-target adducts using tandem liquid chromatography - mass spectrometry (LC-MS). Figure A.1 shows the predicted weight of the benzimidazole-Notch adduct. We have generated a small synthetic peptide based on the sequence of Notch1 and observe a mass/charge (m/z) ratio of 3700 when analyzed by LC-MS, based on the charged states of the ions present in the spectra (Figure A.2). While the optimal conditions for analysis remain to be determined, preliminary data shows the presence of the predicted benzimidazole-Notch peptide adduct at 4042 in panel C of figure A.3. Unreacted/unbound benzimidazole and peptide are seen at Peaks A and D respectively. Panel B shows an additional, unidentified species. It is important to note that we also observe a species at 342.2 when Rabeprazole is analyzed by itself that we believe corresponds to the lost of a water molecule (Figure A.4).

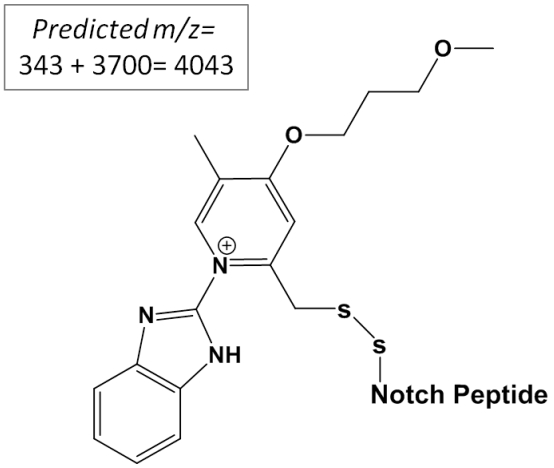

Figure A.1: Predicted m/z for benzimidazole-Notch peptide adduct

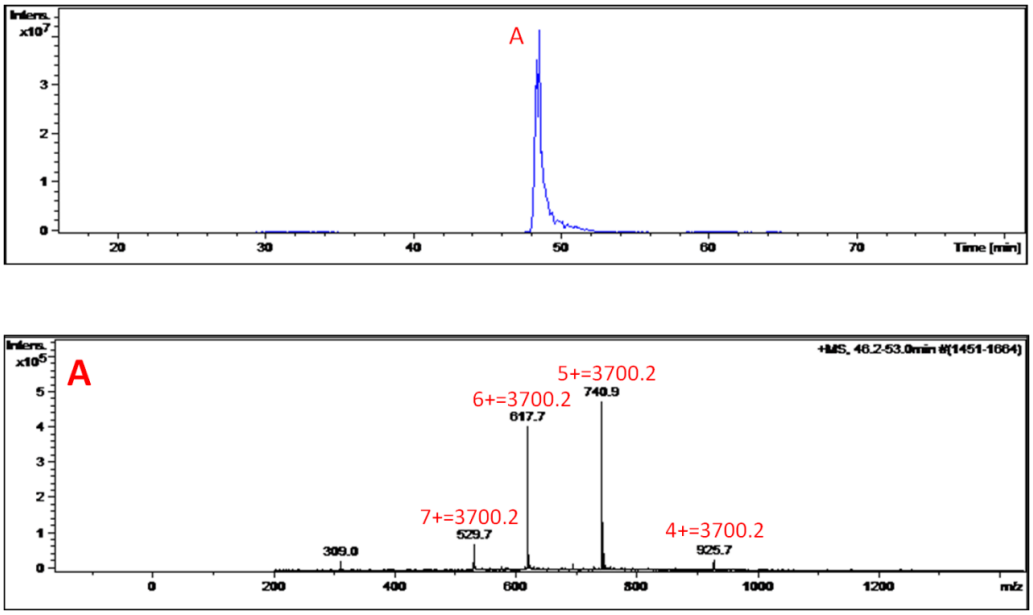

Figure A.2: LC-MS analysis of synthetic Notch1 peptide (250pmol)

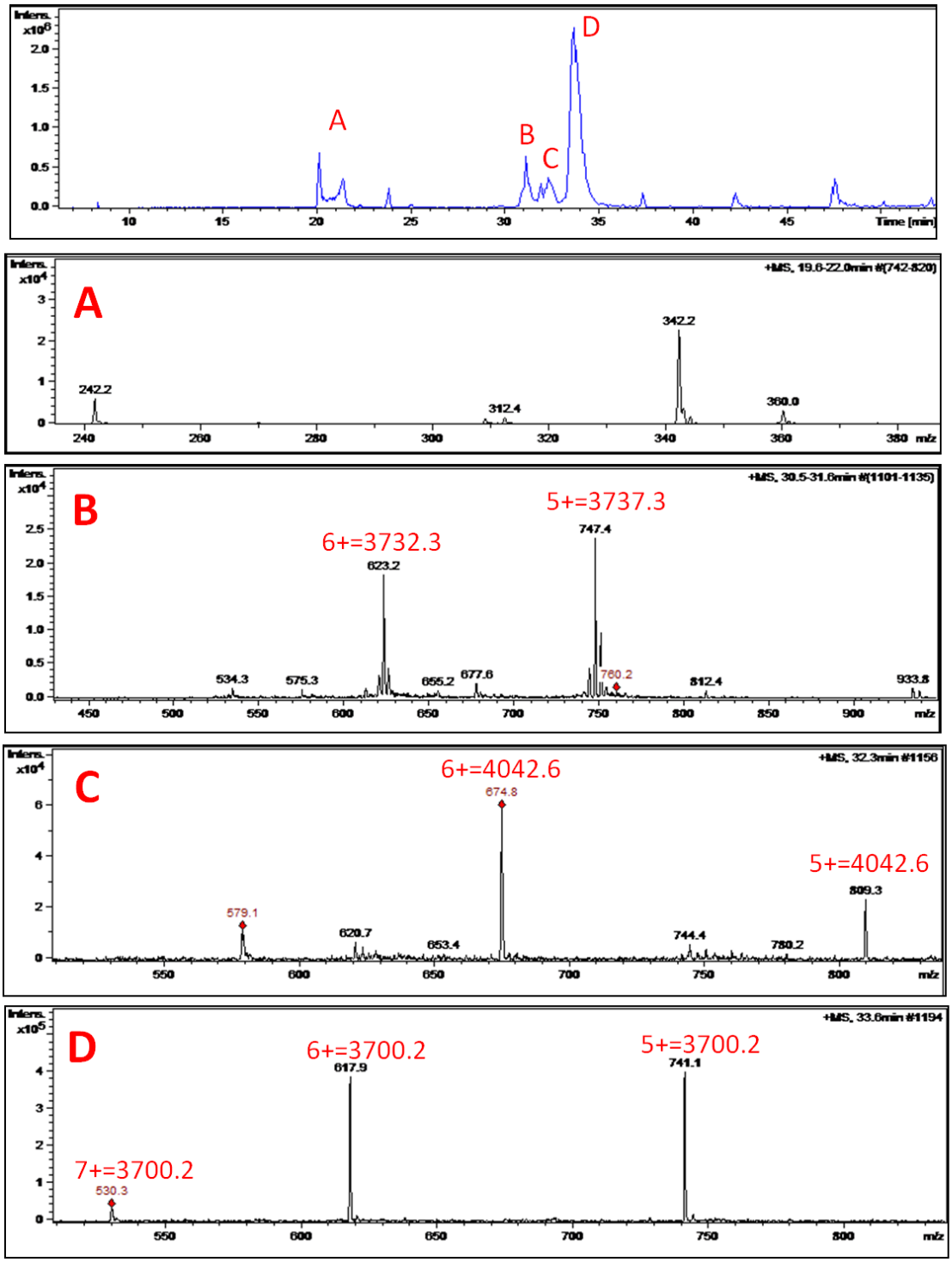

Figure A.3: LC-MS analysis of Rabeprazole (250pmol) incubated with synthetic Notch1 peptide (250pmol) for 1 hour prior to injection into LC-MS. Compound and peptide were both dissolved in DMSO.

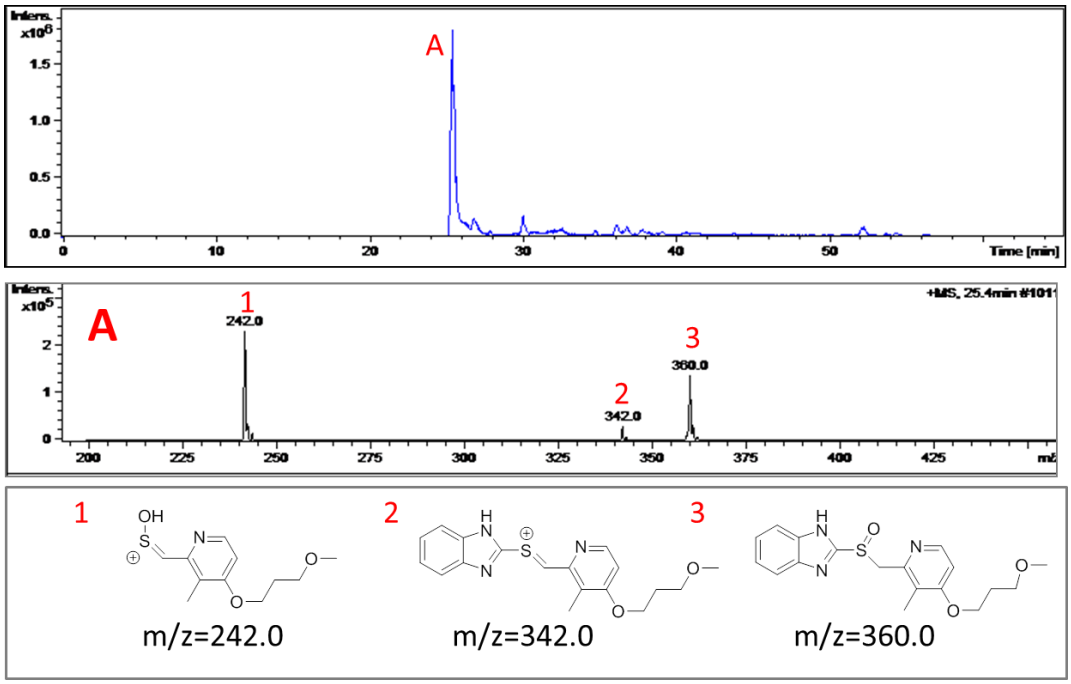

Figure A.4. LC-MS analysis of Rabeprazole (250pmol).

APPENDIX B: *SPECS compound screen*

In an effort to discover novel Notch-specific gamma-secretase inhibitors, we have collaborated with SPECS (The Netherlands). Dr. Deming Chau directed the initial high-throughput screen and Dr. Qi Liu synthesized various analogues. I have followed up with an extensive structure-activity relationship analysis as detailed below.

More than 80 compounds were tested in our one-pot *in vitro* gamma-secretase assay (Table B.1) (See Chapter 2 for detailed methods). Compounds were originally screened at 2.5, 5 and 10μM. IC_{50} values and selectivity margins were calculated for the most promising compounds (Table B.2).

The compound below served as our lead compound and was used as a starting point for designing and comparing analogues. It has an IC_{50} value of approximately 1μM and is roughly 30x selective.

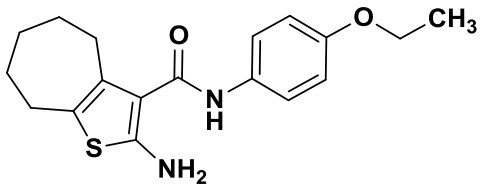

Figure B.1. Lead compound in SPECS screen for Notch selective inhibitors

In summary, we've found that the free amine of the thiophene is absolutely required for selective inhibition of Notch cleavage. Five, six, seven and eight membered-rings attached to the thiophene are tolerated, and the potency and

selectivity of MSK-49 demonstrates that the ring is not required for activity, although it is worth noting that MSK-51 does not inhibit NICD production. A wide range of substitutions are allowable on the benzene ring, including complete substitution to a pyridine ring with the nitrogen at the para, meta, or ortho positions. Adding an extra carbon between the amide and the benzene increases potency approximately 2-fold and increases selectivity to nearly 40x, as demonstrated with one of the most promising compounds, MSK-50.

Table B.1. Results of *in* vitro gamma-secretase assay for each SPECS compound. The requirement for being considered an inhibitor of NICD in second column was IC_{50}<10μM. For IC_{50} assays, normalized AlphaLISA signals were converted to percent vehicle values and used to create dose-response curves which were fitted to 3 parameter curves using GraphPad Prism version 6 (GraphPad Software, San Diego, CA). Selectivity margins were calculated by dividing Aβ40 IC_{50} by NICD IC_{50}. Selectivity for compounds with * in notes column were calculated assuming IC_{50} for Aβ40=25. Compounds with ** assume Aβ40 IC_{50}=100. Five-fold difference in NICD IC_{50} compared to Aβ40 required to be considered selective.

			NICD		*AB40*			
Compound	**Inhibits NICD?**	**Selective?**	**Avg. IC50 (μM)**	**SD (μM)**	**Avg. IC50 (μM)**	**SD (μM)**	**Selectivity**	**Notes**
MSK-1	no							crude
MSK-2	no							crystallized
MSK-3	no							crude
MSK-4	yes	yes	0.93	0.25	17.84	11.52	19	purified
MSK-5	yes	yes	0.81	0.32	20.67	14.97	26	crude
MSK-6	yes	no						purified
MSK-7	yes	no						fraction 2
MSK-8	no							fraction 3
MSK-9	no							crude
MSK-10	no							crude
MSK-11	yes	no						fraction 1
MSK-12	no							fraction 2
MSK-13	no							crude
MSK-14	yes	no						crystallized
MSK-15	yes	yes						fraction 2
MSK-16	no							
MSK-17	yes	yes						
MSK-18	yes	yes	1.18		18.73		16	
MSK-19	no							
MSK-20	no							

Table B.1. Results of *in* vitro gamma-secretase assay for each SPECS compound. (Continued)

			NICD		*AB40*			
Compound	Inhibits NICD?	Selective?	Avg. IC50 (μM)	SD (μM)	Avg. IC50 (μM)	SD (μM)	Selectivity	Notes
MSK-21	no							
MSK-22	yes	no	1.91	0.59	3.62	0.58	2	
MSK-23	yes	no						
MSK-24	no							
MSK-25	no							
MSK-26	no							
MSK-27	no		220.1		568.4			
MSK-28	yes	no	2.01	1.47	2.68	1.82	1	
MSK-29	yes	yes	0.36		13.63		38	
MSK-30	yes	no	7.739	3.34	14.86	1.70	2	
MSK-31	yes	yes	1.14	0.54	15.71	18.21	14	
MSK-32	yes	yes	0.87		8.8		10	
MSK-33	yes	yes	0.66		5		8	
MSK-34	yes	yes	0.55		2.66		5	
MSK-35	yes	yes	0.52		4.4		8	
MSK-36	yes	yes	0.71		>25		35	*
MSK-37	yes	yes	1.01		>25		25	*
MSK-38	yes	yes	0.35		4.65		13	
MSK-39	yes	yes	0.96		6.039		6	
MSK-40	yes	yes	0.75		23.2		33	*
MSK-41	yes	no	1.6		4.5		3	
MSK-42	yes	yes	2.05		>100		49	
MSK-43	yes	yes	1.1		12		11	
MSK-44	yes	yes	4.35		29.05			
MSK-45	yes	yes	6.87		>100		15	**
MSK-46	yes	yes	1.22		>25		20	*
MSK-47	yes	yes	1.892		19		13	*
MSK-48	yes	yes	4.58		>25		5	*
MSK-49	yes	yes	1.58		>25		16	*
MSK-50	yes	yes	0.65		>25		38	*
MSK-51	no							
MSK-52	yes	yes	0.34	0.21				
MSK-53	yes	yes	0.28	0.13				
MSK-54	yes	yes	0.15	0.15				
MSK-55	yes	no	0.88	0.60	3.591	0.871		
MSK-56	yes	yes	1.46	1.20				
MSK-57	yes	yes	0.25	0.11				
MSK-58	yes	yes	0.13					
MSK-59	yes	yes	1.76	0.30	>10			
MSK-60	yes	yes	1.05	0.20	>10			
MSK-61	no							
MSK-62	yes	no	1.71		2.45			

Table B.1. Results of *in* vitro gamma-secretase assay for each SPECS compound. (Continued)

			NICD		*AB40*			
Compound	**Inhibits NICD?**	**Selective?**	**Avg. IC50 (μM)**	**SD (μM)**	**Avg. IC50 (μM)**	**SD (μM)**	**Selectivity**	**Notes**
MSK-63	yes	no	3.07		10.00			
MSK-64	yes	yes	1.49		3.86			
MSK-65	yes	no	0.70		0.13			
MSK-66	yes	yes	0.71	0.21	4.19			
MSK-67	yes	no	0.57		0.43			
MSK-68	yes	yes	0.81		3.74			
MSK-69	yes	yes	0.12	0.004	>10			
MSK-70	yes	no	0.72		0.47			
MSK-71	yes	no	1.83		1.27			
MSK-72	yes	no	2.33		0.76			
MSK-73	yes	yes	0.86	0.51	4.00			
MSK-74	yes	no	1.06		1.67			
MSK-75	yes	yes	1.24		10.18			
MSK-76	yes		0.41		1.42			
MSK-77	yes	no	1.43		2.78			
MSK-78	yes	yes	0.38	0.13	>10			
MSK-79	no		>10					
MSK-80	no		>10					
MSK-81	yes	no	1.58		1.69			
MSK-82	yes	no	0.60		0.63			
MSK-83	yes	yes	2.23	1.15	≈10			
MSK-84	yes	yes	2.86	1.15	>10			
MSK-85	yes	yes	2.77		>10			
MSK-86	yes	yes	2.82	1.92	>10			

Table B.2. Chemical structures of screened SPECS compounds

Compound		Compound	
MSK-34,35	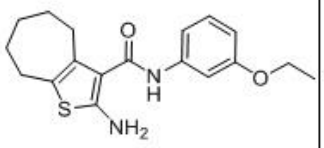	MSK-43	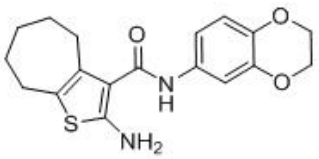
MSK-36,37	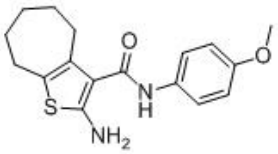	MSK-44	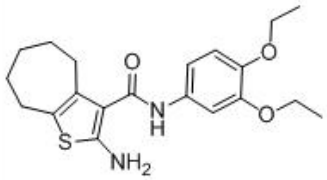
MSK-38	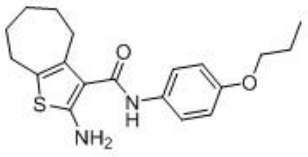	MSK-45	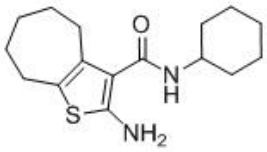
MSK-39	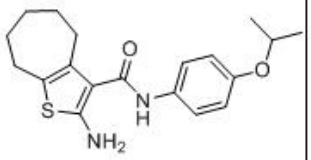	MSK-46,47	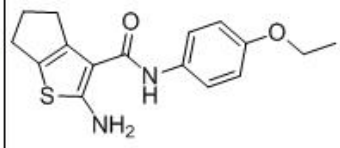
MSK-40	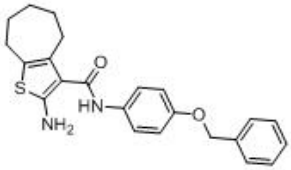	MSK-48	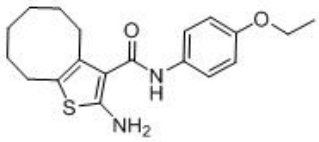
MSK-41	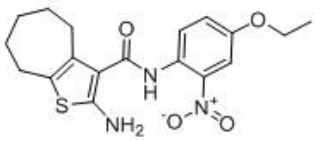	MSK-49	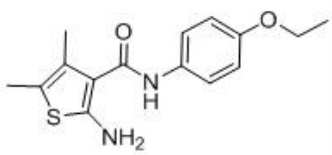
MSK-42	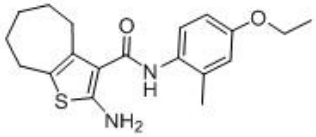	MSK-50	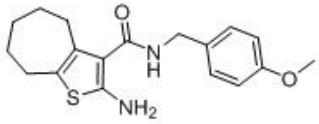

Table B.2. Chemical structures of screened SPECS compounds (continued)

Compound		Compound	
MSK-51	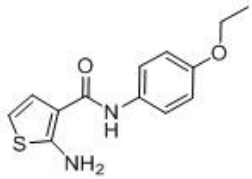	MSK-58	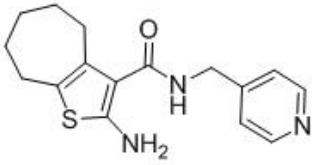
MSK-52	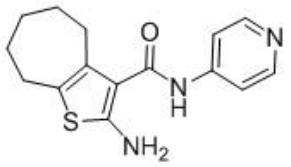	MSK-59	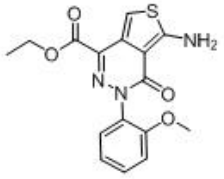
MSK-53	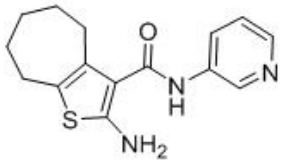	MSK-60	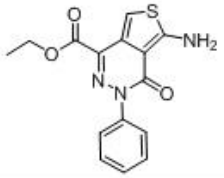
MSK-54	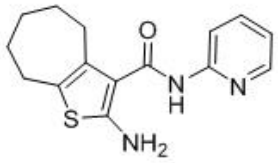	MSK-61	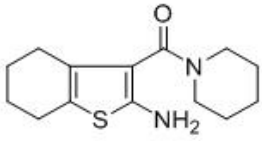
MSK-55	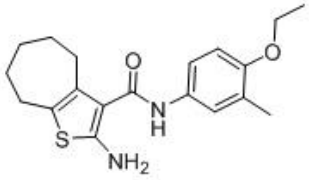	MSK-62	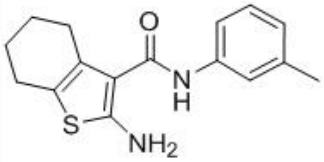
MSK-56	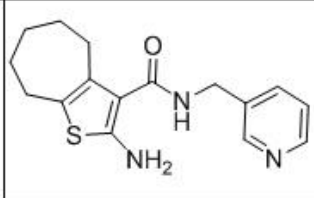	MSK-63	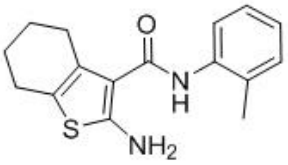
MSK-57	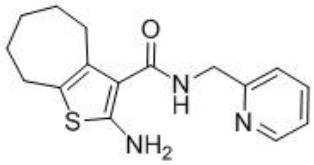	MSK-64	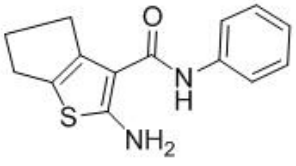

Table B.2. Chemical structures of screened SPECS compounds (continued)

Compound		Compound	
MSK-65	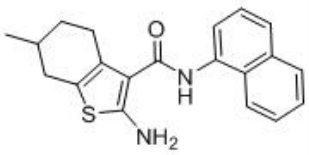	MSK-72	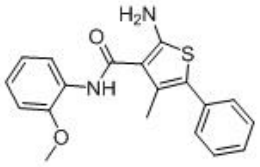
MSK-66	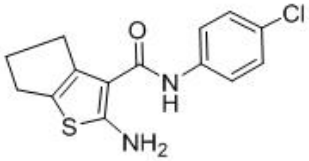	MSK-73	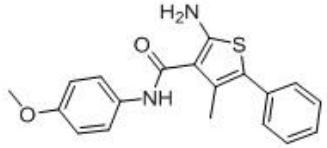
MSK-67	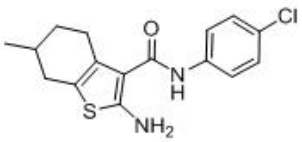	MSK-74	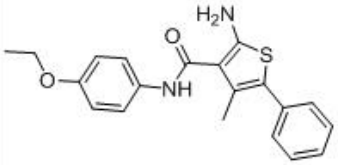
MSK-68	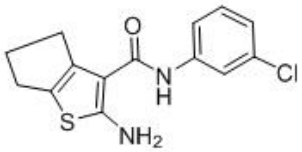	MSK-75	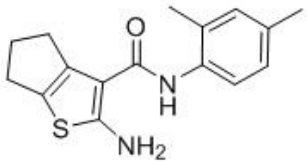
MSK-69	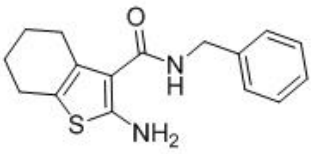	MSK-76	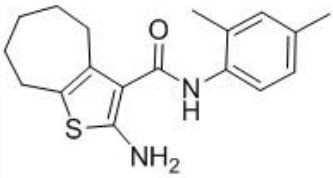
MSK-70	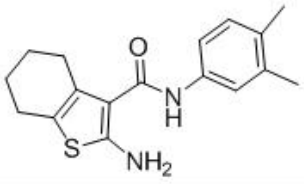	MSK-77	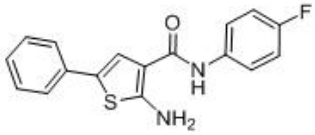
MSK-71	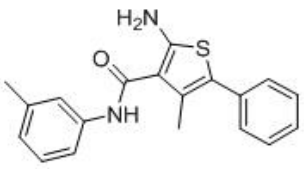	MSK-78	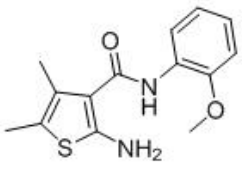

Table B.2. Chemical structures of screened SPECS compounds (continued)

Compound		Compound	
MSK-79	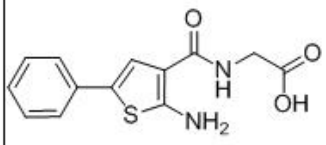	MSK-86	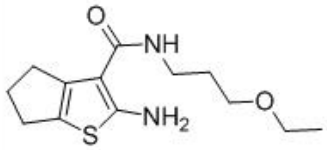
MSK-80	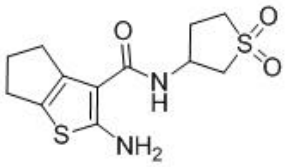		
MSK-81	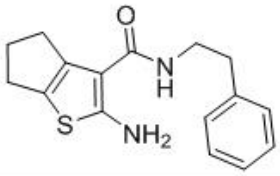		
MSK-82	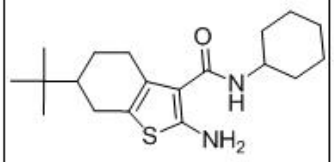		
MSK-83	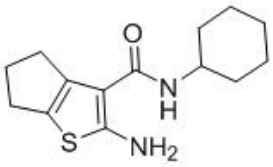		
MSK-84	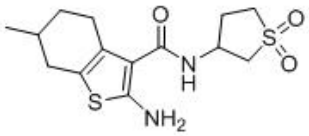		
MSK-85	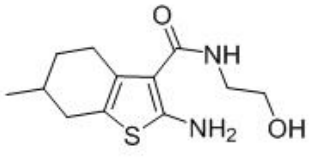		

When the most potent compounds from our screen were tested in our cell-based gamma-secretase assay, we did not detect any inhibition of Notch cleavage (Figure B.2). We hypothesize that this may be due to ionization of the free amine under physiological conditions. Potential "pro-drug" analogues that mask the free amine are currently under development.

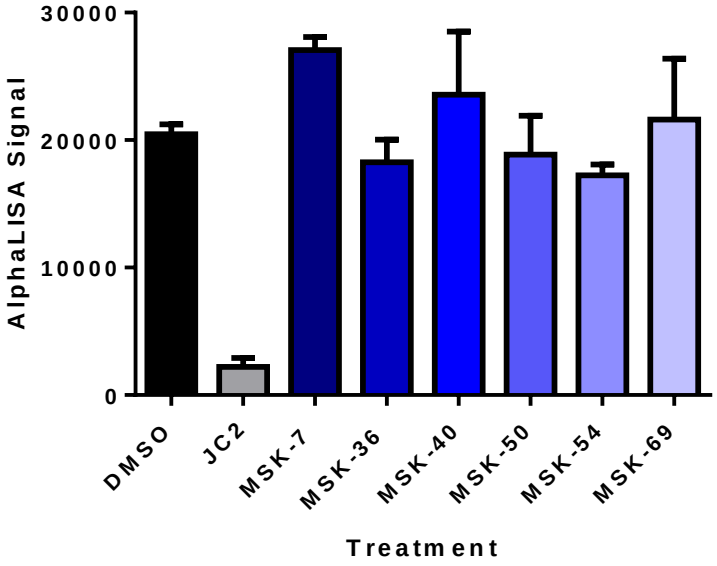

Figure B.2: SPECS compounds tested in cell-based gamma-secretase assay for Notch cleavage. None of the analogues tested exhibit NICD inhibition in cells. DMSO is the vehicle and used as a positive control, JC2, a potent gamma-secretase inhibitor used as a negative control.

APPENDIX C: *GSI-34 Optimization*

GSI-34 is a potent gamma-secretase inhibitor commonly used in the laboratory to investigate enzyme function[255]. It has also been shown to sensitize human colon adenocarcinoma cell lines to chemotherapy and was found to be synergistic with oxaliplatin, 5-FU, and SN-38 in an assay for cell viability [256]. Furthermore, GSI-34 effectively blocks migration and invasion of aggressive breast cancer lines and reduced primary tumor burden and lung metastasis in a breast cancer mouse model[61]. In an effort to further develop the sulfonamide GSI for use a potential cancer therapeutic we have generated a series of GSI-34 analogues and tested their potency in our one-pot *in vitro* gamma-secretase activity assay. The most promising compound, C21, was tested in our cellular gamma-secretase assay, but was not as effective as GSI-34 treatment (Figure C.1).

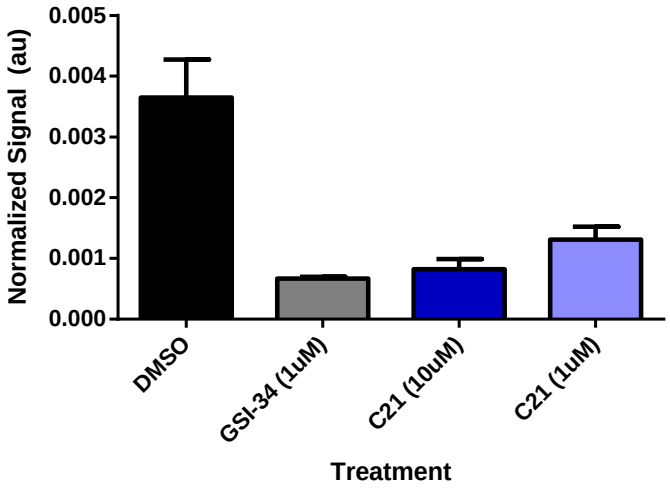

Figure C.1: Cell-based gamma-secretase activity assay. Treatment with the lead compound, C21, is not as effective as treatment with GSI-34.

Table C.1: Summary of *in vitro* gamma-secretase assay data for GSI-34 analogues.

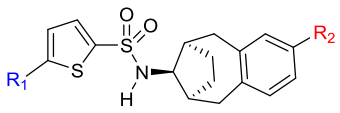

Entry	R_1	R_2	IC_{50}/nM
1	H	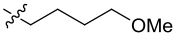	1
2	H	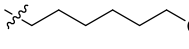	>100
3	H	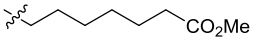	6
4	F		20
5	F		>100
6	F	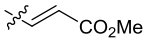	1
7	F	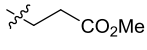	1
8	F	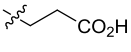	>100
9	F	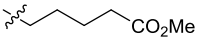	0.6
10	F	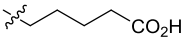	100
11	Cl		20
12	Cl		100
13	Cl	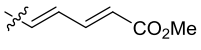	2
14	Cl	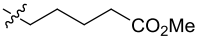	2
15	Cl	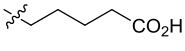	20
16	Cl	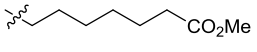	10
17	Cl	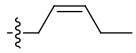	24
18	Cl	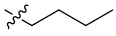	23
19	Cl	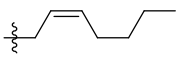	12
20	Cl	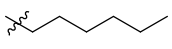	6
21	Cl	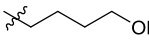	0.2
22	Cl	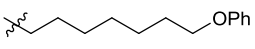	11

CHAPTER 6:

References

1. Haass, C. and D.J. Selkoe, *Cellular processing of beta-amyloid precursor protein and the genesis of amyloid beta-peptide.* Cell, 1993. **75**(6): p. 1039-42.
2. Wolfe, M.S., *Intramembrane-cleaving proteases.* J Biol Chem, 2009. **284**(21): p. 13969-73.
3. Wolfe, M.S., *Intramembrane proteolysis.* Chem Rev, 2009. **109**(4): p. 1599-612.
4. Freeman, M., *Proteolysis within the membrane: rhomboids revealed.* Nat Rev Mol Cell Biol, 2004. **5**(3): p. 188-97.
5. Suguna, K., et al., *Binding of a reduced peptide inhibitor to the aspartic proteinase from Rhizopus chinensis: implications for a mechanism of action.* Proc Natl Acad Sci U S A, 1987. **84**(20): p. 7009-13.
6. De Strooper, B., T. Iwatsubo, and M.S. Wolfe, *Presenilins and gamma-secretase: structure, function, and role in Alzheimer Disease.* Cold Spring Harb Perspect Med, 2012. **2**(1): p. a006304.
7. Wolfe, M.S., *Structure, mechanism and inhibition of gamma-secretase and presenilin-like proteases.* Biol Chem, 2010. **391**(8): p. 839-47.
8. Dries, D.R. and G. Yu, *Assembly, maturation, and trafficking of the gamma-secretase complex in Alzheimer's disease.* Curr Alzheimer Res, 2008. **5**(2): p. 132-46.
9. Edbauer, D., et al., *Reconstitution of gamma-secretase activity.* Nat Cell Biol, 2003. **5**(5): p. 486-8.
10. Sato, T., et al., *Active gamma-secretase complexes contain only one of each component.* J Biol Chem, 2007. **282**(47): p. 33985-93.
11. Thinakaran, G., et al., *Endoproteolysis of presenilin 1 and accumulation of processed derivatives in vivo.* Neuron, 1996. **17**(1): p. 181-90.
12. Ahn, K., et al., *Activation and intrinsic gamma-secretase activity of presenilin 1.* Proc Natl Acad Sci U S A, 2010. **107**(50): p. 21435-40.
13. Beher, D., et al., *Selected non-steroidal anti-inflammatory drugs and their derivatives target gamma-secretase at a novel site. Evidence for an allosteric mechanism.* J Biol Chem, 2004. **279**(42): p. 43419-26.
14. Lai, M.T., et al., *Presenilin-1 and presenilin-2 exhibit distinct yet overlapping gamma-secretase activities.* J Biol Chem, 2003. **278**(25): p. 22475-81.
15. Gu, Y., et al., *The presenilin proteins are components of multiple membrane-bound complexes that have different biological activities.* J Biol Chem, 2004. **279**(30): p. 31329-36.
16. Alzheimer's Disease Collaborative, G., *The structure of the presenilin 1 (S182) gene and identification of six novel mutations in early onset AD families.* Nat Genet, 1995. **11**(2): p. 219-22.
17. Sherrington, R., et al., *Cloning of a gene bearing missense mutations in early-onset familial Alzheimer's disease.* Nature, 1995. **375**(6534): p. 754-60.
18. Levy-Lahad, E., et al., *Candidate gene for the chromosome 1 familial Alzheimer's disease locus.* Science, 1995. **269**(5226): p. 973-7.

19. Levitan, D. and I. Greenwald, *Facilitation of lin-12-mediated signalling by sel-12, a Caenorhabditis elegans S182 Alzheimer's disease gene.* Nature, 1995. **377**(6547): p. 351-4.
20. Scheuner, D., et al., *Secreted amyloid beta-protein similar to that in the senile plaques of Alzheimer's disease is increased in vivo by the presenilin 1 and 2 and APP mutations linked to familial Alzheimer's disease.* Nat Med, 1996. **2**(8): p. 864-70.
21. Borchelt, D.R., et al., *Familial Alzheimer's disease-linked presenilin 1 variants elevate Abeta1-42/1-40 ratio in vitro and in vivo.* Neuron, 1996. **17**(5): p. 1005-13.
22. Citron, M., et al., *Mutant presenilins of Alzheimer's disease increase production of 42-residue amyloid beta-protein in both transfected cells and transgenic mice.* Nat Med, 1997. **3**(1): p. 67-72.
23. Duff, K., et al., *Increased amyloid-beta42(43) in brains of mice expressing mutant presenilin 1.* Nature, 1996. **383**(6602): p. 710-3.
24. Siman, R., et al., *Presenilin-1 P264L knock-in mutation: differential effects on abeta production, amyloid deposition, and neuronal vulnerability.* J Neurosci, 2000. **20**(23): p. 8717-26.
25. Flood, D.G., et al., *FAD mutant PS-1 gene-targeted mice: increased A beta 42 and A beta deposition without APP overproduction.* Neurobiol Aging, 2002. **23**(3): p. 335-48.
26. De Strooper, B., et al., *Deficiency of presenilin-1 inhibits the normal cleavage of amyloid precursor protein.* Nature, 1998. **391**(6665): p. 387-90.
27. De Strooper, B., et al., *A presenilin-1-dependent gamma-secretase-like protease mediates release of Notch intracellular domain.* Nature, 1999. **398**(6727): p. 518-22.
28. Struhl, G. and I. Greenwald, *Presenilin is required for activity and nuclear access of Notch in Drosophila.* Nature, 1999. **398**(6727): p. 522-5.
29. Wolfe, M.S., et al., *Two transmembrane aspartates in presenilin-1 required for presenilin endoproteolysis and gamma-secretase activity.* Nature, 1999. **398**(6727): p. 513-7.
30. Steiner, H., et al., *Glycine 384 is required for presenilin-1 function and is conserved in bacterial polytopic aspartyl proteases.* Nat Cell Biol, 2000. **2**(11): p. 848-51.
31. Li, Y.M., et al., *Photoactivated gamma-secretase inhibitors directed to the active site covalently label presenilin 1.* Nature, 2000. **405**(6787): p. 689-94.
32. Laudon, H., et al., *A nine-transmembrane domain topology for presenilin 1.* J Biol Chem, 2005. **280**(42): p. 35352-60.
33. Spasic, D., et al., *Presenilin-1 maintains a nine-transmembrane topology throughout the secretory pathway.* J Biol Chem, 2006. **281**(36): p. 26569-77.
34. Lee, J.H., et al., *Lysosomal proteolysis and autophagy require presenilin 1 and are disrupted by Alzheimer-related PS1 mutations.* Cell, 2010. **141**(7): p. 1146-58.
35. Nyabi, O., et al., *Presenilins mutated at Asp-257 or Asp-385 restore Pen-2 expression and Nicastrin glycosylation but remain catalytically inactive in the absence of wild type Presenilin.* J Biol Chem, 2003. **278**(44): p. 43430-6.
36. Levitan, D., et al., *PS1 N- and C-terminal fragments form a complex that functions in APP processing and Notch signaling.* Proc Natl Acad Sci U S A, 2001. **98**(21): p. 12186-90.
37. Yu, G., et al., *Nicastrin modulates presenilin-mediated notch/glp-1 signal transduction and betaAPP processing.* Nature, 2000. **407**(6800): p. 48-54.

38. LaVoie, M.J., et al., *Assembly of the gamma-secretase complex involves early formation of an intermediate subcomplex of Aph-1 and nicastrin.* J Biol Chem, 2003. **278**(39): p. 37213-22.
39. Dries, D.R., et al., *Glu-333 of nicastrin directly participates in gamma-secretase activity.* J Biol Chem, 2009. **284**(43): p. 29714-24.
40. Chavez-Gutierrez, L., et al., *Glu(332) in the Nicastrin ectodomain is essential for gamma-secretase complex maturation but not for its activity.* J Biol Chem, 2008. **283**(29): p. 20096-105.
41. Chen, F., et al., *Nicastrin binds to membrane-tethered Notch.* Nat Cell Biol, 2001. **3**(8): p. 751-4.
42. Shah, S., et al., *Nicastrin functions as a gamma-secretase-substrate receptor.* Cell, 2005. **122**(3): p. 435-47.
43. Hayashi, I., et al., *Neutralization of the gamma-secretase activity by monoclonal antibody against extracellular domain of nicastrin.* Oncogene, 2012. **31**(6): p. 787-98.
44. Zhang, X., et al., *Identification of a tetratricopeptide repeat-like domain in the nicastrin subunit of gamma-secretase using synthetic antibodies.* Proc Natl Acad Sci U S A, 2012. **109**(22): p. 8534-9.
45. Pamren, A., et al., *Mutations in nicastrin protein differentially affect amyloid beta-peptide production and Notch protein processing.* J Biol Chem, 2011. **286**(36): p. 31153-8.
46. Zhao, G., et al., *Gamma-secretase composed of PS1/Pen2/Aph1a can cleave notch and amyloid precursor protein in the absence of nicastrin.* J Neurosci, 2010. **30**(5): p. 1648-56.
47. Francis, R., et al., *aph-1 and pen-2 are required for Notch pathway signaling, gamma-secretase cleavage of betaAPP, and presenilin protein accumulation.* Dev Cell, 2002. **3**(1): p. 85-97.
48. Takasugi, N., et al., *The role of presenilin cofactors in the gamma-secretase complex.* Nature, 2003. **422**(6930): p. 438-41.
49. Luo, W.J., et al., *PEN-2 and APH-1 coordinately regulate proteolytic processing of presenilin 1.* J Biol Chem, 2003. **278**(10): p. 7850-4.
50. Bammens, L., et al., *Functional and topological analysis of Pen-2, the fourth subunit of the gamma-secretase complex.* J Biol Chem, 2011. **286**(14): p. 12271-82.
51. Placanica, L., et al., *Pen2 and presenilin-1 modulate the dynamic equilibrium of presenilin-1 and presenilin-2 gamma-secretase complexes.* J Biol Chem, 2009. **284**(5): p. 2967-77.
52. Levitan, D., et al., *APH-2/nicastrin functions in LIN-12/Notch signaling in the Caenorhabditis elegans somatic gonad.* Dev Biol, 2001. **240**(2): p. 654-61.
53. Goutte, C., et al., *APH-1 is a multipass membrane protein essential for the Notch signaling pathway in Caenorhabditis elegans embryos.* Proc Natl Acad Sci U S A, 2002. **99**(2): p. 775-9.
54. Shirotani, K., et al., *Immature nicastrin stabilizes APH-1 independent of PEN-2 and presenilin: identification of nicastrin mutants that selectively interact with APH-1.* J Neurochem, 2004. **89**(6): p. 1520-7.
55. Serneels, L., et al., *gamma-Secretase heterogeneity in the Aph1 subunit: relevance for Alzheimer's disease.* Science, 2009. **324**(5927): p. 639-42.
56. Shirotani, K., et al., *Identification of distinct gamma-secretase complexes with different APH-1 variants.* J Biol Chem, 2004. **279**(40): p. 41340-5.

57. Haapasalo, A. and D.M. Kovacs, *The many substrates of presenilin/gamma-secretase.* J Alzheimers Dis, 2011. **25**(1): p. 3-28.
58. Lleo, A., *Activity of gamma-secretase on substrates other than APP.* Curr Top Med Chem, 2008. **8**(1): p. 9-16.
59. Herreman, A., et al., *Presenilin 2 deficiency causes a mild pulmonary phenotype and no changes in amyloid precursor protein processing but enhances the embryonic lethal phenotype of presenilin 1 deficiency.* Proc Natl Acad Sci U S A, 1999. **96**(21): p. 11872-7.
60. Lee, J., et al., *Identification of presenilin 1-selective gamma-secretase inhibitors with reconstituted gamma-secretase complexes.* Biochemistry, 2011. **50**(22): p. 4973-80.
61. Villa, J.C., et al., *Nontranscriptional role of Hif-1alpha in activation of gamma-secretase and notch signaling in breast cancer.* Cell Rep, 2014. **8**(4): p. 1077-92.
62. He, G., et al., *Gamma-secretase activating protein is a therapeutic target for Alzheimer's disease.* Nature, 2010. **467**(7311): p. 95-8.
63. Chu, J., et al., *Pharmacological modulation of GSAP reduces amyloid-beta levels and tau phosphorylation in a mouse model of Alzheimer's disease with plaques and tangles.* J Alzheimers Dis, 2014. **41**(3): p. 729-37.
64. Tian, Y., et al., *An APP inhibitory domain containing the Flemish mutation residue modulates gamma-secretase activity for Abeta production.* Nat Struct Mol Biol, 2010. **17**(2): p. 151-8.
65. Esler, W.P., et al., *Activity-dependent isolation of the presenilin- gamma -secretase complex reveals nicastrin and a gamma substrate.* Proc Natl Acad Sci U S A, 2002. **99**(5): p. 2720-5.
66. Beher, D., et al., *In vitro characterization of the presenilin-dependent gamma-secretase complex using a novel affinity ligand.* Biochemistry, 2003. **42**(27): p. 8133-42.
67. Tian, G., et al., *The mechanism of gamma-secretase: multiple inhibitor binding sites for transition state analogs and small molecule inhibitors.* J Biol Chem, 2003. **278**(31): p. 28968-75.
68. Tian, G., et al., *Linear non-competitive inhibition of solubilized human gamma-secretase by pepstatin A methylester, L685458, sulfonamides, and benzodiazepines.* J Biol Chem, 2002. **277**(35): p. 31499-505.
69. Berezovska, O., et al., *Amyloid precursor protein associates with a nicastrin-dependent docking site on the presenilin 1-gamma-secretase complex in cells demonstrated by fluorescence lifetime imaging.* J Neurosci, 2003. **23**(11): p. 4560-6.
70. Kornilova, A.Y., et al., *The initial substrate-binding site of gamma-secretase is located on presenilin near the active site.* Proc Natl Acad Sci U S A, 2005. **102**(9): p. 3230-5.
71. Annaert, W.G., et al., *Presenilin 1 controls gamma-secretase processing of amyloid precursor protein in pre-golgi compartments of hippocampal neurons.* J Cell Biol, 1999. **147**(2): p. 277-94.
72. Pasternak, S.H., et al., *Presenilin-1, nicastrin, amyloid precursor protein, and gamma-secretase activity are co-localized in the lysosomal membrane.* J Biol Chem, 2003. **278**(29): p. 26687-94.
73. Ray, W.J., et al., *Cell surface presenilin-1 participates in the gamma-secretase-like proteolysis of Notch.* J Biol Chem, 1999. **274**(51): p. 36801-7.
74. Vassar, R., et al., *Beta-secretase cleavage of Alzheimer's amyloid precursor protein by the transmembrane aspartic protease BACE.* Science, 1999. **286**(5440): p. 735-41.

75. Sannerud, R., et al., *Restricted Location of PSEN2/gamma-Secretase Determines Substrate Specificity and Generates an Intracellular Abeta Pool.* Cell, 2016.
76. Carroll, C.M. and Y.M. Li, *Physiological and pathological roles of the gamma-secretase complex.* Brain Res Bull, 2016.
77. Beel, A.J. and C.R. Sanders, *Substrate specificity of gamma-secretase and other intramembrane proteases.* Cell Mol Life Sci, 2008. **65**(9): p. 1311-34.
78. Bekris, L.M., et al., *Genetics of Alzheimer disease.* J Geriatr Psychiatry Neurol, 2010. **23**(4): p. 213-27.
79. Selkoe, D.J. and J. Hardy, *The amyloid hypothesis of Alzheimer's disease at 25 years.* EMBO Mol Med, 2016. **8**(6): p. 595-608.
80. Zheng, H. and E.H. Koo, *Biology and pathophysiology of the amyloid precursor protein.* Mol Neurodegener, 2011. **6**(1): p. 27.
81. Takami, M., et al., *gamma-Secretase: successive tripeptide and tetrapeptide release from the transmembrane domain of beta-carboxyl terminal fragment.* J Neurosci, 2009. **29**(41): p. 13042-52.
82. Fukumori, A., et al., *Three-amino acid spacing of presenilin endoproteolysis suggests a general stepwise cleavage of gamma-secretase-mediated intramembrane proteolysis.* J Neurosci, 2010. **30**(23): p. 7853-62.
83. Hecimovic, S., et al., *Mutations in APP have independent effects on Abeta and CTFgamma generation.* Neurobiol Dis, 2004. **17**(2): p. 205-18.
84. Page, R.M., et al., *Generation of Abeta38 and Abeta42 is independently and differentially affected by familial Alzheimer disease-associated presenilin mutations and gamma-secretase modulation.* J Biol Chem, 2008. **283**(2): p. 677-83.
85. Czirr, E., et al., *Independent generation of Abeta42 and Abeta38 peptide species by gamma-secretase.* J Biol Chem, 2008. **283**(25): p. 17049-54.
86. Lammich, S., et al., *Constitutive and regulated alpha-secretase cleavage of Alzheimer's amyloid precursor protein by a disintegrin metalloprotease.* Proc Natl Acad Sci U S A, 1999. **96**(7): p. 3922-7.
87. Postina, R., et al., *A disintegrin-metalloproteinase prevents amyloid plaque formation and hippocampal defects in an Alzheimer disease mouse model.* J Clin Invest, 2004. **113**(10): p. 1456-64.
88. Iwatsubo, T., et al., *Visualization of A beta 42(43) and A beta 40 in senile plaques with end-specific A beta monoclonals: evidence that an initially deposited species is A beta 42(43).* Neuron, 1994. **13**(1): p. 45-53.
89. Kuperstein, I., et al., *Neurotoxicity of Alzheimer's disease Abeta peptides is induced by small changes in the Abeta42 to Abeta40 ratio.* EMBO J, 2010. **29**(19): p. 3408-20.
90. Kumar-Singh, S., et al., *Mean age-of-onset of familial alzheimer disease caused by presenilin mutations correlates with both increased Abeta42 and decreased Abeta40.* Hum Mutat, 2006. **27**(7): p. 686-95.
91. Jonsson, T., et al., *A mutation in APP protects against Alzheimer's disease and age-related cognitive decline.* Nature, 2012. **488**(7409): p. 96-9.
92. Corder, E.H., et al., *Gene dose of apolipoprotein E type 4 allele and the risk of Alzheimer's disease in late onset families.* Science, 1993. **261**(5123): p. 921-3.
93. Ward, A., et al., *Prevalence of apolipoprotein E4 genotype and homozygotes (APOE e4/4) among patients diagnosed with Alzheimer's disease: a systematic review and meta-analysis.* Neuroepidemiology, 2012. **38**(1): p. 1-17.

94. Kim, J., J.M. Basak, and D.M. Holtzman, *The role of apolipoprotein E in Alzheimer's disease.* Neuron, 2009. **63**(3): p. 287-303.
95. Mohr, O.L., *Character Changes Caused by Mutation of an Entire Region of a Chromosome in Drosophila.* Genetics, 1919. **4**(3): p. 275-82.
96. Artavanis-Tsakonas, S., M.D. Rand, and R.J. Lake, *Notch signaling: cell fate control and signal integration in development.* Science, 1999. **284**(5415): p. 770-6.
97. Kopan, R. and M.X. Ilagan, *The canonical Notch signaling pathway: unfolding the activation mechanism.* Cell, 2009. **137**(2): p. 216-33.
98. Kovall, R.A. and S.C. Blacklow, *Mechanistic insights into Notch receptor signaling from structural and biochemical studies.* Curr Top Dev Biol, 2010. **92**: p. 31-71.
99. Rand, M.D., et al., *Calcium depletion dissociates and activates heterodimeric notch receptors.* Mol Cell Biol, 2000. **20**(5): p. 1825-35.
100. Guruharsha, K.G., M.W. Kankel, and S. Artavanis-Tsakonas, *The Notch signalling system: recent insights into the complexity of a conserved pathway.* Nat Rev Genet, 2012. **13**(9): p. 654-66.
101. Fischer, A. and M. Gessler, *Delta-Notch--and then? Protein interactions and proposed modes of repression by Hes and Hey bHLH factors.* Nucleic Acids Res, 2007. **35**(14): p. 4583-96.
102. Ellisen, L.W., et al., *TAN-1, the human homolog of the Drosophila notch gene, is broken by chromosomal translocations in T lymphoblastic neoplasms.* Cell, 1991. **66**(4): p. 649-61.
103. Weng, A.P., et al., *Activating mutations of NOTCH1 in human T cell acute lymphoblastic leukemia.* Science, 2004. **306**(5694): p. 269-71.
104. Houde, C., et al., *Overexpression of the NOTCH ligand JAG2 in malignant plasma cells from multiple myeloma patients and cell lines.* Blood, 2004. **104**(12): p. 3697-704.
105. Chiaramonte, R., et al., *A wide role for NOTCH1 signaling in acute leukemia.* Cancer Lett, 2005. **219**(1): p. 113-20.
106. Fabbri, G., et al., *Analysis of the chronic lymphocytic leukemia coding genome: role of NOTCH1 mutational activation.* J Exp Med, 2011. **208**(7): p. 1389-401.
107. Ranganathan, P., K.L. Weaver, and A.J. Capobianco, *Notch signalling in solid tumours: a little bit of everything but not all the time.* Nat Rev Cancer, 2011. **11**(5): p. 338-51.
108. Hanlon, L., et al., *Notch1 functions as a tumor suppressor in a model of K-ras-induced pancreatic ductal adenocarcinoma.* Cancer Res, 2010. **70**(11): p. 4280-6.
109. Plentz, R., et al., *Inhibition of gamma-secretase activity inhibits tumor progression in a mouse model of pancreatic ductal adenocarcinoma.* Gastroenterology, 2009. **136**(5): p. 1741-9 e6.
110. Puente, X.S., et al., *Whole-genome sequencing identifies recurrent mutations in chronic lymphocytic leukaemia.* Nature, 2011. **475**(7354): p. 101-5.
111. Thiery, J.P., et al., *Epithelial-mesenchymal transitions in development and disease.* Cell, 2009. **139**(5): p. 871-90.
112. Li, Y.M., et al., *Presenilin 1 is linked with gamma-secretase activity in the detergent solubilized state.* Proc Natl Acad Sci U S A, 2000. **97**(11): p. 6138-43.
113. Chun, J., et al., *Stereoselective synthesis of photoreactive peptidomimetic gamma-secretase inhibitors.* J Org Chem, 2004. **69**(21): p. 7344-7.
114. Tarassishin, L., et al., *Processing of Notch and amyloid precursor protein by gamma-secretase is spatially distinct.* Proc Natl Acad Sci U S A, 2004. **101**(49): p. 17050-5.

115. Placanica, L., J.W. Chien, and Y.M. Li, *Characterization of an atypical gamma-secretase complex from hematopoietic origin.* Biochemistry, 2010. **49**(13): p. 2796-804.
116. Shelton, C.C., et al., *Modulation of gamma-secretase specificity using small molecule allosteric inhibitors.* Proc Natl Acad Sci U S A, 2009. **106**(48): p. 20228-33.
117. Crump, C.J., et al., *Development of clickable active site-directed photoaffinity probes for gamma-secretase.* Bioorg Med Chem Lett, 2012. **22**(8): p. 2997-3000.
118. Gertsik, N., D.M. Chau, and Y.M. Li, *gamma-Secretase Inhibitors and Modulators Induce Distinct Conformational Changes in the Active Sites of gamma-Secretase and Signal Peptide Peptidase.* ACS Chem Biol, 2015. **10**(8): p. 1925-31.
119. Doody, R.S., et al., *A phase 3 trial of semagacestat for treatment of Alzheimer's disease.* N Engl J Med, 2013. **369**(4): p. 341-50.
120. Martone, R.L., et al., *Begacestat (GSI-953): a novel, selective thiophene sulfonamide inhibitor of amyloid precursor protein gamma-secretase for the treatment of Alzheimer's disease.* J Pharmacol Exp Ther, 2009. **331**(2): p. 598-608.
121. Gillman, K.W., et al., *Discovery and Evaluation of BMS-708163, a Potent, Selective and Orally Bioavailable gamma-Secretase Inhibitor.* ACS Med Chem Lett, 2010. **1**(3): p. 120-4.
122. Chavez-Gutierrez, L., et al., *The mechanism of gamma-Secretase dysfunction in familial Alzheimer disease.* EMBO J, 2012. **31**(10): p. 2261-74.
123. Crump, C.J., et al., *BMS-708,163 targets presenilin and lacks notch-sparing activity.* Biochemistry, 2012. **51**(37): p. 7209-11.
124. Coric, V., et al., *Safety and tolerability of the gamma-secretase inhibitor avagacestat in a phase 2 study of mild to moderate Alzheimer disease.* Arch Neurol, 2012. **69**(11): p. 1430-40.
125. Zheng, H. and E.H. Koo, *The amyloid precursor protein: beyond amyloid.* Mol Neurodegener, 2006. **1**: p. 5.
126. Mitani, Y., et al., *Differential effects between gamma-secretase inhibitors and modulators on cognitive function in amyloid precursor protein-transgenic and nontransgenic mice.* J Neurosci, 2012. **32**(6): p. 2037-50.
127. Yin, Y.I., et al., *{gamma}-Secretase Substrate Concentration Modulates the Abeta42/Abeta40 Ratio: IMPLICATIONS FOR ALZHEIMER DISEASE.* J Biol Chem, 2007. **282**(32): p. 23639-44.
128. Weggen, S., et al., *A subset of NSAIDs lower amyloidogenic Abeta42 independently of cyclooxygenase activity.* Nature, 2001. **414**(6860): p. 212-6.
129. Green, R.C., et al., *Effect of tarenflurbil on cognitive decline and activities of daily living in patients with mild Alzheimer disease: a randomized controlled trial.* JAMA, 2009. **302**(23): p. 2557-64.
130. Crump, C.J., D.S. Johnson, and Y.M. Li, *Development and mechanism of gamma-secretase modulators for Alzheimer's disease.* Biochemistry, 2013. **52**(19): p. 3197-216.
131. Narlawar, R., et al., *Conversion of the LXR-agonist TO-901317--from inverse to normal modulation of gamma-secretase by addition of a carboxylic acid and a lipophilic anchor.* Bioorg Med Chem Lett, 2007. **17**(19): p. 5428-31.
132. Zall, A., et al., *NSAID-derived gamma-secretase modulation requires an acidic moiety on the carbazole scaffold.* Bioorg Med Chem, 2011. **19**(16): p. 4903-9.

133. Portelius, E., et al., *Acute effect on the Abeta isoform pattern in CSF in response to gamma-secretase modulator and inhibitor treatment in dogs.* J Alzheimers Dis, 2010. **21**(3): p. 1005-12.
134. Borgegard, T., et al., *First and second generation gamma-secretase modulators (GSMs) modulate amyloid-beta (Abeta) peptide production through different mechanisms.* J Biol Chem, 2012. **287**(15): p. 11810-9.
135. Takahashi, Y., et al., *Sulindac sulfide is a noncompetitive gamma-secretase inhibitor that preferentially reduces Abeta 42 generation.* J Biol Chem, 2003. **278**(20): p. 18664-70.
136. Clarke, E.E., et al., *Intra- or intercomplex binding to the gamma-secretase enzyme. A model to differentiate inhibitor classes.* J Biol Chem, 2006. **281**(42): p. 31279-89.
137. Kukar, T. and T.E. Golde, *Possible mechanisms of action of NSAIDs and related compounds that modulate gamma-secretase cleavage.* Curr Top Med Chem, 2008. **8**(1): p. 47-53.
138. Kukar, T.L., et al., *Substrate-targeting gamma-secretase modulators.* Nature, 2008. **453**(7197): p. 925-9.
139. Botev, A., et al., *The amyloid precursor protein C-terminal fragment C100 occurs in monomeric and dimeric stable conformations and binds gamma-secretase modulators.* Biochemistry, 2011. **50**(5): p. 828-35.
140. Lleo, A., et al., *Nonsteroidal anti-inflammatory drugs lower Abeta42 and change presenilin 1 conformation.* Nat Med, 2004. **10**(10): p. 1065-6.
141. Uemura, K., et al., *Substrate docking to gamma-secretase allows access of gamma-secretase modulators to an allosteric site.* Nat Commun, 2010. **1**: p. 130.
142. Crump, C.J., et al., *Piperidine acetic acid based gamma-secretase modulators directly bind to Presenilin-1.* ACS Chem Neurosci, 2011. **2**(12): p. 705-710.
143. Crump, C.J., D.S. Johnson, and Y.M. Li, *Target of gamma-secretase modulators, presenilin marks the spot.* EMBO J, 2011. **30**(23): p. 4696-8.
144. Ebke, A., et al., *Novel gamma-secretase enzyme modulators directly target presenilin protein.* J Biol Chem, 2011. **286**(43): p. 37181-6.
145. Ohki, Y., et al., *Phenylpiperidine-type gamma-secretase modulators target the transmembrane domain 1 of presenilin 1.* EMBO J, 2011. **30**(23): p. 4815-24.
146. Jumpertz, T., et al., *Presenilin is the molecular target of acidic gamma-secretase modulators in living cells.* PLoS One, 2012. **7**(1): p. e30484.
147. Pozdnyakov, N., et al., *gamma-Secretase modulator (GSM) photoaffinity probes reveal distinct allosteric binding sites on presenilin.* J Biol Chem, 2013. **288**(14): p. 9710-20.
148. De Strooper, B., *Lessons from a failed gamma-secretase Alzheimer trial.* Cell, 2014. **159**(4): p. 721-6.
149. So, J.Y., et al., *HES1-mediated inhibition of Notch1 signaling by a Gemini vitamin D analog leads to decreased CD44(+)/CD24(-/low) tumor-initiating subpopulation in basal-like breast cancer.* J Steroid Biochem Mol Biol, 2015. **148**: p. 111-21.
150. Huynh, C., et al., *The novel gamma secretase inhibitor RO4929097 reduces the tumor initiating potential of melanoma.* PLoS One, 2011. **6**(9): p. e25264.
151. Tolcher, A.W., et al., *Phase I study of RO4929097, a gamma secretase inhibitor of Notch signaling, in patients with refractory metastatic or locally advanced solid tumors.* J Clin Oncol, 2012. **30**(19): p. 2348-53.

152. Strosberg, J.R., et al., *A phase II study of RO4929097 in metastatic colorectal cancer.* Eur J Cancer, 2012. **48**(7): p. 997-1003.
153. Kolb, E.A., et al., *Initial testing (stage 1) by the pediatric preclinical testing program of RO4929097, a gamma-secretase inhibitor targeting notch signaling.* Pediatr Blood Cancer, 2012. **58**(5): p. 815-8.
154. LoConte, N.K., et al., *A multicenter phase 1 study of gamma -secretase inhibitor RO4929097 in combination with capecitabine in refractory solid tumors.* Invest New Drugs, 2015. **33**(1): p. 169-76.
155. Richter, S., et al., *A phase I study of the oral gamma secretase inhibitor R04929097 in combination with gemcitabine in patients with advanced solid tumors (PHL-078/CTEP 8575).* Invest New Drugs, 2014. **32**(2): p. 243-9.
156. Sahebjam, S., et al., *A phase I study of the combination of ro4929097 and cediranib in patients with advanced solid tumours (PJC-004/NCI 8503).* Br J Cancer, 2013. **109**(4): p. 943-9.
157. Debeb, B.G., et al., *Pre-clinical studies of Notch signaling inhibitor RO4929097 in inflammatory breast cancer cells.* Breast Cancer Res Treat, 2012. **134**(2): p. 495-510.
158. Schott, A.F., et al., *Preclinical and clinical studies of gamma secretase inhibitors with docetaxel on human breast tumors.* Clin Cancer Res, 2013. **19**(6): p. 1512-24.
159. Krop, I., et al., *Phase I pharmacologic and pharmacodynamic study of the gamma secretase (Notch) inhibitor MK-0752 in adult patients with advanced solid tumors.* J Clin Oncol, 2012. **30**(19): p. 2307-13.
160. Fouladi, M., et al., *Phase I trial of MK-0752 in children with refractory CNS malignancies: a pediatric brain tumor consortium study.* J Clin Oncol, 2011. **29**(26): p. 3529-34.
161. Lin, C.Y., K.Q. Barry-Holson, and K.H. Allison, *Breast cancer stem cells: are we ready to go from bench to bedside?* Histopathology, 2016. **68**(1): p. 119-37.
162. Yuan, X., et al., *Notch signaling: an emerging therapeutic target for cancer treatment.* Cancer Lett, 2015. **369**(1): p. 20-7.
163. Lopez-Guerra, M., et al., *The gamma-secretase inhibitor PF-03084014 combined with fludarabine antagonizes migration, invasion and angiogenesis in NOTCH1-mutated CLL cells.* Leukemia, 2015. **29**(1): p. 96-106.
164. Messersmith, W.A., et al., *A Phase I, dose-finding study in patients with advanced solid malignancies of the oral gamma-secretase inhibitor PF-03084014.* Clin Cancer Res, 2015. **21**(1): p. 60-7.
165. Bai, X.C., et al., *An atomic structure of human gamma-secretase.* Nature, 2015. **525**(7568): p. 212-7.
166. Chau, D.M., et al., *Familial Alzheimer disease presenilin-1 mutations alter the active site conformation of gamma-secretase.* J Biol Chem, 2012. **287**(21): p. 17288-96.
167. Shih Ie, M. and T.L. Wang, *Notch signaling, gamma-secretase inhibitors, and cancer therapy.* Cancer Res, 2007. **67**(5): p. 1879-82.
168. Karran, E., M. Mercken, and B. De Strooper, *The amyloid cascade hypothesis for Alzheimer's disease: an appraisal for the development of therapeutics.* Nat Rev Drug Discov, 2011. **10**(9): p. 698-712.
169. Groth, C. and M.E. Fortini, *Therapeutic approaches to modulating Notch signaling: current challenges and future prospects.* Semin Cell Dev Biol, 2012. **23**(4): p. 465-72.
170. Cheng, X.J., et al., *Sodium Chloride Increases Abeta Levels by Suppressing Abeta Clearance in Cultured Cells.* PLoS One, 2015. **10**(6): p. e0130432.

171. Maia, L.F., et al., *Changes in amyloid-beta and Tau in the cerebrospinal fluid of transgenic mice overexpressing amyloid precursor protein.* Sci Transl Med, 2013. **5**(194): p. 194re2.
172. Xiong, Z., et al., *Curcumin mediates presenilin-1 activity to reduce beta-amyloid production in a model of Alzheimer's Disease.* Pharmacol Rep, 2011. **63**(5): p. 1101-8.
173. Frykman, S., et al., *Identification of two novel synaptic gamma-secretase associated proteins that affect amyloid beta-peptide levels without altering Notch processing.* Neurochem Int, 2012. **61**(1): p. 108-18.
174. Feyt, C., et al., *Phosphorylation of APP695 at Thr668 decreases gamma-cleavage and extracellular Abeta.* Biochem Biophys Res Commun, 2007. **357**(4): p. 1004-10.
175. Luistro, L., et al., *Preclinical profile of a potent gamma-secretase inhibitor targeting notch signaling with in vivo efficacy and pharmacodynamic properties.* Cancer Res, 2009. **69**(19): p. 7672-80.
176. Wei, P., et al., *Evaluation of selective gamma-secretase inhibitor PF-03084014 for its antitumor efficacy and gastrointestinal safety to guide optimal clinical trial design.* Mol Cancer Ther, 2010. **9**(6): p. 1618-28.
177. Feng, Z., H. Wen, and Q. Liao, *[Expression of Notch1, Jagged1 and NICD in epithelial ovarian carcinomas and a preliminary study on the activity of gamma-secretase in epithelial ovarian carcinoma cell lines].* Zhonghua Fu Chan Ke Za Zhi, 2014. **49**(10): p. 780-6.
178. Ilagan, M.X. and R. Kopan, *Monitoring Notch activation in cultured mammalian cells: luciferase complementation imaging assays.* Methods Mol Biol, 2014. **1187**: p. 155-68.
179. Ilagan, M.X., et al., *Real-time imaging of notch activation with a luciferase complementation-based reporter.* Sci Signal, 2011. **4**(181): p. rs7.
180. Hancock, M.K., L. Kopp, and K. Bi, *High-throughput screening compatible cell-based assay for interrogating activated notch signaling.* Assay Drug Dev Technol, 2009. **7**(1): p. 68-79.
181. Khorkova, O.E., et al., *Modulation of amyloid precursor protein processing by compounds with various mechanisms of action: detection by liquid phase electrochemiluminescent system.* J Neurosci Methods, 1998. **82**(2): p. 159-66.
182. Clarke, E.E. and M.S. Shearman, *Quantitation of amyloid-beta peptides in biological milieu using a novel homogeneous time-resolved fluorescence (HTRF) assay.* J Neurosci Methods, 2000. **102**(1): p. 61-8.
183. Olsson, A., et al., *Simultaneous measurement of beta-amyloid(1-42), total tau, and phosphorylated tau (Thr181) in cerebrospinal fluid by the xMAP technology.* Clin Chem, 2005. **51**(2): p. 336-45.
184. Shelton, C.C., et al., *An exo-cell assay for examining real-time gamma-secretase activity and inhibition.* Mol Neurodegener, 2009. **4**: p. 22.
185. Chau, D.M., et al., *A novel high throughput 1536-well Notch1 gamma -secretase AlphaLISA assay.* Comb Chem High Throughput Screen, 2013. **16**(6): p. 415-24.
186. McKee, T.D., et al., *An improved cell-based method for determining the gamma-secretase enzyme activity against both Notch and APP substrates.* J Neurosci Methods, 2013. **213**(1): p. 14-21.
187. Lleo, A., et al., *Notch1 competes with the amyloid precursor protein for gamma-secretase and down-regulates presenilin-1 gene expression.* J Biol Chem, 2003. **278**(48): p. 47370-5.

188. Svedruzic, Z.M., et al., *Modulation of gamma-secretase activity by multiple enzyme-substrate interactions: implications in pathogenesis of Alzheimer's disease.* PLoS One, 2012. **7**(3): p. e32293.
189. Morohashi, Y., et al., *C-terminal fragment of presenilin is the molecular target of a dipeptidic gamma-secretase-specific inhibitor DAPT (N-[N-(3,5-difluorophenacetyl)-L-alanyl]-S-phenylglycine t-butyl ester).* J Biol Chem, 2006. **281**(21): p. 14670-6.
190. Burton, C.R., et al., *The amyloid-beta rise and gamma-secretase inhibitor potency depend on the level of substrate expression.* J Biol Chem, 2008. **283**(34): p. 22992-3003.
191. Shearman, M.S., et al., *L-685,458, an aspartyl protease transition state mimic, is a potent inhibitor of amyloid beta-protein precursor gamma-secretase activity.* Biochemistry, 2000. **39**(30): p. 8698-704.
192. Henley, D.B., et al., *Development of semagacestat (LY450139), a functional gamma-secretase inhibitor, for the treatment of Alzheimer's disease.* Expert Opin Pharmacother, 2009. **10**(10): p. 1657-64.
193. Shin, J.M., et al., *The site of action of pantoprazole in the gastric H+/K(+)-ATPase.* Biochim Biophys Acta, 1993. **1148**(2): p. 223-33.
194. Shin, J.M., Y.M. Cho, and G. Sachs, *Chemistry of covalent inhibition of the gastric (H+, K+)-ATPase by proton pump inhibitors.* J Am Chem Soc, 2004. **126**(25): p. 7800-11.
195. Besancon, M., et al., *Sites of reaction of the gastric H,K-ATPase with extracytoplasmic thiol reagents.* J Biol Chem, 1997. **272**(36): p. 22438-46.
196. Roche, V.F., *The chemically elegant proton pump inhibitors.* Am J Pharm Educ, 2006. **70**(5): p. 101.
197. Badiola, N., et al., *The proton-pump inhibitor lansoprazole enhances amyloid beta production.* PLoS One, 2013. **8**(3): p. e58837.
198. Schechter, I. and A. Berger, *On the size of the active site in proteases. I. Papain. 1967.* Biochem Biophys Res Commun, 2012. **425**(3): p. 497-502.
199. Kuniyasu, A., *[Identification of the ligand binding sites and novel drug target molecules by photoaffinity labeling].* Yakugaku Zasshi, 2003. **123**(8): p. 673-9.
200. Rennhack, A., et al., *Synthesis of a potent photoreactive acidic gamma-secretase modulator for target identification in cells.* Bioorg Med Chem, 2012. **20**(21): p. 6523-32.
201. Seiffert, D., et al., *Presenilin-1 and -2 are molecular targets for gamma-secretase inhibitors.* J Biol Chem, 2000. **275**(44): p. 34086-91.
202. Mantafounis, D. and J. Pitts, *Protein engineering of chymosin; modification of the optimum pH of enzyme catalysis.* Protein Eng, 1990. **3**(7): p. 605-9.
203. Banay-Schwartz, M., et al., *The pH dependence of breakdown of various purified brain proteins by cathepsin D preparations.* Neurochem Int, 1985. **7**(4): p. 607-14.
204. Athauda, S.B., et al., *Enzymic and structural characterization of nepenthesin, a unique member of a novel subfamily of aspartic proteinases.* Biochem J, 2004. **381**(Pt 1): p. 295-306.
205. Wolfe, M.S., *Gamma-secretase: structure, function, and modulation for Alzheimer's disease.* Curr Top Med Chem, 2008. **8**(1): p. 2-8.
206. Sun, L., X. Li, and Y. Shi, *Structural biology of intramembrane proteases: mechanistic insights from rhomboid and S2P to gamma-secretase.* Curr Opin Struct Biol, 2016. **37**: p. 97-107.

207. Johnson, D.S., E. Weerapana, and B.F. Cravatt, *Strategies for discovering and derisking covalent, irreversible enzyme inhibitors.* Future Med Chem, 2010. **2**(6): p. 949-64.
208. Bateman, L.A., et al., *An alkyne-aspirin chemical reporter for the detection of aspirin-dependent protein modification in living cells.* J Am Chem Soc, 2013. **135**(39): p. 14568-73.
209. Cohen, M.S., H. Hadjivassiliou, and J. Taunton, *A clickable inhibitor reveals context-dependent autoactivation of p90 RSK.* Nat Chem Biol, 2007. **3**(3): p. 156-60.
210. Roth, G.J., N. Stanford, and P.W. Majerus, *Acetylation of prostaglandin synthase by aspirin.* Proc Natl Acad Sci U S A, 1975. **72**(8): p. 3073-6.
211. Van Der Ouderaa, F.J., et al., *Acetylation of prostaglandin endoperoxide synthetase with acetylsalicylic acid.* Eur J Biochem, 1980. **109**(1): p. 1-8.
212. Fellenius, E., et al., *Substituted benzimidazoles inhibit gastric acid secretion by blocking (H+ + K+)ATPase.* Nature, 1981. **290**(5802): p. 159-61.
213. Robinson, M., *Proton pump inhibitors: update on their role in acid-related gastrointestinal diseases.* Int J Clin Pract, 2005. **59**(6): p. 709-15.
214. Lindberg, P., et al., *The mechanism of action of the gastric acid secretion inhibitor omeprazole.* J Med Chem, 1986. **29**(8): p. 1327-9.
215. Shin, J.M., et al., *Characterization of the inhibitory activity of tenatoprazole on the gastric H+,K+ -ATPase in vitro and in vivo.* Biochem Pharmacol, 2006. **71**(6): p. 837-49.
216. Shin, J.M., et al., *Continuing development of acid pump inhibitors: site of action of pantoprazole.* Aliment Pharmacol Ther, 1994. **8 Suppl 1**: p. 11-23.
217. Shin, J.M. and G. Sachs, *Differences in binding properties of two proton pump inhibitors on the gastric H+,K+-ATPase in vivo.* Biochem Pharmacol, 2004. **68**(11): p. 2117-27.
218. Besancon, M., et al., *Membrane topology and omeprazole labeling of the gastric H+,K(+)-adenosinetriphosphatase.* Biochemistry, 1993. **32**(9): p. 2345-55.
219. Baskin, J.M., et al., *Copper-free click chemistry for dynamic in vivo imaging.* Proc Natl Acad Sci U S A, 2007. **104**(43): p. 16793-7.
220. Su, Y., et al., *Multiplex imaging and cellular target identification of kinase inhibitors via an affinity-based proteome profiling approach.* Sci Rep, 2015. **5**: p. 7724.
221. Jang, S., et al., *Development of a simple method for protein conjugation by copper-free click reaction and its application to antibody-free Western blot analysis.* Bioconjug Chem, 2012. **23**(11): p. 2256-61.
222. Debets, M.F., et al., *Bioconjugation with strained alkenes and alkynes.* Acc Chem Res, 2011. **44**(9): p. 805-15.
223. Sletten, E.M. and C.R. Bertozzi, *From mechanism to mouse: a tale of two bioorthogonal reactions.* Acc Chem Res, 2011. **44**(9): p. 666-76.
224. Selvaraj, R. and J.M. Fox, *trans-Cyclooctene--a stable, voracious dienophile for bioorthogonal labeling.* Curr Opin Chem Biol, 2013. **17**(5): p. 753-60.
225. Devaraj, N.K. and R. Weissleder, *Biomedical applications of tetrazine cycloadditions.* Acc Chem Res, 2011. **44**(9): p. 816-27.
226. Seckute, J. and N.K. Devaraj, *Expanding room for tetrazine ligations in the in vivo chemistry toolbox.* Curr Opin Chem Biol, 2013. **17**(5): p. 761-7.

227. Blackman, M.L., M. Royzen, and J.M. Fox, *Tetrazine ligation: fast bioconjugation based on inverse-electron-demand Diels-Alder reactivity.* J Am Chem Soc, 2008. **130**(41): p. 13518-9.
228. Saccomani, G., et al., *Characterization of gastric mucosal membranes. IX. Fractionation and purification of K+-ATPase-containing vesicles by zonal centrifugation and free-flow electrophoresis technique.* Biochim Biophys Acta, 1977. **465**(2): p. 311-30.
229. Skrabanja, A.T., J.J. De Pont, and S.L. Bonting, *The H+/ATP transport ratio of the (K+ + H+)-ATPase of pig gastric membrane vesicles.* Biochim Biophys Acta, 1984. **774**(1): p. 91-5.
230. Dach, I., et al., *Active detergent-solubilized H+,K+-ATPase is a monomer.* J Biol Chem, 2012. **287**(50): p. 41963-78.
231. Shin, J.M., et al., *Characterization of a novel potassium-competitive acid blocker of the gastric H,K-ATPase, 1-[5-(2-fluorophenyl)-1-(pyridin-3-ylsulfonyl)-1H-pyrrol-3-yl]-N-methylmethanamin e monofumarate (TAK-438).* J Pharmacol Exp Ther, 2011. **339**(2): p. 412-20.
232. Soumarmon, A., F. Grelac, and M.J. Lewin, *Solubilization of active (H+ + K+)-ATPase from gastric membrane.* Biochim Biophys Acta, 1983. **732**(3): p. 579-85.
233. Rabon, E.C., et al., *Radiation inactivation analysis of oligomeric structure of the H,K-ATPase.* J Biol Chem, 1988. **263**(31): p. 16189-94.
234. Shin, J.M. and G. Sachs, *Dimerization of the gastric H+, K(+)-ATPase*. J Biol Chem, 1996. **271**(4): p. 1904-8.
235. Abe, K., et al., *Correlation between the activities and the oligomeric forms of pig gastric H/K-ATPase.* Biochemistry, 2003. **42**(51): p. 15132-8.
236. Abe, K., et al., *Evidence for a relationship between activity and the tetraprotomeric assembly of solubilized pig gastric H/K-ATPase.* J Biochem, 2005. **138**(3): p. 293-301.
237. Shin, J.M., et al., *Functional consequences of the oligomeric form of the membrane-bound gastric H,K-ATPase.* Biochemistry, 2005. **44**(49): p. 16321-32.
238. Murrey, H.E., et al., *Systematic Evaluation of Bioorthogonal Reactions in Live Cells with Clickable HaloTag Ligands: Implications for Intracellular Imaging.* J Am Chem Soc, 2015. **137**(35): p. 11461-75.
239. Mollenhauer, J., et al., *DMBT1, a new member of the SRCR superfamily, on chromosome 10q25.3-26.1 is deleted in malignant brain tumours.* Nat Genet, 1997. **17**(1): p. 32-9.
240. Takeshita, H., et al., *Expression of the DMBT1 gene is frequently suppressed in human lung cancer.* Jpn J Cancer Res, 1999. **90**(9): p. 903-8.
241. Mori, M., et al., *Lack of DMBT1 expression in oesophageal, gastric and colon cancers.* Br J Cancer, 1999. **79**(2): p. 211-3.
242. Mollenhauer, J., et al., *DMBT1 encodes a protein involved in the immune defense and in epithelial differentiation and is highly unstable in cancer.* Cancer Res, 2000. **60**(6): p. 1704-10.
243. Prakobphol, A., et al., *Salivary agglutinin, which binds Streptococcus mutans and Helicobacter pylori, is the lung scavenger receptor cysteine-rich protein gp-340.* J Biol Chem, 2000. **275**(51): p. 39860-6.
244. Fiorini, G., et al., *Newer agents for Helicobacter pylori eradication.* Clin Exp Gastroenterol, 2012. **5**: p. 109-12.

245. Blandizzi, C., et al., *Acid-independent gastroprotective effects of lansoprazole in experimental mucosal injury.* Dig Dis Sci, 1999. **44**(10): p. 2039-50.
246. Renner, M., et al., *DMBT1 confers mucosal protection in vivo and a deletion variant is associated with Crohn's disease.* Gastroenterology, 2007. **133**(5): p. 1499-509.
247. Paresi, C.J., Q. Liu, and Y.M. Li, *Benzimidazole covalent probes and the gastric H(+)/K(+)-ATPase as a model system for protein labeling in a copper-free setting.* Mol Biosyst, 2016. **12**(6): p. 1772-80.
248. Haenisch, B., et al., *Risk of dementia in elderly patients with the use of proton pump inhibitors.* Eur Arch Psychiatry Clin Neurosci, 2015. **265**(5): p. 419-28.
249. Gomm, W., et al., *Association of Proton Pump Inhibitors With Risk of Dementia: A Pharmacoepidemiological Claims Data Analysis.* JAMA Neurol, 2016. **73**(4): p. 410-6.
250. Rojo, L.E., et al., *Selective interaction of lansoprazole and astemizole with tau polymers: potential new clinical use in diagnosis of Alzheimer's disease.* J Alzheimers Dis, 2010. **19**(2): p. 573-89.
251. Shah, N.H., et al., *Proton Pump Inhibitor Usage and the Risk of Myocardial Infarction in the General Population.* PLoS One, 2015. **10**(6): p. e0124653.
252. Juurlink, D.N., et al., *Proton pump inhibitors and the risk of adverse cardiac events.* PLoS One, 2013. **8**(12): p. e84890.
253. Gude, N. and M. Sussman, *Notch signaling and cardiac repair.* J Mol Cell Cardiol, 2012. **52**(6): p. 1226-32.
254. Aquila, G., et al., *The role of Notch pathway in cardiovascular diseases.* Glob Cardiol Sci Pract, 2013. **2013**(4): p. 364-71.
255. Lewis, S.J., et al., *A novel series of potent gamma-secretase inhibitors based on a benzobicyclo[4.2.1]nonane core.* Bioorg Med Chem Lett, 2005. **15**(2): p. 373-8.
256. Meng, R.D., et al., *gamma-Secretase inhibitors abrogate oxaliplatin-induced activation of the Notch-1 signaling pathway in colon cancer cells resulting in enhanced chemosensitivity.* Cancer Res, 2009. **69**(2): p. 573-82.